DANIEL KROEHLING RODRIGUES CARDOSO

SORPTION AND STABILITY OF TRACE ELEMENTS ON ALUMINUM-SUBSTITUTED IRON OXIDES

Dissertation submitted to the Soil Science and Plant Nutrition Graduate Program of the Universidade Federal de Viçosa in partial fulfillment of the requirements for the degree of *Magister Scientiae*.

Adviser: Isabela Cristina Filardi Vasques

Co-adviser: Jaime Wilson Vargas de Mello

VIÇOSA – MINAS GERAIS
2023

Ficha catalográfica elaborada pela Biblioteca Central da Universidade Federal de Viçosa - Campus Viçosa

T

C268s
2023

Cardoso, Daniel Kroehling Rodrigues, 1996-
Sorption and stability of trace elements on aluminum-substituted iron oxides / Daniel Kroehling Rodrigues Cardoso. – Viçosa, MG, 2023.
1 dissertação eletrônica (82 f.): il. (algumas color.).

Texto em inglês.
Inclui apêndice.
Orientador: Isabela Cristina Filardi Vasques.
Dissertação (mestrado) - Universidade Federal de Viçosa, Departamento de Solos, 2023.
Inclui bibliografia.
DOI: https://doi.org/10.47328/ufvbbt.2023.294
Modo de acesso: World Wide Web.

1. Drenagem ácida de minas. 2. Precipitação (Química). 3. Garimpo. 4. Arsênio. 5. Goethita. I. Vasques, Isabela Cristina Filardi , 1990-. II. Universidade Federal de Viçosa. Departamento de Solos. Programa de Pós-Graduação em Solos e Nutrição de Plantas. III. Título.

CDD 22. ed. 628.16832

Bibliotecário(a) responsável: Alice Regina Pinto Pires CRB-6/2523

DANIEL KROEHLING RODRIGUES CARDOSO

SORPTION AND STABILITY OF TRACE ELEMENTS ON ALUMINUM-SUBSTITUTED IRON OXIDES

Dissertation submitted to the Soil Science and Plant Nutrition Graduate Program of the Universidade Federal de Viçosa in partial fulfillment of the requirements for the degree of *Magister Scientiae*.

APPROVED: April 27, 2023.

Assent:

Documento assinado digitalmente
gov.br DANIEL KROEHLING RODRIGUES CARDOSO
Data: 24/05/2023 11:20:12-0300
Verifique em https://validar.iti.gov.br

Daniel Kroehling Rodrigues Cardoso
Author

Documento assinado digitalmente
gov.br ISABELA CRISTINA FILARDI VASQUES
Data: 24/05/2023 06:11:59-0300
Verifique em https://validar.iti.gov.br

Isabela Cristina Filardi Vasques
Adviser

AGRADECIMENTOS

Agradeço à Coordenação de Aperfeiçoamento de Pessoal de Nível Superior (CAPES), ao Conselho Nacional de Desenvolvimento Científico e Tecnológico (CNPq) e à Fundação de Amparo à Pesquisa do Estado de Minas Gerais (FAPEMIG) pelo financiamento e incentivo à pesquisa científica no nosso país.

Agradeço também à Universidade Federal de Viçosa (UFV), ao Departamento de Solos (DPS) e ao Programa de Pós-Graduação em Solos e Nutrição de Plantas (PPG-SNP) pela infraestrutura, os laboratórios, equipamentos e reagentes usados neste trabalho.

A meus queridos orientadores, Isabela Vasques e Jaime Mello, agradeço a sugestão do trabalho, os ensinamentos, e a guia no jogo e nas regras da ciência. A Renato Veloso Calango, pelo apoio na montagem do experimento e pelos “pitacos”.

Aos imprescindíveis estagiários, Marcelo Oliveira e Gisele Braathen, agradeço a confiança e as horas de trabalho tedioso.

A todo pessoal do DPS que apoiou e fortaleceu, em especial a João Milagres, Humberto Rosado, Júlio Nunes, Daniela Costa, Ludmila Gonçalves, Karin Ferraz, Edvaldo Cardoso, Amanda Abreu, Josemar Barros e Janilson Rocha.

Aos admirados professores Carlos Schaefer, Irene Cardoso, Bruno Vasconcelos, Edgar Júnior, Cristine Muggler, Catarina Kasuya, Hidelblandi Melo, André Carvalho, Igor Assis e Maurício Fontes, agradeço as lições em ciências da Terra e da natureza.

Mãe, pai e Rafa, mesmo distantes, estão sempre comigo. Assim como toda a família Kroehling e Cardoso, vocês sempre me incentivaram na carreira cientifica, me enchem de amor e orgulho, e eu sempre volto para casa. Este trabalho é nosso.

Gratidão à Tribo do Morro, Capoeira Angoleiros do Mar, por despertar em mim o forte e acordá-lo mais um pouco. Aos mandingueiros Daniel Angoleiro, Nath Vespinha, Tiago Gafanhoto, Marco Tulio Tato, Jhonny Calango, e toda a Tribo, obrigado pela brincadeira de luta, amor e carinho.

A Davi, Felipe e João, obrigado pela recepção fraternal. Os dias e as noites em Viçosa são melhores com vocês.

Obrigado, Julia, por ter me feito uma pessoa melhor com muito amor e cuidado. Aos amigos de Bom Despacho e Belo Horizonte, Netinho, Dedé, Gusui, Ian, Pedro, João Luiz, Sinuhê, Pinico, Léo, Victor, Thaís, Jordan, Dondon e tantos outros, estou morrendo de saudades.

A ciência brasileira não tem pernas, mas ela caminha.

ABSTRACT

KROEHLING, Daniel Rodrigues Cardoso, M.Sc., Universidade Federal de Viçosa, April 2023. **Sorption and stability of trace elements on aluminum-substituted iron oxides**. Adviser: Isabela Cristina Filardi Vasques. Co-adviser: Jaime Wilson Vargas de Mello.

The trace elements arsenic (As), antimony (Sb), lead (Pb), and cadmium (Cd) are present in orogenic gold deposits positively correlated with gold. Others, such as the rare earth elements lanthanum (La) and ytterbium (Yb), do not present correlation with gold. The weathering of these rocks, intensified by mining activity, leads to a redistribution throughout the local drainage basin. Iron oxides precipitating from weathering products immobilize part of these elements. High contents of gold in secondary deposits attract artisanal mining (*garimpo*), which historically contaminates watercourses with mercury (Hg). In this study, iron oxides were precipitated from a solution containing As, Pb, Sb, Cd, La, Yb, and Hg in the presence and in the absence of aluminum (Al). The stability of the coprecipitates was evaluated through BCR and SBET extraction procedures. Most of the initial content of As, Pb, Yb, and Sb was coprecipitated with Fe-oxides in only two hours, while Cd and La persisted longer in solution. Aluminum isomorphic substitution in Fe-oxides favored La and Yb immobilization in the short-term, but favored As and Cd immobilization in the long-term. Goethite with Al substitution (Al-goethite) was the only phase identified in treatments with Al, and lepidocrocite precipitation was favored at high concentrations of trace elements. Arsenic and Cd were more stable coprecipitated with Al-goethite. On the other hand, La and Yb were more stable with Al-free-goethite or lepidocrocite. The extraction percentages of As, Cd and Sb from precipitates were lower than Pb, La and Yb, which might be related to higher incorporation of As, Cd and Sb into the oxides structure. The precipitates had high bioaccessible contents of As and, therefore, higher risk to oral exposure for children ($HQ > 1$). Mercury did not interfere with other elements sorption or stability, therefore the hypothesis that *garimpo* can remobilize other elements through desorption from Fe-oxides due to Hg introduction was not confirmed. The results were useful for enhancing comprehension of interactions between iron oxides and trace elements in natural systems, including aspects such as sorption mechanisms, stability, bioavailability, and toxicity.

Keywords: Coprecipitation. Acid mine drainage. Garimpo. Arsenic. Goethite.

RESUMO

KROEHLING, Daniel Rodrigues Cardoso, M.Sc., Universidade Federal de Viçosa, abril de 2023. **Sorção e estabilidade de elementos-traço em óxidos de ferro com substituição por alumínio**. Orientadora: Isabela Cristina Filardi Vasques. Coorientador: Jaime Wilson Vargas de Mello.

Os elementos-traço arsênio (As), antimônio (Sb), chumbo (Pb) e cádmio (Cd) estão presentes em depósitos orogênicos correlacionados positivamente com o ouro. Outros, como os elementos terras raras lantânio (La) e itérbio (Yb), não apresentam correlação com o ouro. O intemperismo dessas rochas, intensificado pela atividade de mineração, redistribui os elementos na bacia hidrográfica local. Óxidos de ferro precipitados a partir dos produtos do intemperismo imobilizam parte desses elementos. Altos teores de ouro nos depósitos secundários atraem garimpeiros, que historicamente contaminam os cursos d'água com mercúrio (Hg). Neste estudo, óxidos de ferro foram precipitados de uma solução contendo As, Pb, Sb, Cd, La, Yb e Hg na presença e ausência de alumínio (Al). A estabilidade dos coprecipitados foi avaliada por meio dos procedimentos de extração BCR e SBET. A maior parte do conteúdo inicial de As, Pb, Yb e Sb foi coprecipitada com os óxidos de Fe em apenas duas horas, enquanto Cd e La persistiram em solução por mais tempo. A substituição isomórfica do Al nos óxidos de Fe durante a coprecipitação favoreceu a imobilização de La e Yb em curto prazo, porém só favoreceu a imobilização de As e Cd em longo prazo. Goethita com substituição por Al (Al-goethita) foi a única fase identificada nos tratamentos com Al, e a precipitação de lepidocrocita foi favorecida em altas concentrações de elementos traço. Arsênio e Cd foram mais estáveis coprecipitados com Al-goethita. Por outro lado, La e Yb foram mais estáveis com goethita e lepidocrocita sem Al. As porcentagens de extração de As, Cd e Sb dos precipitados foram menores que as de Pb, La e Yb, o que pode estar relacionado à maior incorporação de As, Cd e Sb na estrutura dos óxidos de Fe. Os precipitados apresentaram altos teores bioacessíveis de As e, por isso, maior risco à exposição oral de crianças ($HQ > 1$). O mercúrio não interferiu na sorção ou estabilidade dos outros elementos, portanto a hipótese de que o garimpo pode remobilizar outros elementos por dessorção dos óxidos de Fe, devido à introdução de Hg não foi confirmada. Os resultados foram úteis para ampliar a compreensão das interações entre óxidos de ferro e elementos-traço em sistemas naturais, incluindo aspectos como mecanismos de sorção, estabilidade, biodisponibilidade e toxicidade.

Palavras-chave: Coprecipitação. Drenagem ácida de mina. Garimpo. Arsênio. Goethita.

SUMMARY

INTRODUÇÃO GERAL

Depósitos de ouro orogênicos são uma classe de depósitos hidrotermais formados em cinturões orogênicos e apresentam padrões geoquímicos semelhantes (Goldfarb et al., 2001; Groves et al., 1998; Ridley, 2013). Minerais sulfetados, como pirita, arsenopirita ou pirrotita, estão comumente associados ao ouro nos veios mineralizados. Esses sulfetos são quimicamente instáveis sob condições ambientais e se oxidam na presença de oxigênio e água. A oxidação produz acidez e mobiliza elementos potencialmente tóxicos, processo conhecido como drenagem ácida de mina (Mello et al., 2006; Simate and Ndlovu, 2014).

Um exemplo de depósito de ouro orogênico é encontrado na mina Morro do Ouro, em Paracatu, Brasil (Oliver et al., 2015). Análises geoquímicas da formação Paracatu mostram que alguns elementos-traço estão positivamente correlacionados com o ouro (e.g., As, Sb, Pb, Cd), enquanto outros apresentam variações sutis ao longo da rocha hospedeira (e.g., La, Yb). Todos esses elementos são naturalmente distribuídos no ambiente há milhares de anos por intemperismo e erosão, mas a mineração acelera a distribuição ao escavar a rocha e expor os sulfetos ao ambiente oxidante. Além disso, o comportamento geoquímico de tais elementos nos solos, sedimentos e água pode não apresentar as mesmas correlações encontradas na rocha.

Altos teores de ouro nos depósitos aluvionares atraem garimpeiros, responsáveis pela alta concentração de mercúrio nos sedimentos dos cursos d'água das regiões auríferas (Rezende et al., 2018). Os garimpeiros remexem os sedimentos e quebram os fragmentos de rocha, usando mercúrio para facilitar a extração do ouro (UNEP, 2018). Essa atividade compromete a qualidade das águas, mas ainda são desconhecidos os efeitos do garimpo na redistribuição dos elementos-traço.

Óxidos, hidróxidos e oxihidróxidos de ferro (ou simplesmente "óxidos de ferro") são alguns dos minerais mais importantes no controle da mobilidade de elementos-traço em solos e sedimentos. Nanopartículas de óxidos de ferro estão amplamente dispersas no meio ambiente, além de serem produto da oxidação dos sulfetos de ferro. Os óxidos de ferro são precipitados a partir da oxidação do Fe(II) ou supersaturação da solução (Schwertmann and Cornell, 2000; Waychunas et al., 2005). Em sistemas naturais a precipitação não ocorre isoladamente, mas na presença de outras substâncias solúveis que influenciam a formação do óxido (Freitas et al., 2016; Yang et al., 2021).

Os elementos-traço podem ser adsorvidos à superfície (Ladeira and Ciminelli, 2004; Silva et al., 2010) ou coprecipitados com os óxidos de Fe (Freitas et al., 2016, 2015). A coprecipitação ocorre quando diferentes elementos em solução precipitam simultaneamente (Ford, 2012;

Sposito, 2008). Este processo se revelou altamente eficaz para a remoção de elementos-traço de soluções contaminadas através da coprecipitação com óxidos de ferro e alumínio (Barcelos et al., 2018; Mello et al., 2018; Pietralonga et al., 2017; Vasques et al., 2018a, 2018b).

De fato, a coprecipitação pode ser muito mais eficaz para a imobilização de contaminantes do que a simples adsorção superficial, posto que muitos íons coprecipitados podem ser incorporados na estrutura do mineral em formação (Jeong et al., 2017; Lu et al., 2011). A mobilidade dos elementos-traço e a estabilidade dos óxidos de ferro coprecipitados podem ser avaliadas através de métodos de extração que simulam diferentes condições ambientais. Procedimentos de extrações sequenciais e testes de bioacessibilidade são métodos de custo relativamente baixo que indicam mecanismos de sorção e força de ligação entre elemento-traço e fase mineral (Barcelos et al., 2018; Ciminelli et al., 2018; Vasques et al., 2018a).

Íons solvatados e fracamente adsorvidos na superfície mineral através de complexos de esfera externa podem ser facilmente solubilizados por esses extratores. Por outro lado, íons fortemente adsorvidos que compartilham elétrons e formam complexos de esfera interna não são facilmente dessorvidos da fase mineral, a menos que a ligação seja rompida. Por sua vez, íons incorporados à estrutura formando uma solução sólida são extraídos apenas com a dissolução da fase sólida.

Este trabalho avaliou a eficiência de óxidos de ferro e alumínio em remover As, Sb, Cd, La, Yb e Hg de soluções contaminadas através da coprecipitação em laboratório. A estabilidade dos óxidos e elementos coprecipitados também foi avaliada através dos procedimentos de extração BCR (*Community Bureau of Reference*) e SBET (*Simplified Bioaccessibility Extraction Test*). As hipóteses deste trabalho foram: (1) os elementos-traço correlacionados na rocha não apresentam a mesma correlação durante a coprecipitação em condições ambientais; (2) a substituição isomórfica por alumínio influencia a imobilização dos elementos-traço; e (3) o mercúrio compete com os outros elementos-traço por sítios de adsorção nos óxidos de ferro. Além disso, a pesquisa teve como objetivo sugerir mecanismos de sorção para elementos-traço, definir quais elementos formam ligações mais estáveis com os óxidos de ferro, e avaliar o risco humano à exposição aos precipitados. Espera-se que os resultados obtidos possam contribuir para um melhor entendimento sobre as interações entre óxidos de ferro e elementos-traço, incluindo mecanismos de sorção, estabilidade e, consequentemente, biodisponibilidade desses elementos no ambiente.

REFERÊNCIAS

Barcelos, G.S., Veloso, R.W., de Mello, J.W.V., Gasparon, M., 2018. Immobilization of Eu and Ho from synthetic acid mine drainage by precipitation with Fe and Al (hydr)oxides. Environmental Science and Pollution Research 25, 18813–18822. https://doi.org/10.1007/s11356-018-2100-5

Ciminelli, V.S.T., Antônio, D.C., Caldeira, C.L., Freitas, E.T.F., Delbem, I.D., Fernandes, M.M., Gasparon, M., Ng, J.C., 2018. Low arsenic bioaccessibility by fixation in nanostructured iron (Hydr)oxides: Quantitative identification of As-bearing phases. J Hazard Mater 353, 261–270. https://doi.org/10.1016/j.jhazmat.2018.03.037

Ford, R.G., 2012. Chemisorption and Precipitation Reactions. Handbook of Soil Sciences: Properties and Processes.

Freitas, E.T.F., Montoro, L.A., Gasparon, M., Ciminelli, V.S.T., 2015. Natural attenuation of arsenic in the environment by immobilization in nanostructured hematite. Chemosphere 138, 340–347. https://doi.org/10.1016/j.chemosphere.2015.05.101

Freitas, E.T.F., Stroppa, D.G., Montoro, L.A., de Mello, J.W.V., Gasparon, M., Ciminelli, V.S.T., 2016. Arsenic entrapment by nanocrystals of Al-magnetite: The role of Al in crystal growth and As retention. Chemosphere 158, 91–99. https://doi.org/10.1016/j.chemosphere.2016.05.044

Goldfarb, R.J., Groves, D.I., Gardoll, S., 2001. Orogenic gold and geologic time: a global synthesis. Ore Geol Rev 18, 1–75. https://doi.org/10.1016/S0169-1368(01)00016-6

Groves, D.I., Goldfarb, R.J., Gebre-Mariam, M., Hagemann, S.G., Robert, F., 1998. Orogenic gold deposits: A proposed classification in the context of their crustal distribution and relationship to other gold deposit types. Ore Geol Rev 13, 7–27. https://doi.org/10.1016/S0169-1368(97)00012-7

Jeong, S., Yang, K., Jho, E.H., Nam, K., 2017. Importance of chemical binding type between As and iron-oxide on bioaccessibility in soil: Test with synthesized two line ferrihydrite. J Hazard Mater 330, 157–164. https://doi.org/10.1016/j.jhazmat.2017.02.009

Ladeira, A.C.Q., Ciminelli, V.S.T., 2004. Adsorption and desorption of arsenic on an oxisol and its constituents. Water Res 38, 2087–2094. https://doi.org/10.1016/j.watres.2004.02.002

Lu, P., Nuhfer, N.T., Kelly, S., Li, Q., Konishi, H., Elswick, E., Zhu, C., 2011. Lead coprecipitation with iron oxyhydroxide nano-particles. Geochim Cosmochim Acta 75, 4547–4561. https://doi.org/10.1016/j.gca.2011.05.035

Mello, J.W.V. de, Dias, L.E., Daniel, A.M., Abrahão, W.A.P., Deschamps, E., Schaefer, C.E.G.R., 2006. Preliminary evaluation of acid mine drainage in Minas Gerais State, Brazil. Rev Bras Cienc Solo 30, 365–375. https://doi.org/10.1590/S0100-06832006000200016

Mello, J.W.V., Gasparon, M., Silva, J., 2018. Effectiveness of arsenic co-precipitation with Fe-Al hydroxides for treatment of contaminated water. Rev Bras Cienc Solo 42. https://doi.org/10.1590/18069657rbcs20170261

Mello, J.W. V., Nepomuceno, A.L., Matos, A.A.S., Guimarães, P.J., Mendonça, G. V., Silva, S.C., unpublished. Antimony, mercury and other elements as tracers for geogenic origin and impacts of artisanal mining on arsenic distribution in sediments from an orogenic gold mineralization area. Unsubmitted.

Oliver, N.H.S., Thomson, B., Freitas-Silva, F.H., Holcombe, R.J., Rusk, B., Almeida, B.S., Faure, K., Davidson, G.R., Esper, E.L., Guimarães, P.J., Dardenne, M.A., 2015. Local and Regional Mass Transfer During Thrusting, Veining, and Boudinage in the Genesis of the Giant Shale-Hosted Paracatu Gold Deposit, Minas Gerais, Brazil. Economic Geology 110, 1803–1834. https://doi.org/10.2113/econgeo.110.7.1803

Pietralonga, A.G., de Mendonça, B.A.F., Barcelos, G.S., de Mello, J.W.V., Abrahão, W.A.P., 2017. Lanthanum immobilization by iron and aluminum colloids. Environ Earth Sci 76. https://doi.org/10.1007/s12665-017-6583-z

Rezende, P.S., Silva, N.C., Moura, W.D., Windmöller, C.C., 2018. Quantification and speciation of mercury in streams and rivers sediment samples from Paracatu, MG, Brazil, using a direct mercury analyzer®. Microchemical Journal 140, 199–206. https://doi.org/10.1016/j.microc.2018.04.006

Ridley, J., 2013. Ore Deposit Geology. Cambridge University Press.

Schwertmann, U., Cornell, R.M., 2000. Iron Oxides in the Laboratary. Wiley-VCH Verlag GmbH. https://doi.org/10.1002/9783527613229

Silva, J., Mello, J.W.V., Gasparon, M., Abrahão, W.A.P., Ciminelli, V.S.T., Jong, T., 2010. The role of Al-Goethites on arsenate mobility. Water Res 44, 5684–5692. https://doi.org/10.1016/j.watres.2010.06.056

Simate, G.S., Ndlovu, S., 2014. Acid mine drainage: Challenges and opportunities. J Environ Chem Eng 2, 1785–1803. https://doi.org/10.1016/j.jece.2014.07.021

Sposito, G., 2008. The Chemistry of Soils, Second ed. Oxford University Press, New York.

UNEP, 2018. Global Mercury Assessment. United Nations Environment Programme. Geneva, Switzerland.

Vasques, Isabela C.F., de Mello, J.W.V., Veloso, R.W., Ferreira, V.P., Abrahão, W.A.P., 2018a. Arsenite removal from contaminated water by precipitation of aluminum, ferrous and ferric (hydr)oxides. Environmental Science and Pollution Research 25, 12967–12980. https://doi.org/10.1007/s11356-018-1458-8

Vasques, Isabela C.F., de Mello, J.W. V., Veloso, R.W., Ferreira, V. de P., Abrahão, W.A.P., 2018b. Effectiveness of Ferric, Ferrous, and Aluminum (Hydr)Oxide Coprecipitation to Treat Water Contaminated with Arsenate. J Environ Qual 47, 1339–1346. https://doi.org/10.2134/jeq2018.01.0014

Waychunas, G.A., Kim, C.S., Banfield, J.F., 2005. Nanoparticulate Iron Oxide Minerals in Soils and Sediments: Unique Properties and Contaminant Scavenging Mechanisms. Journal of Nanoparticle Research 7, 409–433. https://doi.org/10.1007/s11051-005-6931-x

Yang, M., Liang, X., Li, Y., He, H., Zhu, R., Arai, Y., 2021. Ferrihydrite Transformation Impacted by Adsorption and Structural Incorporation of Rare Earth Elements. ACS Earth Space Chem 5, 2768–2777. https://doi.org/10.1021/acsearthspacechem.1c00159

COPRECIPITATION OF ALUMINUM-SUBSTITUTED IRON OXIDES AND TRACE ELEMENTS FROM AN OROGENIC GOLD DEPOSIT ENVIRONMENT

Graphical Abstract

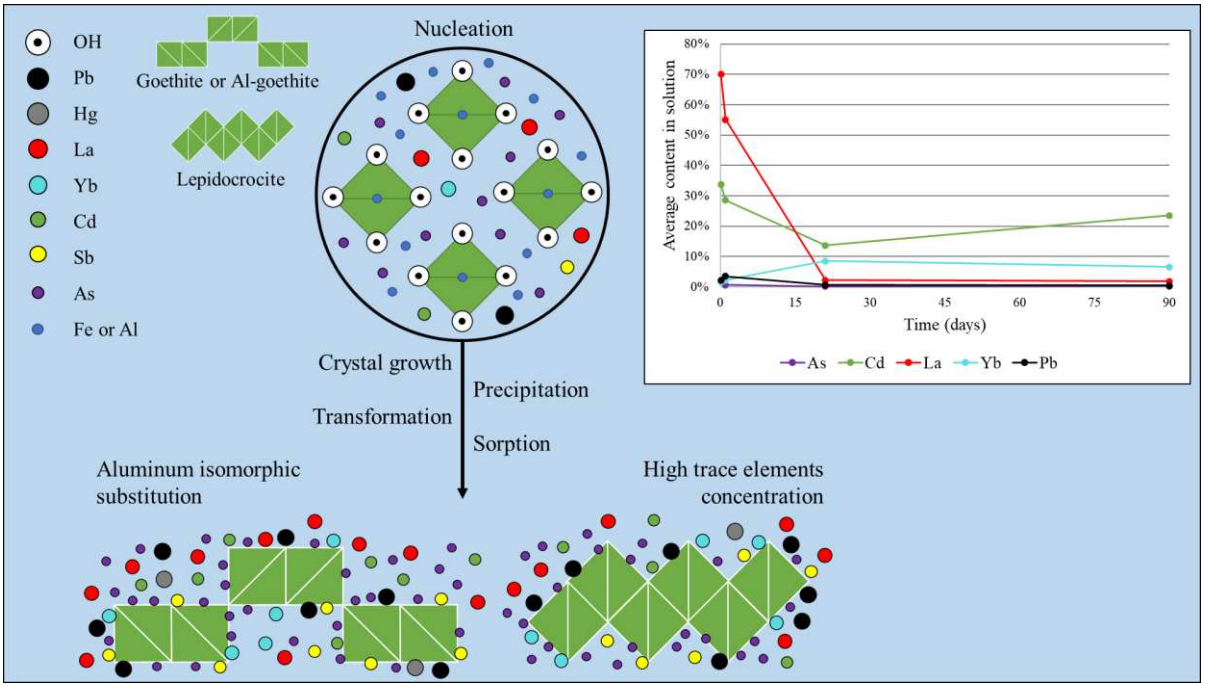

Highlights

- More than 99% of the soluble trace elements was coprecipitated with iron oxides.
- As, Pb, Yb and Sb were faster sorbed to iron oxides than Cd and La.
- Al isomorphic substitution in iron oxides favored La and Yb removal in the short-term, whilst favored As and Cd removal in the long-term.
- High concentrations of trace elements favored precipitation of lepidocrocite.
- Hg did not interfere significantly in other trace elements sorption.

ABSTRACT

Trace elements, such as arsenic (As), antimony (Sb), lead (Pb), and cadmium (Cd), are commonly present in sulfide deposits positively correlated with gold. Others, such as the rare earth elements lanthanum (La) and ytterbium (Yb), show subtle variations throughout the mineralization profile. The weathering of these rocks, intensified by mining activity, leads to a redistribution throughout local soils and sediments. Iron oxides precipitating as weathering products immobilize part of these elements. High contents of gold in secondary deposits are attractive for artisanal mining (*garimpo*), which traditionally introduces mercury (Hg) in waterways. The dynamics of iron oxides coprecipitation with trace elements is revealed in this study. The trace elements were identified in the orogenic gold deposit in Morro do Ouro mine (Paracatu, Brazil). Arsenic, Pb, Yb, and Sb were faster sorbed to iron oxides, while Cd and La persisted longer in solution. Lepidocrocite precipitation was favored at high concentrations of trace elements. Al-goethite was the only phase identified in treatments with aluminum. Isomorphic substitution of Fe by Al in goethite presented different effects: it favored La and Yb immobilization in the short-term, whilst it favored As and Cd immobilization in the long-term. This effect was related to the progress of iron oxide formation and crystal growth. After ninety days, more than 99% of the initial trace elements soluble content was coprecipitated with Fe-oxides, but the limit for effluent discharged was not attained for As, Cd and Fe. Mercury did not interfere significantly with other elements sorption and the hypothesis that *garimpo* can remobilize other elements through desorption from Fe-oxides due to Hg introduction was not confirmed.

Keywords: Acid mine drainage. Rare Earth Elements. Soil contamination. Arsenic. Garimpo.

1. INTRODUCTION

Orogenic gold deposits are a class of hydrothermal, vein and replacement deposit in metamorphic and intrusive igneous rocks, formed in actively evolving orogenic belts, and show typical geochemical patterns (Goldfarb et al., 2001; Groves et al., 1998; John Ridley, 2013). Sulfide minerals are usual components of mineralized veins, being pyrite, pyrrhotite, and arsenopyrite the main sulfides associated with gold. Under environmental conditions, at or near the Earth's surface, sulfides are chemically unstable and oxidize in the presence of oxygen and water. These reactions produce acidity, releasing potentially toxic elements to the environment, a process known as acid mine drainage (Mello et al., 2006; Simate and Ndlovu, 2014).

An example of orogenic gold deposit is found in Morro do Ouro mine, at Paracatu Formation, in the state of Minas Gerais, Brazil (Oliver et al., 2015). Geochemical analysis of the Paracatu Formation has shown that some trace elements are positively correlated to gold (e.g., As, Sb, Pb, Cd), but others show subtle variations throughout the mineralization (e.g., La, Yb). All these elements are naturally distributed on the local basin through weathering and erosion over thousands of years, but mining activities accelerate this distribution by digging and exposing the sulfide-rich rock to atmosphere. These elements are expected to present a different geochemical behavior under environmental conditions. Then, the geochemistry of such elements in soils, sediments and water, in general, does not follow the same pattern, but may correlate to the contents found in the lithotype.

High contents of gold in watercourses are attractive for artisanal mining operations, known as *garimpo*, which are responsible for high mercury (Hg) concentration in sediments of streams and rivers around gold deposits (Rezende et al., 2018). The miners roll and crush rock fragments, using Hg to improve gold extraction (UNEP, 2018). This activity undoubtedly causes severe impacts in water quality, but it is still unknown the effects of *garimpo* on the natural redistribution of the above-mentioned elements. Gil-Díaz et al. (2021) showed that Hg^{2+} presents high affinity for iron (hydr)oxides nanoparticles. These iron (hydr)oxides, in addition to being wide-spread in tropical soils and sediments, are also expected products of iron sulfides oxidation. Therefore, the Hg introduced in streams by *garimpo* might compete with other trace elements for iron (hydr)oxides sorption sites.

Indeed, the mobility of trace elements in tropical soils and sediments is controlled mainly by their sorption onto iron oxides, oxyhydroxides and hydroxides (Veloso et al., 2019), from now on referred to as 'iron oxides'. Trace elements can be adsorbed onto the surface (Ladeira and Ciminelli, 2004; Silva et al., 2010) or coprecipitated within the iron oxides (Freitas et al.,

2016, 2015). Coprecipitation is the process of incorporation of an element as a trace or minor constituent within a precipitating phase (Ford, 2012; Sposito, 2008). It takes place when different elements in solution precipitate simultaneously. This process proved to be highly effective for water decontamination through precipitation of Fe and Al oxides (Barcelos et al., 2018; Mello et al., 2018; Pietralonga et al., 2017; Vasques et al., 2018a, 2018b).

The isomorphic substitution of Fe by Al in Fe-oxides is a phenomenon widely observed in nature (Schwertmann and Carlson, 1994). It is well known that Al-for-Fe substitution leads to a decrease of the Fe-oxide unit-cell dimension, which can be estimated as proposed by Schulze (1984). Souza et al. (2021) revealed that structural defects in ferrihydrite due to Al-substitution are compensated by an increase in surface Fe-OH and Al-OH groups, which could enhance As(V) adsorption. Moreover, Freitas et al. (2016, 2015) showed that Al induces oriented attachment-based growth on Al-magnetite and Al-hematite, leading to strong As retention in the Fe-oxide structure. Vasques et al. (2018a) reported that coprecipitation of Fe-oxides with structural Al favored As removal from water in the long-term but impaired it in the short-term. Therefore, although extensively studied, the effects of Al substitution in Fe-oxides for trace elements sorption are still controverse.

This study evaluated the capacity of Fe-Al-oxides to remove As, Sb, Cd, La, and Yb from contaminated water through coprecipitation in laboratory. These trace elements are commonly found in orogenic gold deposits and in acid mine drainage. They were also found in watershed sediments around Morro do Ouro mine in preliminary studies (Mello et al. unpublished). The hypotheses are: (1) the elements correlated in the lithotype do not present the same behavior during coprecipitation under environmental conditions; (2) aluminum for iron substitution influences the Fe-oxides mineralogy and also the trace elements removal from water; (3) mercury can compete with other trace elements for sorption sites on Fe-oxides. This would indicate that *garimpo* operations, aside contaminating the watercourses with Hg, could favor the remobilization of geogenic toxic elements from sediments settled down in watercourses. Understanding the geochemical dynamics and affinities of these elements with iron oxides can be helpful on distinguishing the effects of human activities from the natural geogenic distribution of toxic elements in the environment.

2. MATERIALS AND METHODS

2.1 Coprecipitation of Fe-Al-oxides and trace elements

Iron oxides with and without aluminum were synthesized following Schwertmann and Cornell (2000) guidelines for goethite preparation from Fe(II) systems adapted to the coprecipitation with trace elements (Barcelos et al., 2018; Mello et al., 2018; Pietralonga et al., 2017; Vasques et al., 2018a, 2018b). The concentration of the sorbents ([Fe] + [Al] = 500 mmol L^{-1}) was proposed in order to precipitate around 30 g of Fe-oxides in 0.800 L of each experimental unit (Table 1). The solutions were prepared using $FeSO_4.7H_2O$ and $Al_2(SO_4)_3.18H_2O$. Sulfates were preferred over chlorides in order to simulate the environment affected by acid mine drainage, since SO_4^{2-} is mobilized due to sulfides oxidation from orogenic gold deposits.

Table 1 – Factors under study in the coprecipitation experiment.

Factor*	Element	Concentration			
		mmol L^{-1}	mg L^{-1}	mmol L^{-1}	mg L^{-1}
a		Without Al		With Al	
	Fe:Al	500:0	28,000:0	450:50	25,200:1,350
		Low concentration		High concentration	
b	As	5.00	374.60	10.00	749.21
	Pb	0.10	20.88	0.20	41.77
	La	0.10	13.90	0.20	27.80
	Yb	0.01	1.83	0.02	3.65
	Sb	0.01	1.22	0.02	2.44
	Cd	0.01	1.15	0.02	2.31
c		Without Hg		With Hg	
	Hg	0	0	0.01	2.05
d		Pure Fe-hydroxides		Pure Fe-Al-hydroxides	
	Fe:Al	500:0	28,000:0	450:50	25,200:1,350

* a) Adsorbents; b) Geogenics; c) Anthropogenic; d) Control treatments.

Paracatu Formation samples presented four trace elements (As, Sb, Pb, Cd) positively correlated to gold and two trace elements (La, Yb) not correlated but present throughout the mineralized and barren sequence (Mello et al. unpublished; Oliver et al., 2015) (Figure 1). The 'Low' trace elements concentrations in the experiment were based on the average proportions to Fe contents (Table 1). The 'High' trace elements concentrations represented a worst-case scenario of higher contents found in the local gold mineralization (75-125 m depth), which was

the double of the 'Low' concentrations (75-125 m depth) (Figure 1). The reagents used were: As_2O_3, Sb standard solution (10.000 mg L^{-1}), $Pb(NO_3)_2$, $CdSO_4.8/3H_2O$, $La_2(SO_4)_3$ and Yb_2O_3, all analytical grade.

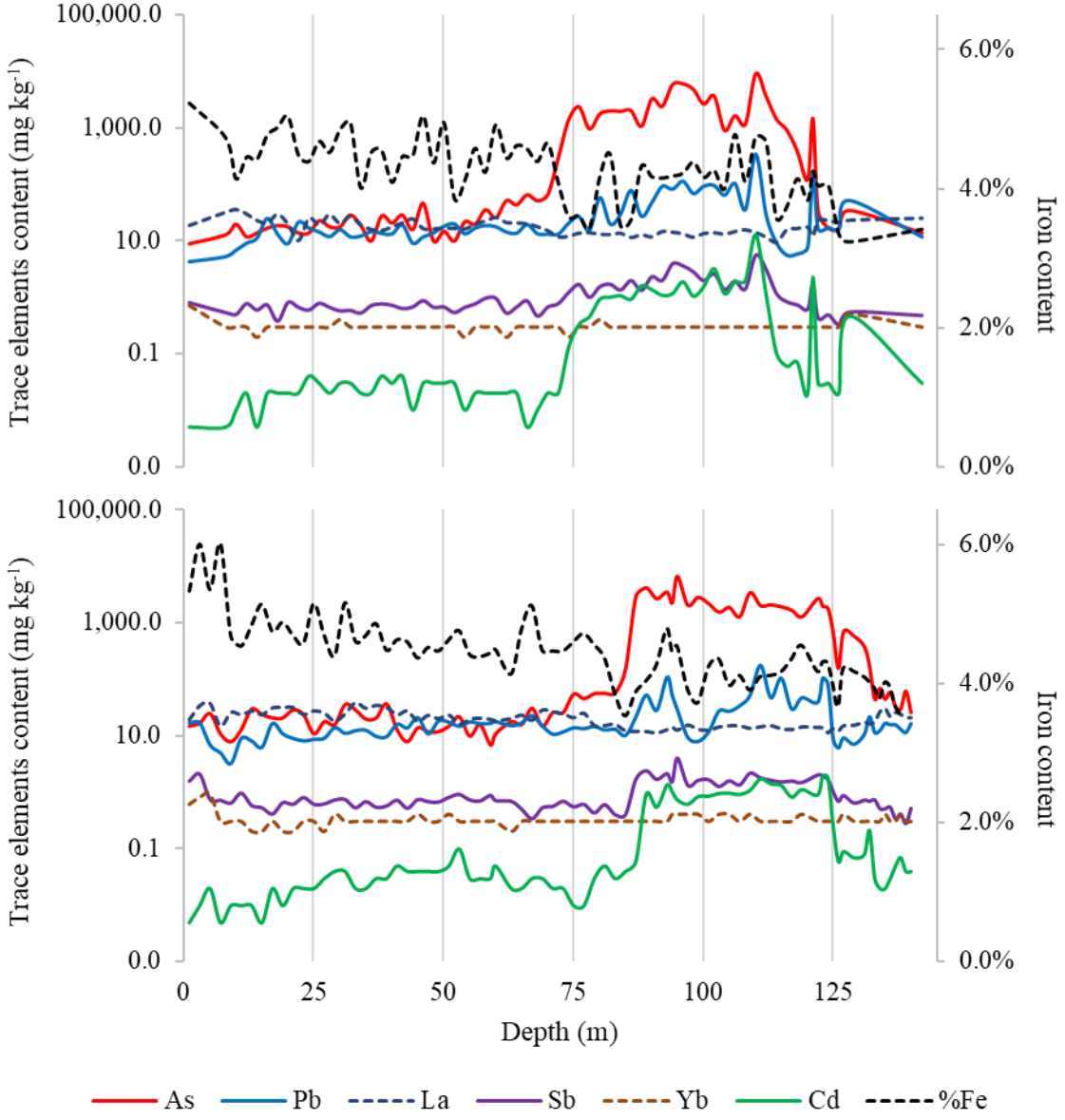

Figure 1 – Content of trace elements at two drill holes in Paracatu Formation. Notice the correlations with As, except for Fe, La and Yb (Retrieved from Mello et al. (unpublished)).

Mercury (Hg) was also a factor in this study because it is not always naturally present in orogenic gold deposits (e.g., in Paracatu Formation) but it is introduced in the environment by *garimpo* operations. The hypothesis is that Hg handling in watercourses can mobilize other toxic elements by competing for sorption sites in Fe-oxides. Mello et al. (unpublished) reported a Hg average content of around 6.0 mg kg^{-1} in the fine fraction (< 2 mm) of the sediments from a basin adjacent to the Morro do Ouro mine. Therefore, the soluble concentration of Hg in the

experiment was 0.01 mmol L^{-1} (Table 1), as $HgCl_2$, in order to achieve the Hg content in the precipitates close to that in the sediments. It is noteworthy that this concentration is twelve-times higher than the prevention value considered for soils in Minas Gerais State, suggesting that it is high enough to cause negative ecotoxicological effects (COPAM, 2011).

The contaminant solutions were prepared separately and added to 2.0 L polyethylene bottles in order to obtain the desired concentrations. Then, iron and aluminum solutions were added separately to the bottles and pH was adjusted to 8.0 with KOH 5.0 mol L^{-1} to promote Al-Fe-oxides precipitation. The volume of each experimental unit was completed to 0.800 L with ultra-pure water. Compressed air was pumped into the suspensions every day for one hour in order to promote homogenization and oxygenation.

2.2 Supernatants collection and analyses

Aliquots of supernatant solutions were periodically collected from the experimental units at 2 hours, 1 day, 21 and 90 days from the experimental units after the first pH adjustment. The supernatant aliquots were maintained under refrigeration and acidified with concentrated HNO_3 to prevent precipitation until analysis. The contents of Fe, Al and trace elements in the supernatant aliquots were analyzed by inductively coupled plasma optical emission spectrometry (ICP-OES).

The pH of the suspensions was also periodically measured at zero, 1, 4, 7, 14, 21, 35, 68 and 90 days. Immediately after each pH measurement, KOH 5 M was added to suspensions in order to keep the pH around 8.0. The total remaining supernatants were collected after 90 days by siphoning and properly discharged. Then, the precipitates were freeze-dried and prepared for mineralogical characterization.

2.3 Mineralogical characterization of precipitates

The freeze-dried precipitates were sieved at 106 μm (150#) and water-washed until the electrical conductivity of the supernatants was below 4 μS cm^{-1} in order to remove soluble salts that could impair oxides characterization. The crystalline phases in precipitates were then identified by X-ray diffraction (XRD) with Cu anode diffractometer with a wavelength of 1.54 Å at room temperature. Diffractograms were interpreted according to the International Centre for Diffraction Data (ICDD).

The percentage of Al isomorphic substitution in goethites was estimated according to Schulze (1984). The *c* dimension was calculated from the 110 and 111 diffraction lines and then the Al-substitution was estimated by the equations 1 and 2, as follow:

$$\boldsymbol{c} = \left[\left(\frac{\mathbf{1}}{\mathbf{d(111)}}\right)^{\mathbf{2}} - \left(\frac{\mathbf{1}}{\mathbf{d(110)}}\right)^{\mathbf{2}}\right]^{-\frac{\mathbf{1}}{\mathbf{2}}} \qquad \text{(Eq. 1)}$$

$$\%\,\mathbf{Al} = \mathbf{1730} - \mathbf{572}\boldsymbol{c} \qquad \text{(Eq. 2)}$$

2.4 Statistical analysis

The experiment was performed in a completely randomized design, with eight treatments, two control groups and three replicates, making up thirty experimental units (Table 1). The predictor/explanatory variables were: Fe:Al molar ratio, trace elements concentrations and mercury concentrations. Two levels for each variable were considered in a 2x2x2 factorial design. The control groups (in the absence of trace elements) were not enrolled in the statistical analysis, but only considered for XRD analysis comparisons.

The trace elements concentrations in supernatants were the response variable for evaluation of the Fe-Al-oxides capacity to sorb and immobilize them. The Jarque-Bera test was used to check normality, as the Bartlett and Levene tests were adopted to check homoscedasticity of the data. Whenever one of these conditions was violated, the data were transformed and checked again. Once the assumptions were confirmed, the data were then subject to ANOVA (F test) and contrasts by Holm-Bonferroni test were used to compare Fe:Al molar ratios and mercury significant effects at 5% of α error probability ($P = 0.05$).

3. RESULTS

3.1 Mineralogical characterization of precipitates

Goethite (α-FeOOH), lepidocrocite (γ-FeOOH), magnetite (Fe_3O_4), and maghemite (γ-Fe_2O_3) were the mineralogical phases identified by XRD in the precipitates (Figure 2). No discrete phase for aluminum or trace elements was identified.

Goethite was the main phase and it was detected in all treatments. The 500:0 Fe:Al molar ratio at high concentrations of trace elements favored precipitation of lepidocrocite. Magnetite and maghemite were identified in the 500:0 Fe:Al control treatment and at low concentrations of trace elements without Hg. It was not possible to distinguish magnetite and maghemite peaks because both have the same cubic structure and their lattice parameters are almost identical (Cornell and Schwertmann, 2003).

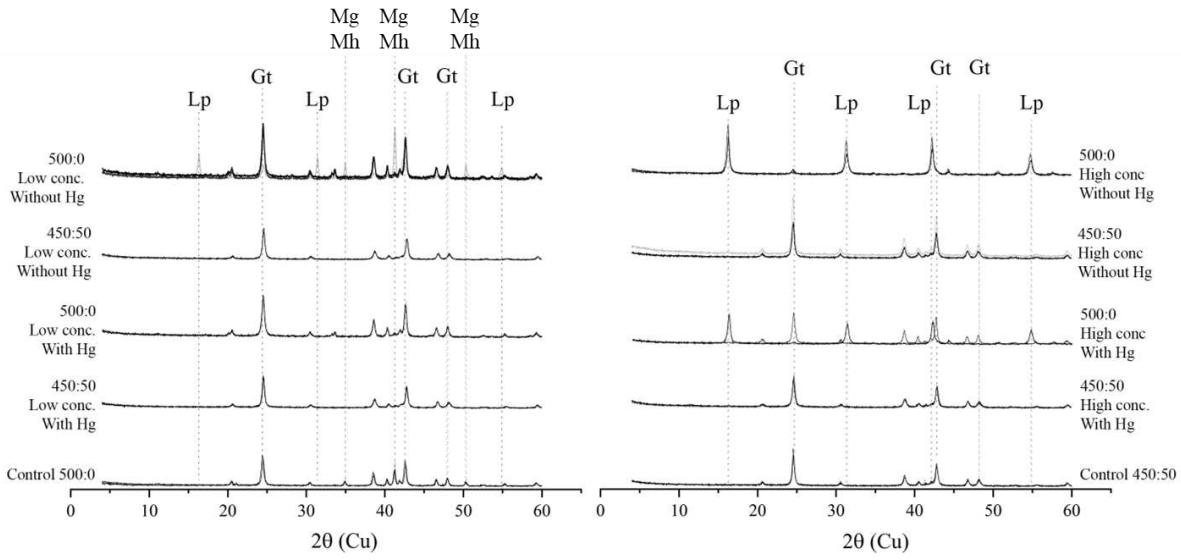

Figure 2 – X-ray diffractograms of the precipitates. Treatments: Fe:Al molar ratio (500:0 or 450:50), trace elements concentration (low or high), mercury (without or with), and controls (only Fe or only Fe and Al). Gt: goethite, Lp: lepidocrocite, Mg: magnetite, Mh: maghemite.

Treatments with aluminum (i.e., 450:50 Fe:Al molar ratio) presented only Al-goethites and no discrete Al-bearing phases (e.g., gibbsite or bayerite) were identified. The Al for Fe isomorphic substitution promoted shifts in the goethite X-ray diffraction lines to smaller d-

values. The percentage of Al-substitution in goethites ranged from 2.5 to 8.3% in the 450:50 treatments (Figure 3).

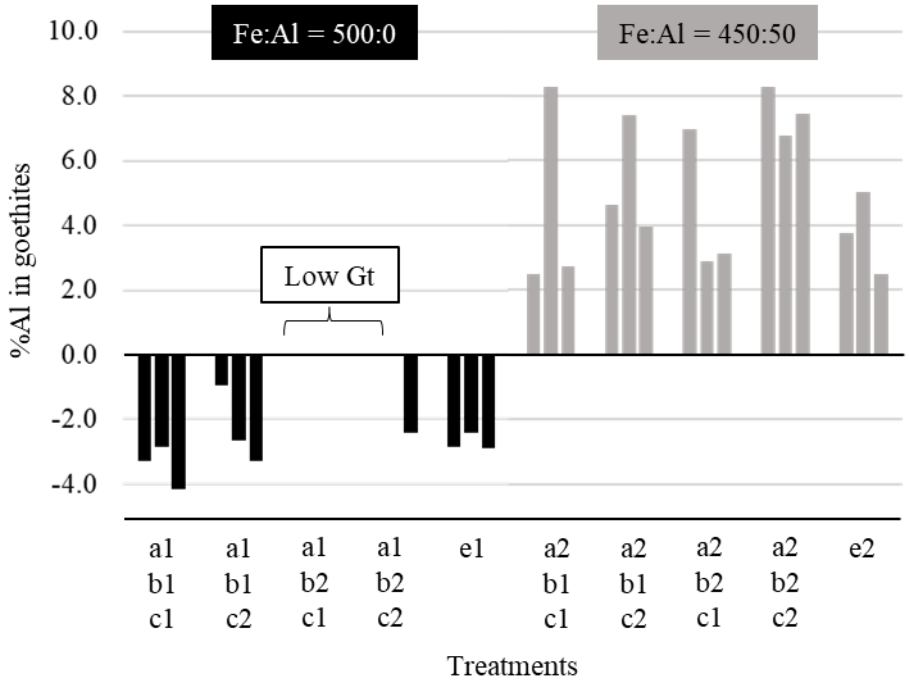

Figure 3 – Percentage of aluminum substitution in goethites calculated by Schulze (1984). a1) Fe:Al = 500:0 and a2) 450:50 molar ratio; b1) Low and b2) High trace elements concentration; c1) Without and c2) With Hg; e1) Control Fe:Al = 500:0 and e2) 450:50 molar ratio. The calculation was not possible for units with low goethite content (Low Gt) due to absence of (111) peak.

3.2 Measured pH

The pH values ranged from 1.8 to 2.4 previously to coprecipitation (time zero) (Figure 4). One day after the first KOH addition, pH reached the highest values, ranging from 6.5 and 7.7. Henceforth there was an overall decrease in pH values, ranging from 4.0 to 6.0 in spite of KOH addition. In general, treatments with 450:50 molar ratios, at high trace elements concentrations presented pH values significantly lower ($P < 0.05$) throughout the experimental period (Table S1).

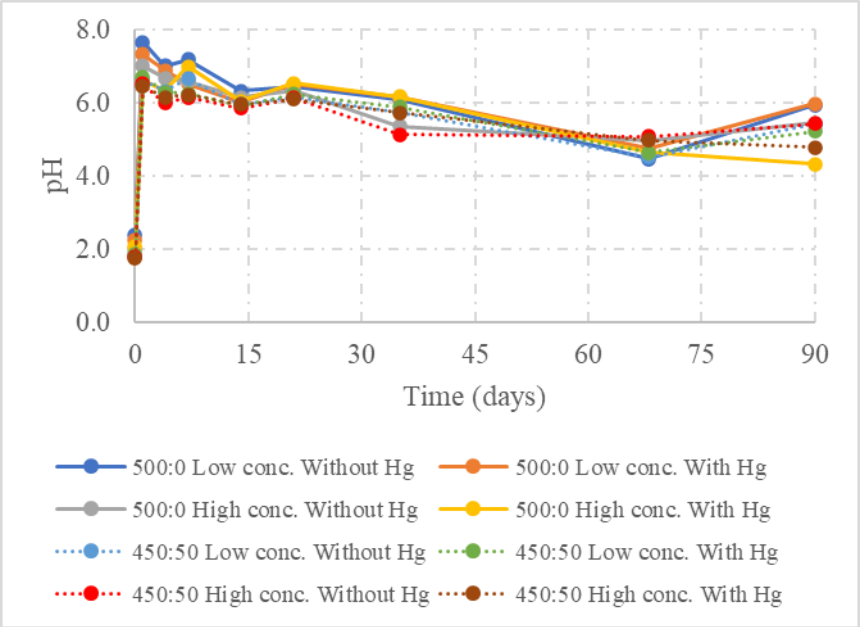

Figure 4 – pH values in supernatants during the coprecipitation experiment. Treatments: Fe:Al molar ratio (500:0 or 450:50), concentration of trace elements (low or high) and mercury (without or with).

3.3 Soluble iron and aluminum concentrations

More than 60% (> 15,000.0 mg L^{-1}) of all initial iron precipitated in two hours (2h) after the first KOH 5 M addition (Figure 5). However, iron concentration kept changing from 2h to one day (1d) even before a second KOH addition, indicating that the system was not in equilibrium in only two hours. Finally, more than 90% (> 23,000.0 mg L^{-1}) of the initial iron was precipitated in every treatment after ninety days.

Concentrations of soluble Al were below the detection limit (< 7.0 mg L^{-1}) in all treatments, meaning that more than 99% of the initial Al (> 1,350 mg L^{-1}) precipitated in only two hours after KOH addition and did not resolubilize. The shift in the X-ray diffraction lines and the estimates for percentage of Al-substitution (Figure 3) suggest that most of this aluminum replaced iron in the Fe-oxides structure.

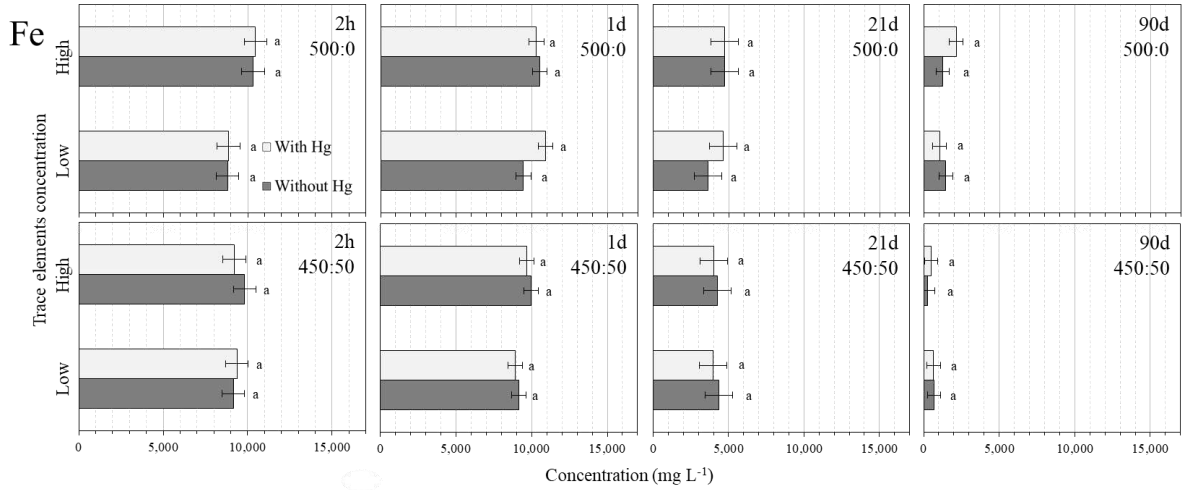

Figure 5 – Iron (Fe) supernatant concentrations (mg L^{-1}) at 2 hours (2h), 1 (1d), 21 (21d) and 90 days (90d) after KOH addition. Fe:Al molar ratio (500:0 or 450:50), concentration of trace elements (low or high) and mercury (without or with). Different lowercase letters and contrast effect (Ĉ*) indicate significant differences ($P \leq 0.05$) due to mercury and Fe:Al ratio, respectively.

3.4 Soluble arsenic and cadmium concentrations

The treatments were in general effective to remove As and Cd from water, but with important differences. The As removal was more effective than Cd removal from supernatants due to Fe and Al coprecipitation, especially in the short-term (Figure 6). More than 97% of the initial As was precipitated in all treatments in two hours (2h) after coprecipitation (> 360 and 720 mg L^{-1} at low and high concentrations of trace elements respectively). At the same time, only 51.5% (1.2 mg L^{-1}) of the initial Cd was immobilized in treatment 450:50 (Fe:Al ratio) at high concentrations of trace elements and with Hg. The highest Cd removal within two hours after coprecipitation was around 85% for treatments 500:0 at low concentrations of trace elements.

Similar to the results for Fe (Figure 5), the soluble As and Cd concentrations changed from two hours to one day after coprecipitation, confirming that the system had not reached equilibrium. The soluble As and Cd in general decreased from two hours to twenty-four hours after the Fe-Al-oxides coprecipitation. Henceforth, the soluble As and Cd decreased until twenty-one days (21d) when they reached the lowest values. From twenty-one to ninety days (90d) the concentrations of soluble As and Cd increased in treatments 500:0 (Fe:Al ratio) at high concentrations of trace elements, which can be ascribed to a decrease in pH (Figure 4).

Treatments with Al (450:50 Fe:Al molar ratio) were less effective than treatments without Al (500:0 Fe:Al) for As and Cd immobilization at two hours and one day after coprecipitation ($P < 0.05$). This was indicated by significant differences (Ĉ*) showing that soluble As and Cd

were lower in the absence of Al. Conversely, the Al effect was reversed at twenty-one and ninety days after coprecipitation, when treatments 450:50 presented significantly lower concentrations of soluble As and Cd, at high concentrations treatments. In ninety days, soluble As and Cd concentrations were below the detection limit (< 1.0 and 0.7 mg L^{-1}, respectively) in treatments 450:50, whilst in treatments 500:0 at high concentrations of trace elements there was more than 2.0 and 0.8 mg L^{-1} of soluble As and Cd, respectively. Mercury did not affect significantly the immobilization of As or Cd at any time.

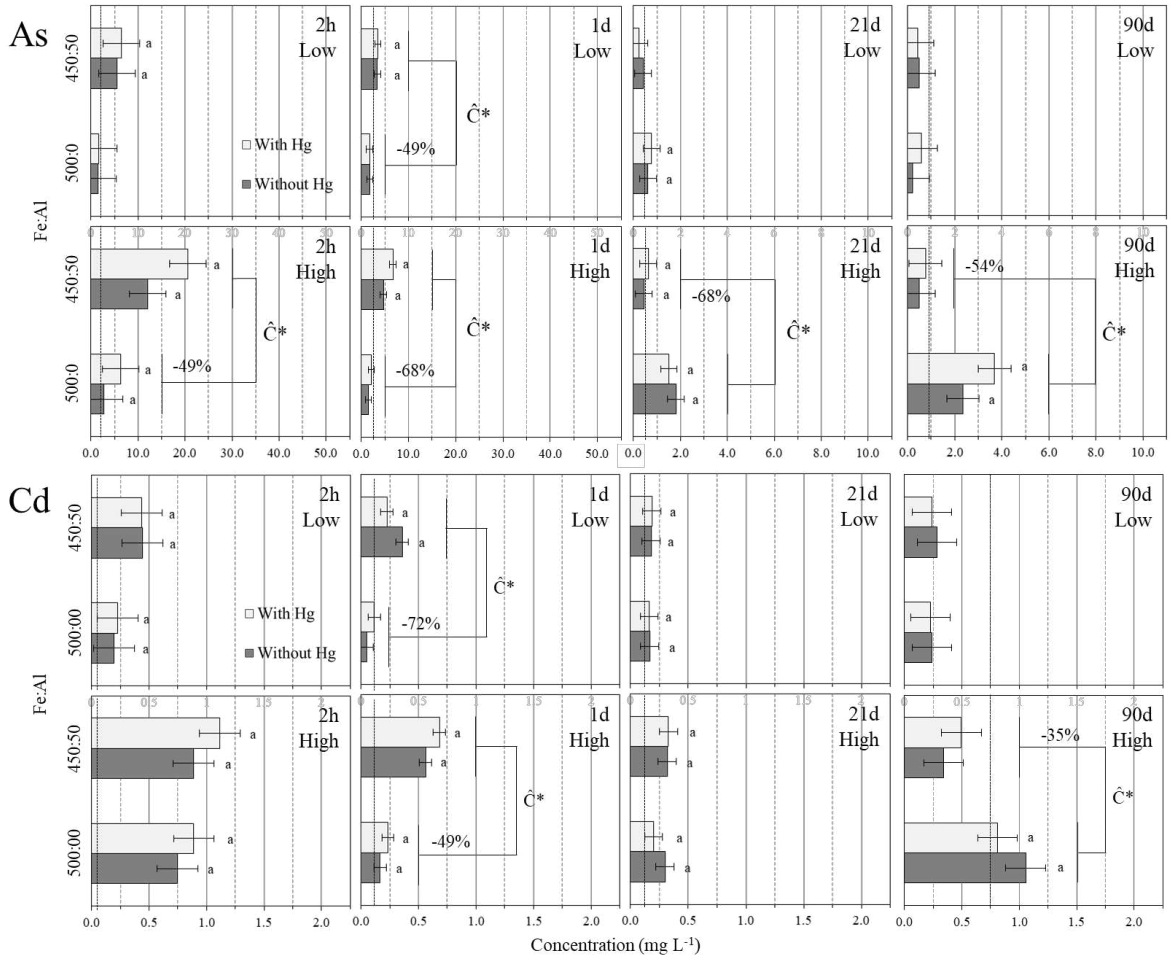

Figure 6 – Arsenic (As) and cadmium (Cd) supernatant concentrations (mg L^{-1}) at 2 hours (2h), 1 (1d), 21 (21d) and 90 days (90d) after KOH addition. Fe:Al molar ratio (500:0 or 450:50), concentration of trace elements (low or high) and mercury (without or with). Different lowercase letters and contrast effect (Ĉ*) indicate significant differences ($P \leq 0.05$) due to mercury and Fe:Al ratio respectively. The dashed line indicates the calculated detection limit.

3.5 Soluble lanthanum and ytterbium concentrations

Most of the initial lanthanum (La) was still in solution two hours (2h) after coprecipitation, whilst treatments were highly efficient for ytterbium removal in the short-term (Figure 7). Treatments 500:0 (Fe:Al molar ratio), at high concentrations of trace elements,

removed less than 10% (< 2.8 mg L^{-1}) of the initial La content in two hours, but at the same time removed more than 95% (> 3.5 mg L^{-1}) of the initial Yb content. The highest La and Yb removals within two hours were for treatments with aluminum (450:50 Fe:Al molar ratio).

The La and Yb ions did not reach equilibrium within two hours, but continued to be removed from solution by coprecipitation with Fe-oxides and their soluble contents were lower after one day (1d). Soluble La kept decreasing until 90 days, when its concentration was lower than the detection limit (< 0.3 mg L^{-1}) for all treatments (> 97% La removal efficiency). Soluble Yb, in turn, increased after the first day and its concentration was more than 0.2 mg L^{-1} in 90 days after coprecipitation in treatments with Al (450:50 Fe:Al molar ratio). At this time, the Yb removal efficiency was between 85 and 92%.

Contrary to As and Cd, the presence of Al contributed significantly ($P < 0.05$) for La and Yb immobilization at the beginning, but impaired it at the end of the experimental period. Within two hours and one day after coprecipitation, treatments with Al (450:50 Fe:Al molar ratio) presented less La and Yb in solution, as indicated by the contrast effects (Ĉ*). Moreover, in twenty-one and ninety days after coprecipitation, there was significantly less soluble La and Yb in treatments 500:0. Mercury did not affect significantly the immobilization of La and Yb at any time.

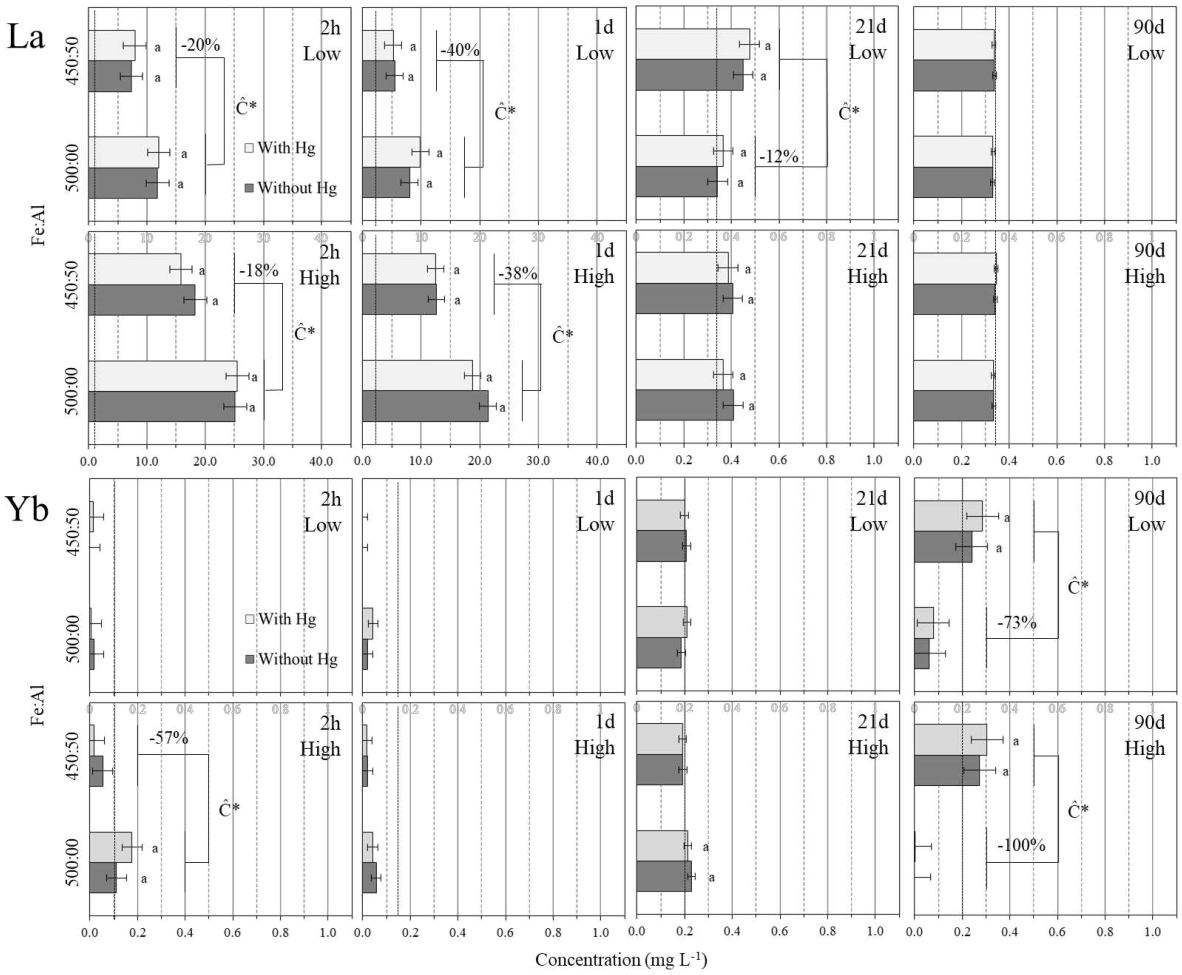

Figure 7 – Lanthanum (La) and ytterbium (Yb) supernatant concentrations (mg L^{-1}) at 2 hours (2h), 1 (1d), 21 (21d) and 90 days (90d) after KOH addition. Fe:Al molar ratio (500:0 or 450:50), concentration of trace elements (low or high) and mercury (without or with). Different lowercase letters and contrast effect (Ĉ*) indicate significant differences ($P \leq 0.05$) due to mercury and Fe:Al ratio respectively. The dashed line indicates the calculated detection limit.

3.6 Soluble lead, antimony and mercury concentrations

Soluble contents of lead, antimony, and mercury were below the ICP-OES detection limit in all samples. Therefore, at least 96% of the initial Pb content was removed within two hours after Fe oxides precipitation (Table 2). In 90 days, more than 99% of the initial Pb soluble content was removed from solution (> 20.7 and 41.4 mg L^{-1} at low and high concentrations of trace elements respectively) (DL = 0.2 mg L^{-1}).

The initial soluble concentrations of Sb and Hg were much lower than Pb (Table 1), hence the removal efficiencies, calculated from the respective ICP-OES detection limits, were also lower. Within two hours after coprecipitation, at least 72.1% and 86.1% of the initial Sb was immobilized at low and high concentrations of the trace elements, respectively. At the same time, at least 66.3% of initial Hg was immobilized despite the concentration of the trace

elements. The soluble Sb and Hg concentrations in 90 days after coprecipitation were below 0.5 and 0.9 mg L^{-1}, respectively.

Table 2 – Lead (Pb), antimony (Sb) and mercury (Hg) supernatants detection limits and minimum removal at 2 hours (2h), 1 (1d), 21 (21d) and 90 days (90d) after coprecipitation.

	Lead (Pb)				Antimony (Sb)				Mercury (Hg)			
Sample time	2h	1d	21d	90d	2h	1d	21d	90d	2h	1d	21d	90d
	mg L^{-1}											
DL[a]	0.9	1.5	0.2	0.2	0.3	0.8	0.5	0.5	0.7	0.7	0.5	0.9
	Minimum removal (%)[b]											
Low conc.[c]	95.7	93.0	98.9	99.2	72.1	38.5	61.5	60.7	66.3	65.4	77.1	56.1
High conc.[c]	97.9	96.5	99.4	99.6	86.1	69.3	80.7	80.3				

The ICP-OES signals were lower than the detection limits in all samples.

[a] Detection limit = (3*(Controls std. dev.)) + (Controls average)

[b] % Minimum removal = (DL) / (Initial soluble content)

[c] Treatments with low and high concentrations of trace elements.

4. DISCUSSION

4.1 Mineralogical phases in precipitates

Formation of iron oxides precipitates from solutions can be understood through reactions of oxidation and hydrolysis of soluble Fe^{2+} with oxygen and water. The reactions can lead to precipitation via green rust, formation of Fe(II) crystals or precipitation of Fe(III) oxides directly (Cornell and Schwertmann, 2003). Although the mineralogical analysis was carried out only at the end of the experiment, a greenish-blue color was observed in the precipitates at the beginning, probably due to this phase transformation.

This intermediate greenish-blue phase, known as green rust, was observed in every experimental unit due to reaction under weakly alkaline conditions (pH 7-8). This complex (formed by Fe(II)-Fe(III) phases) was decomposed through time following KOH additions, daily oxygenation and, consequently, decreasing soluble Fe^{2+} concentration. Furthermore, the suspensions colors changed to reddish-yellow or orange, faster for treatments with aluminum or at high concentrations of trace elements.

The final phases, identified by XRD 90 days after coprecipitation (Figure 2), were goethite (α-FeOOH), lepidocrocite (γ-FeOOH), magnetite (Fe_3O_4), and maghemite (γ-Fe_2O_3). No segregated phases of aluminum or trace elements were identified, probably due to isomorphic substitution in Fe-oxides and the low concentration of these elements relative to iron (≤ 10% mol mol^{-1}). The mineralogy of precipitates was affected by the Fe:Al molar ratio and the concentration of trace elements.

Goethite was the only mineral identified in treatments with aluminum (450:50 Fe:Al molar ratio) (Figure 2). It is well known that goethite precipitation is favored by the presence of Al in the medium, as previously observed by other authors in similar conditions (Barcelos et al., 2018; Mello et al., 2018; Pietralonga et al., 2017; Vasques et al., 2018a, 2018b). Al-hydroxy cations promote hydrolysis of Fe^{2+} and favor precipitation of Al-goethite over lepidocrocite (Taylor, 1988). Furthermore, goethite was identified in every experimental unit but not as the major phase in treatments without aluminum (500:0 Fe:Al) at high concentrations of trace elements.

The preferential formation of lepidocrocite at high concentrations of trace elements in the absence of Al (Figure 2) is also in line with previous researches. It was already known that lepidocrocite is favored through synthesis from Fe(II) salts at high concentrations of other compounds (Barcelos et al., 2018; Pietralonga et al., 2017; Vasques et al., 2018a). Lepidocrocite

is more soluble than goethite and magnetite (Lindsay, 1979) and it is also frequently associated with goethite in reducing environments (Schwertmann and Taylor, 1989). Therefore, it can be assumed that high concentrations of trace elements increased Fe-oxides solubility, since lepidocrocite was favored over goethite in these treatments.

Magnetite and maghemite were identified only in the control treatment 500:0 (Fe:Al) and in one replicate from treatment 500:0 at low concentration of trace elements and without Hg. These suspensions evolved from greenish-blue to darker hues, probably due to magnetite formation, although the solubility product of magnetite was not exceeded (pH ≤ 8.0). Tamaura et al. (1983) suggested that Fe^{2+} ions can interact with Fe(III)-oxides (e.g., goethite and lepidocrocite) to form magnetite. Magnetite is a mixed Fe(II)-Fe(III) ferrimagnetic oxide more resistant to dissolution, so its formation is considered important for trace elements sorption and water treatment. Our results suggest that magnetite and maghemite precipitation is limited to solutions with low contents of Al and trace elements.

4.2 Aluminum isomorphic substitution

As postulated, Al isomorphic substitution in Fe-oxides influenced the mineralogical phases in precipitates and the removal of trace elements from water. The Al^{3+} is smaller than Fe^{3+}, so the Al isomorphic substitution in goethite led to a decrease of the unit-cell dimension confirmed by a shift of XRD lines in relation to Al-free goethites (Schulze, 1984). It is worth to note that goethites from treatments 500:0 (Fe:Al molar ratio) presented negative %Al substitution (Figure 3) probably due to differences in equipment calibration. Therefore, %Al substitution in goethites from treatments 450:50 (Fe:Al molar ratio) might be underestimated.

The absence of segregated Al-phases (e.g., gibbsite or bayerite) in precipitates corroborates that most of Al was incorporated into the Fe-oxide structure. Indeed, goethite (α-FeOOH) was the only mineral detected in the presence of Al (450:50 Fe:Al molar ratio) (Figure 2). Schwertmann and Cornell (2000) suggested that oxidative hydrolysis of Fe^{2+} ions in neutral pH leads to goethite formation that can incorporate up to 0.33 mmol $mmol^{-1}$ of structural Al. This high capacity to incorporate Al in relation to other Fe-oxides is considered to favor goethite formation at low Fe:Al molar ratio (Schwertmann, 1990). Other researchers, under similar experimental conditions, also observed that Al favored Al-goethite precipitation (Mello et al., 2018; Pietralonga et al., 2017; Vasques et al., 2018a) .

The Al-for-Fe isomorphic substitution induces structural defects compensated by Fe-OH and Al-OH groups (Souza et al., 2021) and favors oriented aggregation crystal growth (Freitas

et al., 2016, 2015). These aspects directly affect physicochemical properties of the Fe-oxides, such as secondary mineralization and ion retention capacity (Antônio et al., 2021; Ciminelli et al., 2018). Indeed, immobilization of trace elements by Al-goethites was different in relation to the others Al-free oxides.

The effect of Al on trace elements removal was reversed with time. Arsenic and cadmium (Figure 6) removal was impaired in the presence of Al at the beginning of the experiment (two hours and one day). Conversely, Al favored their removal in the long-term (twenty-one and ninety days after coprecipitation). Vasques et al. (2018a) also observed this reverse effect of Al on As removal by Al-substituted Fe-oxides. On the other hand, treatments with Al favored La and Yb removal at the beginning of the experiment and impaired it at the end (Figure 7). These results indicate that rare earth elements behave differently from other trace elements in terms of interaction with Al-Fe-oxide.

Reports of different and even controversial effects on adsorption of trace elements are not new in literature. Adra et al. (2016), for instance, reported that Al favored immobilization of As(V) in Al-ferrihydrites but impaired sorption of As(III). Souza et al. (2021) ascribed the increase on As(V) uptake by Al-ferrihydrites to increased Metal-OH sites due to Al isomorphic substitution. Furthermore, Al delays the crystallization of Fe-oxides and As(V) is mainly associated with short-range ordered Fe-oxides, as suggested by Violante et al. (2009). Therefore, oxidation of As(III) to As(V) and the poorer crystallization of Al-goethites might explain the reverse effects of Al on As adsorption.

Structural Al also impaired Cd immobilization by Fe-oxides at the beginning but favored it at the end of the experimental period. Randall et al. (1999) suggested that Cd adsorbs to goethite preferentially at (110) crystallographic sharing sites, whilst it adsorbs to lepidocrocite at (100) edge sharing sites. Since Al-for-Fe substitution decreases the d(110) in goethite, it seems fair to assume that Al favored Cd immobilization due to higher amounts of corner sharing sites in the long-term.

Rare earth elements (REE) immobilization can also be impaired or favored by structural Al in Fe-oxides. Pietralonga et al. (2017) suggested that Al can compete with La for adsorption sites on Al-goethites synthesized at lower Fe:Al molar ratio (500:125 and 500:250). On the other hand, Barcelos et al. (2018) reported a higher immobilization of Eu and Ho in treatments with Al (Fe:Al molar ratio = 450:50 and 400:100) than in treatments without Al (500:0) at four days after Fe-oxides coprecipitation.

Although REE are considered to present high chemical affinity for Fe-oxides (Ingri et al., 2000; Koeppenkastrop et al., 1991), the strength and sign of the oxide charge controls surface precipitation of REE on goethite (Fendorf and Fendorf, 1996). Structural Al increases Fe-oxides isoelectric point (Souza et al., 2021) and reduces electrostatic attraction between Al-goethite and REE cations, which could explain the lower removal efficiency of La and Yb in the long-term for treatments with Al. Nevertheless, in the short-term, the high chemical affinity for the surface of Al-goethites overcame the electrostatic repulsion and treatments with Al significantly favored La and Yb immobilization.

It is still not clear why Al-for-Fe isomorphic substitution has a reverse effect in ions sorption, but we can suggest that it is related to the Fe-oxide formation and crystal growth. Changes in the suspensions' colors through time were ascribed to phases transformations of green-rust to lepidocrocite or goethite. It is noteworthy that aspects related to mineralogical phases transformations, such as dissolution and reprecipitation, can drastically change the interactions between solid and solutes. Therefore, these phases transformations can explain differences between short-term and long-term sorption of some trace elements by Al-Fe-oxides.

4.3 Trace elements immobilization

The results support the hypothesis that trace elements correlated at the orogenic gold deposits do not present the same correlation after exposition to atmosphere and remobilization under environmental conditions. Coprecipitation of Fe-oxides presented faster removal of As (Figure 6), Pb (Table 2), Yb (Figure 7) and Sb (Table 2) from water, while for Cd (Figure 6) and La (Figure 7) the removal efficiency was slower. Then, it can be postulated that the geogenic elements are immobilized at different rates and quantities after rock weathering.

All treatments presented high efficiency to remove As from water, which corroborate its high affinity for Fe-oxides (Antônio et al., 2021; Ciminelli et al., 2018; Freitas et al., 2016, 2015). The results also corroborate the high immobilization of As by Fe-oxides in the short-term (two hours and one day), as demonstrated by other authors (Mello et al., 2018; Vasques et al., 2018a, 2018b). Notwithstanding, in 90 days at lower pH, soluble As increased to 2.4 mg L^{-1} in treatments 500:0 (Fe:Al molar ratio) at high concentration of trace elements. This suggest that As sorbed onto lepidocrocite was partially released at lower pH due to competition with other trace elements for adsorption sites.

All treatments presented a high efficiency for Pb removal from water (> 95% in two hours), which is in line with previous findings (Lu et al., 2011; Rahimi et al., 2015). Sposito

(2008) stated that Pb^{2+} is adsorbed by Fe-oxides at pH below the point of zero charge, indicating a specific inner-sphere adsorption mechanism. Rahimi et al. (2015) showed that lepidocrocite and goethite are efficient adsorbents for Pb removal from water. Antimony removal was also rapid and efficient, which is in line with other researchers (Bai et al., 2022; Guo et al., 2014).

On the other hand, the removal efficiency by coprecipitation with Fe-oxides was lower for Cd. This is also in line with other researchers, as Cd presents lower affinity to sorb onto Fe-oxides compared to As, Sb or Pb (Schwertmann and Taylor, 1989). Cadmium is not expected to precipitate below pH 10 (Lindsay, 1979) and neither adsorb onto Fe-oxides at pH lower than 8 (Sposito, 2008). Also, Cd contents in sediments from Paracatu were lower than Cd content in Paracatu Formation (Mello et al. unpublished), indicating Cd high solubility and loss by leaching. Thereupon, Cd removal is considered more challenging than the other trace elements, since it takes longer time to be retained and has severe health effects (ATSDR, 2012).

The removal efficiency of La by coprecipitation with Fe-oxides was low at the beginning of the experiment probably due to competition with other trace elements. Similar to Cd, lanthanum contents in sediments were also lower than in the Paracatu Formation (Mello et al., unpublished). By the end of the experiment, La removal was considered high (> 97%), which is in agreement with other researchers (Fendorf and Fendorf, 1996; Pietralonga et al., 2017). A higher and faster La removal was obtained by Pietralonga et al. (2017) through coprecipitation with Al-Fe-oxides at lower (Fe + Al):La molar ratios (up to 625:125) and higher pH (11.7).

Ytterbium removal was high (> 95%) within two hours after the first KOH addition. It was already suggested that heavy rare earth elements have greater affinity for Fe-oxides than light rare earth elements (Koeppenkastrop et al., 1991; Liu et al., 2018). Nonetheless, soluble contents of Yb were above 0.2 mg L^{-1} in treatments with Al (450:50 Fe:Al) by the end of the experiment, coincident with lower pH period (Figure 4). These results suggest weaker bonds between Yb and Al-goethites, specially at slightly acidic pH.

Mercury was not detected in supernatants at any time, leading to a removal efficiency of at least 56% ninety days after coprecipitation. This relatively low removal efficiency is due to the high ICP-OES detection limit and, therefore, no further discussion on this subject is worthwhile. Anyway, the hypothesis that Hg impairs the mobility of other trace elements was not confirmed because it did not hinder the sorption of any element at any time. Actually, it is very unlikely that Hg at the concentrations found in watersheds around Paracatu Formation could interfere with the mobilization of other trace elements. It is noteworthy that concentrations of Hg used in the experiment were much lower compared to As, Pb and La

(Table 1), which makes it difficult to interfere with the mobilization of these elements. On the other hand, the concentrations of Hg were equivalent to those of Yb, Sb and Cd at low concentrations of trace elements and, therefore, a greater affinity of these elements for Fe-oxides in relation to Hg can be considered.

Finally, more than 99% of the initial trace elements total content was removed from solution after 90 days. Even though, the supernatant solutions would not be proper for discharge in natural water bodies according to Brazilian guidelines (CONAMA, 2011). Treatments 500:0 at high trace elements concentrations presented soluble As and Cd (3.0 and 1.0 mg L^{-1} respectively) above the maximum concentrations for safe effluent discharge (0.5 and 0.2 mg L^{-1} respectively). On the other hand, Pb soluble concentrations were lower than the maximum allowed value for safe discharge (< 0.5 mg L^{-1}). The soluble Fe in all treatments after ninety days (from 300 to 2,150 mg L^{-1}), was also above the maximum value allowed for effluent discharge (15.0 mg L^{-1}). This indicates that more Fe-oxides and trace elements could be coprecipitated with more KOH addition, perhaps attaining the water quality guideline values, since there were still high contents of soluble Fe at the end of the experiment.

5. CONCLUSIONS

Trace elements correlated in orogenic gold deposits do not present the same correlation during coprecipitation with iron oxides under environmental conditions. Even though, coprecipitation is highly effective for decreasing trace elements soluble concentration, depending on trace elements initial content and Al isomorphic substitution. The effect of structural Al on trace elements immobilization might be related to Al-Fe-oxides transformations and crystal growth. Future researches can identify which Al-Fe-oxides phases are formed during the coprecipitation period and relate these phases to ions sorption capacity. Artisanal mining (*garimpo*) operations might remobilize other trace elements through sediments griding and introduction of Hg in watercourses, although it was not possible to confirm it in this study. Therefore, further researches should evaluate if Hg can compete with other trace elements for sorption sites on iron oxides during coprecipitation.

6. REFERENCES

Adra, A., Morin, G., Ona-Nguema, G., Brest, J., 2016. Arsenate and arsenite adsorption onto Al-containing ferrihydrites. Implications for arsenic immobilization after neutralization of acid mine drainage. Applied Geochemistry 64, 2–9. https://doi.org/10.1016/j.apgeochem.2015.09.015

Antônio, D.C., Caldeira, C.L., Freitas, E.T.F., Delbem, I.D., Gasparon, M., Olusegun, S.J., Ciminelli, V.S.T., 2021. Effects of aluminum and soil mineralogy on arsenic bioaccessibility. Environmental Pollution 274. https://doi.org/10.1016/j.envpol.2021.116482

ATSDR, 2012. Toxicological Profile for Cadmium. United States Environmental Protection Agency (USEPA), Atlanta, Georgia.

Bai, Y., Tang, X., Sun, L., Yin, W., Hu, G., Liu, M., Gong, Y., 2022. Application of iron-based materials for removal of antimony and arsenic from water: Sorption properties and mechanism insights. Chemical Engineering Journal 431, 134143. https://doi.org/10.1016/j.cej.2021.134143

Barcelos, G.S., Veloso, R.W., de Mello, J.W. V., Gasparon, M., 2018. Immobilization of Eu and Ho from synthetic acid mine drainage by precipitation with Fe and Al (hydr)oxides. Environmental Science and Pollution Research 25, 18813–18822. https://doi.org/10.1007/s11356-018-2100-5

Chen, P.-Y., 1977. Table of Key Lines in X-ray Powder Diffraction Patterns of Minerals in Clays and Associated Rock. Department of Natural Resources, Bloomington, Indiana.

Ciminelli, V.S.T., Antônio, D.C., Caldeira, C.L., Freitas, E.T.F., Delbem, I.D., Fernandes, M.M., Gasparon, M., Ng, J.C., 2018. Low arsenic bioaccessibility by fixation in nanostructured iron (Hydr)oxides: Quantitative identification of As-bearing phases. J Hazard Mater 353, 261–270. https://doi.org/10.1016/j.jhazmat.2018.03.037

CONAMA, 2011. Resolução 430/2011 (in Portuguese). Brasília, Brazil.

COPAM, 2011. Deliberação Normativa 166/2011 (in Portuguese). Belo Horizonte, Brazil.

Cornell, R.M., Schwertmann, U., 2003. The Iron Oxides. Wiley. https://doi.org/10.1002/3527602097

Fendorf, S., Fendorf, M., 1996. Sorption Mechanisms of Lanthanum on Oxide Minerals. Clays Clay Miner 44, 220–227. https://doi.org/10.1346/CCMN.1996.0440207

Ford, R.G., 2012. Chemisorption and Precipitation Reactions, in: Huang, P.M., Li, Y., Sumner, M.E. (Eds.), Handbook of Soil Sciences: Properties and Processes. CRC Press.

Freitas, E.T.F., Montoro, L.A., Gasparon, M., Ciminelli, V.S.T., 2015. Natural attenuation of arsenic in the environment by immobilization in nanostructured hematite. Chemosphere 138, 340–347. https://doi.org/10.1016/j.chemosphere.2015.05.101

Freitas, E.T.F., Stroppa, D.G., Montoro, L.A., de Mello, J.W.V., Gasparon, M., Ciminelli, V.S.T., 2016. Arsenic entrapment by nanocrystals of Al-magnetite: The role of Al in

crystal growth and As retention. Chemosphere 158, 91–99. https://doi.org/10.1016/j.chemosphere.2016.05.044

Gil-Díaz, M., Rodríguez-Alonso, J., Maffiotte, C.A., Baragaño, D., Millán, R., Lobo, M.C., 2021. Iron nanoparticles are efficient at removing mercury from polluted waters. J Clean Prod 315, 128272. https://doi.org/10.1016/j.jclepro.2021.128272

Goldfarb, R.J., Groves, D.I., Gardoll, S., 2001. Orogenic gold and geologic time: a global synthesis. Ore Geol Rev 18, 1–75. https://doi.org/10.1016/S0169-1368(01)00016-6

Groves, D.I., Goldfarb, R.J., Gebre-Mariam, M., Hagemann, S.G., Robert, F., 1998. Orogenic gold deposits: A proposed classification in the context of their crustal distribution and relationship to other gold deposit types. Ore Geol Rev 13, 7–27. https://doi.org/10.1016/S0169-1368(97)00012-7

Guo, X., Wu, Z., He, M., Meng, X., Jin, X., Qiu, N., Zhang, J., 2014. Adsorption of antimony onto iron oxyhydroxides: Adsorption behavior and surface structure. J Hazard Mater 276, 339–345. https://doi.org/10.1016/j.jhazmat.2014.05.025

Ingri, J., Widerlund, A., Land, M., Gustafsson, Ö., Andersson, P., Öhlander, B., 2000. Temporal variations in the fractionation of the rare earth elements in a boreal river; the role of colloidal particles. Chem Geol 166, 23–45. https://doi.org/10.1016/S0009-2541(99)00178-3

John Ridley, 2013. Ore Deposit Geology. Cambridge University Press.

Koeppenkastrop, D., Decarlo, E.H., Roth, M., 1991. A method to investigate the interaction of rare earth elements in aqueous solution with metal oxides. Journal of Radioanalytical and Nuclear Chemistry Articles 152, 337–346. https://doi.org/10.1007/BF02104687

Ladeira, A.C.Q., Ciminelli, V.S.T., 2004. Adsorption and desorption of arsenic on an oxisol and its constituents. Water Res 38, 2087–2094. https://doi.org/10.1016/j.watres.2004.02.002

Lindsay, W.L., 1979. Chemical Equilibria in Soils. John Wiley & Sons.

Liu, H., Pourret, O., Guo, H., Martinez, R.E., Zouhri, L., 2018. Impact of Hydrous Manganese and Ferric Oxides on the Behavior of Aqueous Rare Earth Elements (REE): Evidence from a Modeling Approach and Implication for the Sink of REE. Int J Environ Res Public Health 15, 2837. https://doi.org/10.3390/ijerph15122837

Lu, P., Nuhfer, N.T., Kelly, S., Li, Q., Konishi, H., Elswick, E., Zhu, C., 2011. Lead coprecipitation with iron oxyhydroxide nano-particles. Geochim Cosmochim Acta 75, 4547–4561. https://doi.org/10.1016/j.gca.2011.05.035

Mello, J.W.V. de, Dias, L.E., Daniel, A.M., Abrahão, W.A.P., Deschamps, E., Schaefer, C.E.G.R., 2006. Preliminary evaluation of acid mine drainage in Minas Gerais State, Brazil. Rev Bras Cienc Solo 30, 365–375. https://doi.org/10.1590/S0100-06832006000200016

Mello, J.W.V., Gasparon, M., Silva, J., 2018. Effectiveness of arsenic co-precipitation with Fe-Al hydroxides for treatment of contaminated water. Rev Bras Cienc Solo 42. https://doi.org/10.1590/18069657rbcs20170261

Mello, J.W. V., Nepomuceno, A.L., Matos, A.A.S., Guimarães, P.J., Mendonça, G. V., Silva, S.C., unpublished. Antimony, mercury and other elements as tracers for geogenic origin and impacts of artisanal mining on arsenic distribution in sediments from an orogenic gold mineralization area (unsubmitted).

Oliver, N.H.S., Thomson, B., Freitas-Silva, F.H., Holcombe, R.J., Rusk, B., Almeida, B.S., Faure, K., Davidson, G.R., Esper, E.L., Guimarães, P.J., Dardenne, M.A., 2015. Local and Regional Mass Transfer During Thrusting, Veining, and Boudinage in the Genesis of the Giant Shale-Hosted Paracatu Gold Deposit, Minas Gerais, Brazil. Economic Geology 110, 1803–1834. https://doi.org/10.2113/econgeo.110.7.1803

Pietralonga, A.G., de Mendonça, B.A.F., Barcelos, G.S., de Mello, J.W.V., Abrahão, W.A.P., 2017. Lanthanum immobilization by iron and aluminum colloids. Environ Earth Sci 76, 266. https://doi.org/10.1007/s12665-017-6583-z

Rahimi, S., Moattari, R.M., Rajabi, L., Derakhshan, A.A., Keyhani, M., 2015. Iron oxide/hydroxide (α,γ-FeOOH) nanoparticles as high potential adsorbents for lead removal from polluted aquatic media. Journal of Industrial and Engineering Chemistry 23, 33–43. https://doi.org/10.1016/j.jiec.2014.07.039

Randall, S.R., Sherman, D.M., Ragnarsdottir, K.V., Collins, C.R., 1999. The mechanism of cadmium surface complexation on iron oxyhydroxide minerals. Geochim Cosmochim Acta 63, 2971–2987. https://doi.org/10.1016/S0016-7037(99)00263-X

Rezende, P.S., Silva, N.C., Moura, W.D., Windmöller, C.C., 2018. Quantification and speciation of mercury in streams and rivers sediment samples from Paracatu, MG, Brazil, using a direct mercury analyzer®. Microchemical Journal 140, 199–206. https://doi.org/10.1016/j.microc.2018.04.006

Schulze, D.G., 1984. The Influence of Aluminum on Iron Oxides. VIII. Unit-Cell Dimensions of Al-Substituted Goethites and Estimation of Al From Them. Clays Clay Miner 32, 36–44. https://doi.org/10.1346/CCMN.1984.0320105

Schwertmann, U., Carlson, L., 1994. Aluminum Influence on Iron Oxides: XVII. Unit-Cell Parameters and Aluminum Substitution of Natural Goethites. Soil Science Society of America Journal 58, 256–261. https://doi.org/10.2136/sssaj1994.03615995005800010039x

Schwertmann, U., Cornell, R.M., 2000. Iron Oxides in the Laboratary. Wiley-VCH Verlag GmbH, Weinheim, Germany. https://doi.org/10.1002/9783527613229

Schwertmann, U., Murad, E., 1990. The Influence of Aluminum on Iron Oxides: XIV. Al-Substituted Magnetite Synthesized at Ambient Temperatures. Clays Clay Miner 38, 196–202. https://doi.org/10.1346/CCMN.1990.0380211

Schwertmann, U., Taylor, R.M., 1989. Iron Oxides. pp. 379–438. https://doi.org/10.2136/sssabookser1.2ed.c8

Silva, J., Mello, J.W.V., Gasparon, M., Abrahão, W.A.P., Ciminelli, V.S.T., Jong, T., 2010. The role of Al-Goethites on arsenate mobility. Water Res 44, 5684–5692. https://doi.org/10.1016/j.watres.2010.06.056

Simate, G.S., Ndlovu, S., 2014. Acid mine drainage: Challenges and opportunities. J Environ Chem Eng 2, 1785–1803. https://doi.org/10.1016/j.jece.2014.07.021

Souza, T.G.F., Freitas, E.T.F., Mohallem, N.D.S., Ciminelli, V.S.T., 2021. Defects induced by Al substitution enhance As(V) adsorption on ferrihydrites. J Hazard Mater 420, 126544. https://doi.org/10.1016/j.jhazmat.2021.126544

Sposito, G., 2008. The Chemistry of Soils, Second edition. ed. Oxford University Press, New York.

Tamaura, Y., Ito, K., Katsura, T., 1983. Transformation of γ-FeO(OH) to Fe3O4 by adsorption of iron(II) ion on γ-FeO(OH). J. Chem. Soc., Dalton Trans. 189–194. https://doi.org/10.1039/DT9830000189

Taylor, R.M., 1988. Proposed mechanism for the formation of soluble Si-Al and Fe (III)-Al hydroxy complexes in soils. Geoderma 42, 65–77. https://doi.org/10.1016/0016-7061(88)90023-7

UNEP, 2018. Global Mercury Assessment. Geneva, Switzerland.

Vasques, I.C.F., de Mello, J.W. V., Veloso, R.W., Ferreira, V. de P., Abrahão, W.A.P., 2018a. Arsenite removal from contaminated water by precipitation of aluminum, ferrous and ferric (hydr)oxides. Environmental Science and Pollution Research 25, 12967–12980. https://doi.org/10.1007/s11356-018-1458-8

Vasques, I.C.F., de Mello, J.W. V., Veloso, R.W., Ferreira, V. de P., Abrahão, W.A.P., 2018b. Effectiveness of Ferric, Ferrous, and Aluminum (Hydr)Oxide Coprecipitation to Treat Water Contaminated with Arsenate. J Environ Qual 47, 1339–1346. https://doi.org/10.2134/jeq2018.01.0014

Veloso, R.W., Mello, J.W.V. de, Abrahão, W.A.P., Glasauer, S., 2019. Seasonal impacts on arsenic mobility and geochemistry in streams surrounding a gold mineralization area, Paracatu, Brazil. Applied Geochemistry 109, 104390. https://doi.org/10.1016/j.apgeochem.2019.104390

Violante, A., Pigna, M., Del Gaudio, S., Cozzolino, V., Banerjee, D., 2009. Coprecipitation of Arsenate with Metal Oxides. 3. Nature, Mineralogy, and Reactivity of Iron(III)−Aluminum Precipitates. Environ Sci Technol 43, 1515–1521. https://doi.org/10.1021/es802229r

BIOACCESSIBILITY AND AVAILABILITY OF TRACE ELEMENTS COPRECIPITATED WITH ALUMINUM-SUBSTITUTED IRON OXIDES

Graphical abstract

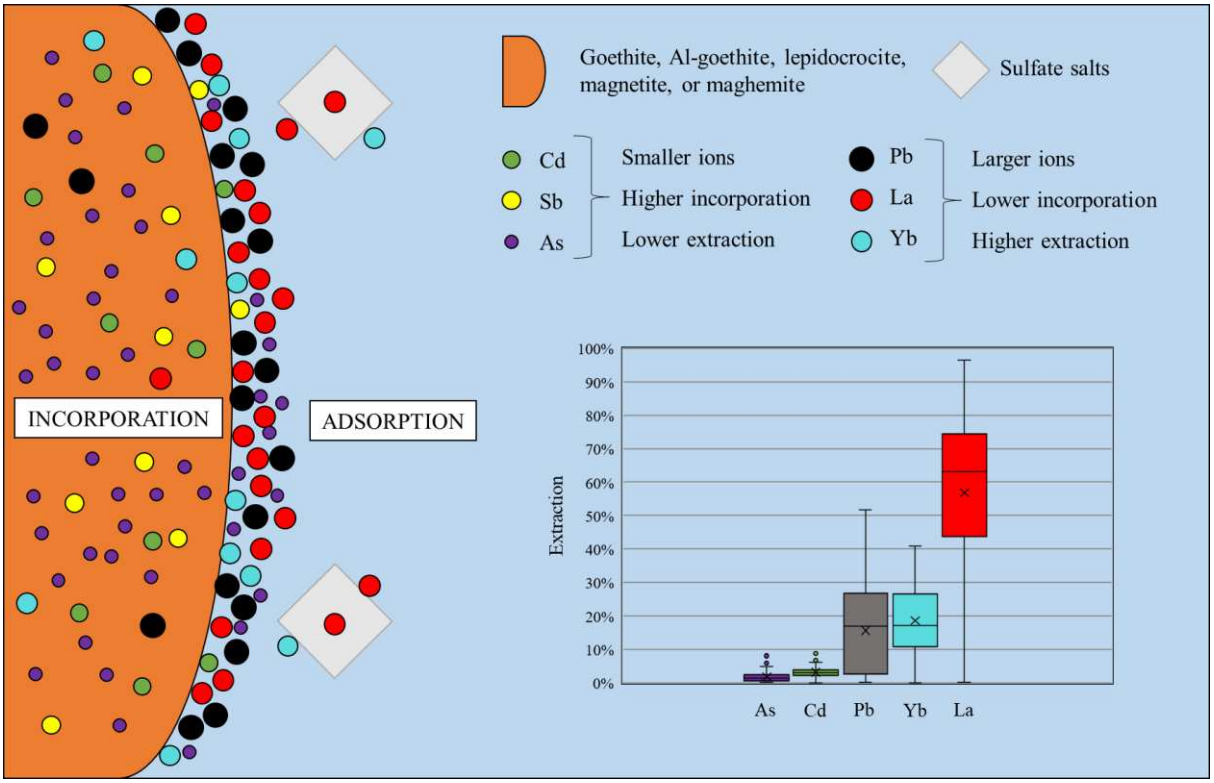

Highlights

- As, Cd and Sb were more stable than La, Yb or Pb in coprecipitated iron oxides;
- The higher stability of trace elements might be related to higher incorporation into iron oxides structure;
- As and Cd coprecipitated with Al-goethites were more stable than with lepidocrocite or Al-free-goethite;
- La and Yb coprecipitated with Al-free-goethite or lepidocrocite were more stable than with Al-goethites.

ABSTRACT

Iron oxides, hydroxides and oxyhydroxides (or simply ‘iron oxides’) nanoparticles are one of the main reservoirs for trace elements in soils and sediments. Trace elements can coprecipitate with iron oxides through the formation of surface complexes or incorporation to the solid phase structure. Iron oxides were precipitated from a solution containing arsenic (As), lead (Pb), antimony (Sb), cadmium (Cd), lanthanum (La), ytterbium (Yb), and mercury (Hg) in the presence and absence of aluminum (Al). The sorption stability of the multiple trace elements coprecipitated was evaluated through BCR and SBET extraction procedures. Low extraction percentages (< 10%) of As, Cd, and Sb were obtained, which was assigned to incorporation of more than 90% of their total contents into iron oxides structure. In turn, La, Pb, and Yb higher extraction percentages (up to 86%, 41% and 37%, respectively) were related to their lower incorporation into iron oxides structure. It was assumed that there is a limit for trace elements incorporation to iron oxides and the remaining not incorporated ions would be only weakly adsorbed and easier extractable. Indeed, at high trace elements concentrations, Cd and Pb sorption stability decreased, increasing their extraction percentages. Arsenic and Cd coprecipitated with Al-goethite were more stable than with lepidocrocite or Al-free-goethite. Conversely, La and Yb coprecipitated with Al-goethites were less stable. The human risk assessment by oral intake revealed that the high bioaccessible content of As in iron oxides represents risk for children health ($HQ > 1$) in every treatment. The results were considered useful for improve the comprehension of interactions between iron oxides and trace elements in natural systems, including aspects such as sorption mechanisms, stability, bioavailability, and toxicity.

Keywords: Arsenic. Cadmium. Goethite. Rare Earth Elements. Health risk.

1. INTRODUCTION

The mobility and fate of elements on the Earth's surface is mainly controlled by minerals sorption reactions in soils and sediments. The sorption stability depends on characteristics of both element and mineral, which controls the toxicity and availability of contaminants and nutrients in the environment (Bauer and Velde, 2014; Schwertmann and Taylor, 1989; Sposito, 2008). The sorption will be stable if the element is immobilized due to a strong interaction with the solid phase. On the other hand, the element can be easily mobilized and available if there is not a high affinity for the mineral sorption sites.

Iron oxides, hydroxides and oxyhydroxides (in this paper referred as 'iron oxides') are some of the most important minerals for controlling the mobility of elements in soils and sediments. Iron oxides nanoparticles are widely spread in the environment and present large and reactive surface area (Cornell and Schwertmann, 2003). The formation of Fe-oxides generally involves iron precipitation from aqueous solution through supersaturation or oxidation (Schwertmann and Cornell, 2000; Waychunas et al., 2005). Even though, Fe-oxides precipitation in natural systems does not occur isolated but in the presence of other aqueous substances that influence crystal growth (Freitas et al., 2016; Yang et al., 2021).

The inorganic substances in soil solution during Fe-oxides precipitation depend directly on the parent material composition. For example, Fe-oxides in soils and sediments from Paracatu (Minas Gerais, Brazil) are enriched in geogenic arsenic (As). This is considered a 'geogenic anomaly' because Paracatu Formation hosts an orogenic gold deposit rich in As (Antônio et al., 2021; Oliver et al., 2015). Previous studies have shown that As has a high affinity for Fe-oxides. Arsenic adsorbs onto the first embryonic Fe nuclei, following crystal growth and is finally entrapped inside Fe-oxides structure (Freitas et al., 2015; Waychunas et al., 2005). The incorporation of As to Fe-oxides structure accounts for the low As bioaccessibility in soil samples from Paracatu (Antônio et al., 2021; Ciminelli et al., 2018).

Indeed, ion incorporation can be much more effective for contaminant immobilization than adsorption and many ions can form solid solutions with Fe-oxides (Jeong et al., 2017; Lu et al., 2011). Cadmium, antimony, lead and rare earth elements can also incorporate into Fe-oxides structure via coprecipitation, diffusion, recrystallization or isomorphic substitution (Burton et al., 2020; Lu et al., 2011; Mo et al., 2021; Yang et al., 2021). Although, it is expected that ions with ionic radii, coordination, and valence number similar to Fe^{3+} and Fe^{2+} would be more easily and to a higher extent incorporated in Fe-oxides.

The mobility of trace elements sorbed onto Fe-oxides can be assessed by using extractions methods developed to evaluate the sorption stability in different environmental conditions. Sequential extractions procedures and bioaccessibility tests are relatively low-cost methods that can indirectly indicate mechanisms and strength of trace elements sorption to solid phases (Barcelos et al., 2018; Ciminelli et al., 2018; Vasques et al., 2018a, 2018b). A well stablished sequential extraction was proposed by the Community Bureau of Reference (BCR), which simulates acidic, reducing, and oxidizing environments (Rauret et al., 1999; Ure, 1991; Ure et al., 1993). Bioaccessibility tests in turn are used to estimate the human health risks from exposure to contaminated material. For example, the Simplified Bioaccessibility Extraction Test (SBET) solution resembles human stomach fluid to simulate adults and children oral exposure to contaminants (USEPA, 2008).

Solvated and loosely adsorbed ions on particle surfaces forming weaker outer-sphere complexes are expected to desorb easily using these extractors. On the other hand, strongly adsorbed ions that share electrons and form inner-sphere complexes are not easily desorbed from the mineral phases unless this strong bond is broken. In turn, ions incorporated to the solid structure forming a solid solution are extracted only with the solid phase dissolution.

Iron oxides are an important sink and reservoir for immobilization of trace elements in sediments and soils, although the mechanism of multiple elements sorption and the competition among them for sorption sites on Fe-oxides remain unclear. Therefore, this study evaluated the sorption stability of trace elements coprecipitated with iron oxides through extraction procedures. The hazard quotient was quantified through bioaccessibility of As, Sb, Pb, Cd, La and Yb in precipitates. It is expected that the results present here may contribute to a better understanding of interactions between iron oxides and trace elements, including sorption mechanisms, stability and, hence, bioavailability of these trace elements in the environment.

2. MATERIALS AND METHODS

The iron oxides were synthesized through coprecipitation from a solution containing As, Pb, Sb, Cd, La, and Yb (Kroehling et al. in press). The elements concentrations in solution were based on the average contents found in carbonaceous phyllites of the Paracatu Formation, which hosts an orogenic gold deposit, in an area affected by acid mine drainage (Oliver et al., 2015). Two Fe:Al molar ratio (500:0 and 450:50 mmol L^{-1}) were used to evaluate the effect of Al isomorphic substitution in Fe-oxides on the trace elements sorption stability.

Mercury (Hg) was considered in this study as a factor aside (without or with Hg) since it is not natural in the region of Paracatu, but Hg has been introduced in the environment by artisanal mining operations (known as *garimpo*). The Fe-oxides were identified by X-ray diffraction (XRD) after 90 days of coprecipitation. A brief resume of the results is presented here, showing the main mineralogical phases detected (Table 3). More information about the synthesis can be found elsewhere (Kroehling et al. in press).

Table 3 – Iron oxides coprecipitated with trace elements identified by XRD (Kroehling et al. in press).

Fe:Al mmol L^{-1}	Trace elements[a]	Mercury (Hg)[b]	Fe-oxides identified by XRD
500:0	Low	Without	Goethite, magnetite and lepidocrocite
500:0	Low	With	Goethite
500:0	High	Without	Lepidocrocite
500:0	High	With	Lepidocrocite and goethite
450:50	Low	Without	Al-goethite
450:50	Low	With	Al-goethite
450:50	High	Without	Al-goethite
450:50	High	With	Al-goethite

[a] As, Pb, La, Sb, Cd and Yb in low (5.23) and high (10.46 mmol L^{-1}) concentration.
[b] With Hg = 0.01 mmol L^{-1}.

2.1 Microwave assisted acid digestion

Representative samples of the precipitates were digested following the Method 3051A, of the SW-846 Manual (USEPA, 2007a). The Brazilian environmental council has also implemented Method 3051A for soil quality guideline values (CONAMA, 2009). This acid extraction method is commonly used to dissolve minerals, such as iron and aluminum oxides, and releasing sorbed elements (Melo et al., 2016).

The microwave assisted acid digestion was used to dissolve 0.50 ± 0.01 g of sample with 9.0 ± 0.1 mL of concentrated HNO_3 and 3.0 ± 0.1 mL concentrated HCl in a fluorocarbon

polymer vessel. The vessel was sealed and heated to 175 ± 5 °C in approximately 5.50 ± 0.25 min; it remained at 175 ± 5 °C for 10 min; and was allowed to cool for around 45 min. The resulting solutions were passed through ashless 0.45 μm paper filters and prepared for analysis of Fe, Al, As, Pb, Sb, Cd, La, Yb, and Hg contents by inductively coupled plasma optical emission spectrometry (ICP-OES), model Optima 8300.

The microwave assisted digestion by concentrated HNO_3 and HCl (Method 3051A) is considered here to extract the 'pseudo-total' contents of the elements under study. The percentage of extraction (%) of the BCR and SBET results, relative to the 'pseudo-total' content were calculated for each sample (*i*) as follow:

$$Extraction_i\ (\%) = \frac{BCR\ or\ SBET\ content_i\ (\mathrm{mg\ kg^{-1}})}{Pseudo{-}total\ content_i\ \ (\mathrm{mg\ kg^{-1}})} \quad \text{(Eq. 3)}$$

2.2 BCR discrete extractions

The stability of Fe, Al, As, Pb, Sb, Cd, La, Yb, and Hg in samples was evaluated through the BCR extraction method (Rauret et al., 1999; Ure, 1991; Ure et al., 1993). This method was adapted in this study for discrete extractions with the same conditions and reagents of the sequential scheme (Mello et al., 2018; Vasques et al., 2018a, 2018b). The main advantage in performing a discrete extraction is to avoid sample losses, yielding extractable contents compatible with those obtained by the sequential procedure (Baig et al., 2009).

The precipitates were sieved in 106 μm previous to extraction. The discrete extraction scheme assessed extractable phases of iron, aluminum and associated trace elements in different environmental conditions:

i. Water extraction: 40 mL of Milli-Q water (18.2 MΩ.cm at 25°C) added to 4.0 g of sample in 50 mL centrifuge tubes, shaken for 2 h at 35 rpm, centrifuged at 3000 *g* for 20 min, and filtered through 0.45 μm micropore filters. This procedure was repeated just one more time since the electrical conductivity of the first extract was above 4.0 μS cm^{-1}. Both extracts were mixed and properly stored at 4°C until analysis.
ii. Acid extraction: 10 mL of 0.11 mol L^{-1} acetic acid (CH_3COOH) added to 0.25 g of sample in 15 mL centrifuge tubes and shaken for 16 h at 35 rpm;
iii. Reducible extraction: 10 mL of 0.5 mol L^{-1} hydroxylammonium chloride ($HONH_2.HCl$) added to 0.25 g of sample in 15 mL centrifuge tubes and shaken for 16 h at 35 rpm;

iv. Oxidant extraction: 5 mL of 8.8 mol L^{-1} hydrogen peroxide (H_2O_2) added to 0.50 g of sample at room temperature for 1 h with the vessel loosely covered, followed by digestion in a water-bath at 85 ± 2°C for 1 h without cover. Addition of more 5 mL of H_2O_2 followed by more 1 h of digestion at 85 ± 2°C. Addition of 25 mL of 1.0 mol L^{-1} ammonium acetate ($C_2H_7NO_2$) followed by shaking for 16 h at 35 rpm and 25 ± 5°C.

The extracts were separated from the solid residue by centrifugation at 3000 *g* for 20 min. The supernatants were passed through 0.45 μm micropore filters and stored at 4°C until analyses by ICP-OES. The solid residues were properly discharged.

2.3 Bioaccessibility and risk assessment

The *in vitro* simplified bioaccessibility extraction test (SBET) is a fast and cheap procedure for evaluation of toxic elements contents solubilized by a solvent that simulates the gastric fluid (USEPA, 2008). The extraction solvent was prepared with 0.4 mol L^{-1} glycine solution and the pH was adjusted to 1.50 ± 0.05 with concentrated HCl. Then, 30 mL of the solvent was added to 0.30 g of sample. The suspensions were shaken at 30 ± 2 rpm for 60 min in water bath at 37°C. The supernatants were then separated from the solid residue through centrifugation at 3000 *g* and filtration through 0.45 μm micropore filters. The extract was analyzed by ICP-OES and the solid residue was properly discharged.

Bioaccessible concentrations (*C,* mg kg^{-1}) were used to evaluate the human health risk assessment by oral bioavailability (USEPA, 2007b) (Table 4). Accidental soil ingestion is one of the main contaminants exposures. The average daily dose (*ADD*) for adults (*a*) or children (*c*) was calculated as follows:

$$\boldsymbol{ADD} = \frac{\boldsymbol{C} \times \boldsymbol{IR(a,c)} \times \boldsymbol{Ef} \times \boldsymbol{ED(a,c)}}{\boldsymbol{Bw\ (a,c)} \times \boldsymbol{At\ (a,c)}} \qquad \text{(Eq. 4)}$$

The risk assessment was calculated through the hazard quotient (*HQ*) (Eq. 5), i.e., the ratio between the average daily dose (*ADD*) and the corresponding reference dose (*RfD*). The samples present health risk if *HQ* is higher than 1.0, otherwise they are considered safe (Table 4).

$$\boldsymbol{HQ} = \frac{\boldsymbol{ADD}}{\boldsymbol{RfD}} \quad \text{(Eq. 5)}$$

Table 4 – Parameters of risk assessment for calculating the average daily dose (*ADD*) and the hazard quotient (*HQ*).

Parameter		Value	Unit	Reference
Ingestion rate adult	*IR(a)*	50	mg day^{-1}	Brazil (2010)
Ingestion rate child	*IR(c)*	100	mg day^{-1}	Brazil (2010)
Exposure frequency	*EF*	250	days $year^{-1}$	USEPA (2007b)
Exposure duration adult	*ED(a)*	25	years	USEPA (2007b)
Exposure duration child	*ED(c)*	6	years	USEPA (2007b)
Body weight adult	*BW(a)*	70	kg	Brazil (2010)
Body weight child	*BW(c)*	15	kg	Brazil (2010)
Average time adult	*AT(a)*	9125	days	USEPA (2007b)
Average time child	*AT(c)*	2190	days	USEPA (2007b)
Reference dose arsenic	*RfD As*	0.0003	mg $(kg\ day)^{-1}$	USEPA (1991)
Reference dose cadmium	*RfD Cd*	0.0035	mg $(kg\ day)^{-1}$	Wang et al. (2023)
Reference dose lead	*RfD Pb*	0.0010	mg $(kg\ day)^{-1}$	Wang et al. (2023)
Reference dose lanthanum	*RfD REE*	0.0200	mg $(kg\ day)^{-1}$	Sun et al. (2017)
Reference dose ytterbium	*RfD REE*	0.0200	mg $(kg\ day)^{-1}$	Sun et al. (2017)

2.4 Statistical analysis

The experiment was performed in a completely randomized factorial design with eight treatments (2x2x2) and three replicates. The predictor/explanatory variables were: Fe:Al molar ratio (500:0 or 450:50), trace elements concentrations (low or high) and mercury (without or with). The response variables were the BCR and SBET contents (mg kg^{-1}) and their percentages (%) relative to pseudo-total contents for evaluation of sorption stability.

Jarque-Bera test was used for testing normality, and Bartlett and Levene for homoscedasticity. Data transformation was performed if one of these assumptions was violated and the assumptions were checked again. The data were then subject to ANOVA (F test) and contrasts by Holm-Bonferroni test at 5% of α error probability ($P = 0.05$) were used to compare Fe:Al molar ratios and mercury significant effects. Moreover, a one-way Bonferroni test was used to evaluate if high concentrations treatments extraction percentages are higher than low concentrations treatments extraction percentages.

3. RESULTS

3.1 Pseudo-total contents

The microwave acid digestion extracted an average of 271,539 and 21,173 mg kg^{-1} of iron and aluminum respectively (Table 5). Aluminum was present only in treatments 450:50 (Fe:Al molar ratio). Arsenic was the major trace element: average of 3,741 and 8,363 mg kg^{-1} from low and high trace elements concentrations, respectively. Antimony and lead presented concentrations around ten times lower than arsenic: 372 and 1,057 mg kg^{-1} of Sb, and 285 and 607 mg kg^{-1} of Pb in low and high trace elements concentrations, respectively. In turn, cadmium and lanthanum concentrations were around half of lead concentration: 137 and 293 mg kg^{-1} of Cd, and 137 and 319 mg kg^{-1} of La. Finally, ytterbium was the minor element: 24 and 52 mg kg^{-1} of Yb. Mercury was below the detection limit in every sample (< 3 mg kg^{-1}).

Table 5 – 'Pseudo-total' contents in precipitates digested with concentrated HNO_3:HCl (9:3 v:v) assisted by microwave following Method 3051A (USEPA, 2007a).

Element	Treatment[a]	Average	Median	Stand. Dev.	Minimum	Maximum
				mg kg^{-1}		
Fe	All treat.	271,539	271,146	25,268	224,683	320,111
Al	Fe:Al 450:50	21,173	21,262	959	19,906	23,402
As	Low concent.	3,741	3,810	529	2,931	4,711
Sb	Low concent.	372	363	68	286	504
Pb	Low concent.	285	287	51	209	393
Cd	Low concent.	137	140	19	108	174
La	Low concent.	137	152	28	99	172
Yb	Low concent.	24	24	4	18	28
As	High concent.	8,363	8,332	1,038	6,384	9,870
Sb	High concent.	1,057	986	161	881	1,352
Pb	High concent.	607	627	60	449	662
Cd	High concent.	293	291	30	243	337
La	High concent.	319	331	43	213	360
Yb	High concent.	52	53	6	38	57
Hg	With Hg	< 3[b]	< 3[b]	-	< 3[b]	< 3[b]

[a] Treatments: 1) Fe:Al atomic ratio in coprecipitation solution = 500:0 or 450:50 mmol L^{-1}; 2) Trace elements initial content in coprecipitation solution: ∑(As, Sb, Pb, Cd, La, Yb) = 5.2 or 10.5 mmol L^{-1} low or high respectively; 3) Factor mercury: without or with Hg.

[b] Detection limit calculated = (3*(Controls std. dev.)) + (Controls average).

3.2 BCR discrete extractions

Less than 1.0% of the pseudo-total content of iron (< 2,600 mg kg^{-1}) was soluble in water or acid (Figure 8). Treatments 500:0 (Fe:Al molar ratio) presented 146.9 times more water-soluble Fe than treatments 450:50 at low concentrations of trace elements ($P < 0.05$). The BCR reducing extractant presented the highest Fe concentrations (up to 7.6% of the pseudo-total content or 21,634 mg kg^{-1}). In general, a higher Fe extraction was observed for treatments 500:0.

Similar to Fe, only a small percentage of the pseudo-total content of aluminum was soluble in water (< 0.3% or < 72.5 mg kg^{-1}), but a higher content of Al was soluble in acid (average 2.5% or 547.2 mg kg^{-1}). The highest Al extractions were also in reducing (average 7.4% or 1,600 mg kg^{-1}) and oxidizing (5.2% or 1,115 mg kg^{-1}) extractions (Figure 8).

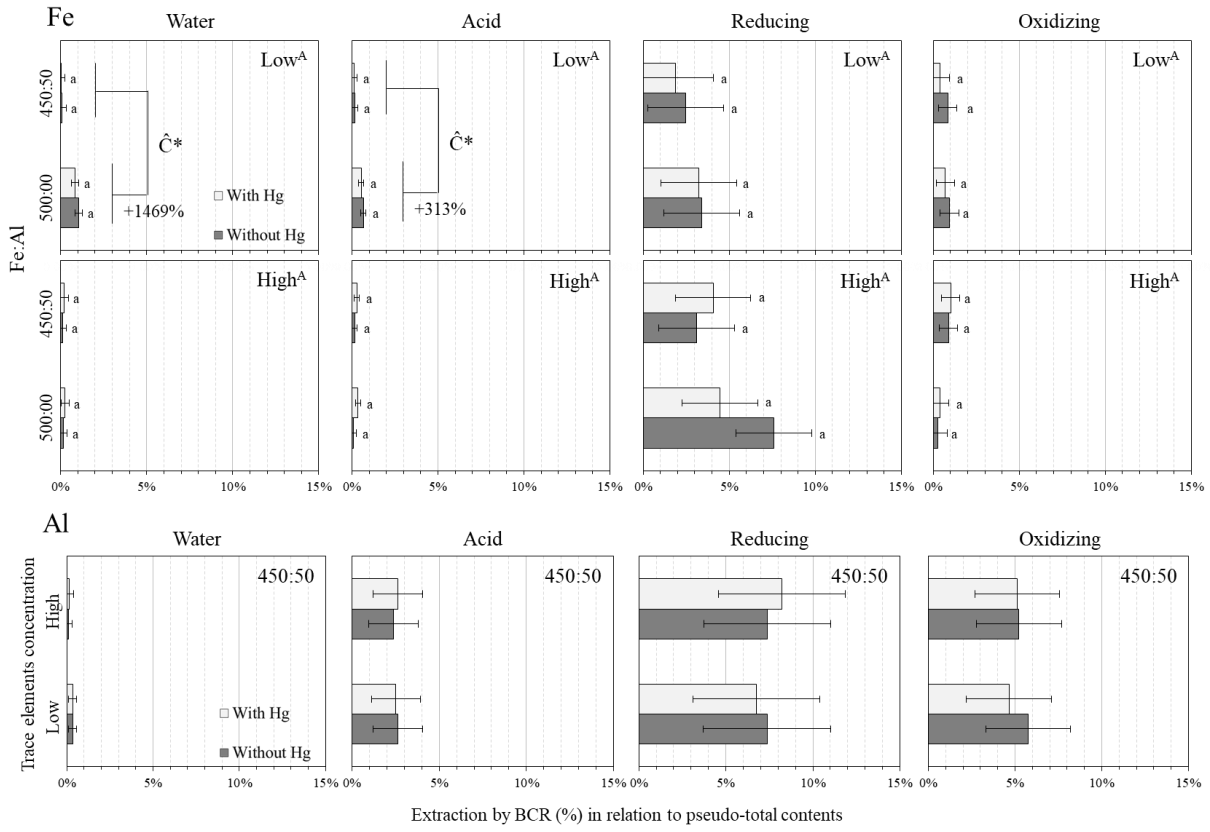

Figure 8 – Extraction (%) of iron (Fe) and aluminum (Al) by BCR discrete extractions (water, acid, reducing and oxidizing) in relation to pseudo-total contents (Method 3051A). Fe:Al molar ratio (500:0 or 450:50), trace elements concentrations (low or high) and mercury (without or with). Different lowercase letters, uppercase letters and contrast effect (Ĉ*) indicate significant differences ($P \leq 0.05$) due to mercury, trace elements concentration and Fe:Al ratio, respectively. Thin lines correspond to experimental standard error.

Arsenic extraction percentages were lower than 7% of the pseudo-total contents in all treatments. Precipitates from 500:0 (Fe:Al molar ratio) treatments presented higher As

extraction than precipitates from 450:50 (Figure 9). There was significantly ($P < 0.05$) more As water-soluble (+126%), reducible (+148%) and oxidizable (+120%) from 500:0 than from 450:50 treatments.

Cadmium extraction was also higher for treatments 500:0 (Fe:Al molar ratio) (Figure 9). The water extraction of treatments 500:0 at low trace elements concentrations presented 319% more Cd than treatments 450:50 at low concentration ($P < 0.05$). Moreover, Cd reducing extraction percentage was significantly higher at high trace elements concentration treatments. A significant difference (+54%) was also found in reducing extraction of Cd due to the absence of Hg in treatments without Al (500:0 Fe:Al) at high trace elements concentrations. Futhermore, Cd extractions were lower than 6% and not so discrepants in distinct solutions.

Conversely, treatments 450:50 (Fe:Al molar ratio) released significantly more Pb than treatments 500:0 in acid extraction, at low and high trace elements concentrations ($P < 0.05$) (Figure 9). Moreover, Pb reducing and oxidizing extractions percentages were significantly higher at high trace elements concentration. Similar to Cd, reducing extraction released significantly more Pb (+40%) in treatments 500:0 at high trace elements concentrations, due to the absence of Hg.

Finally, antimony and mercury concentrations were below the detection limit in all treatments. The detection limits for Sb were: water (22.2 mg kg^{-1} or 4.1% of the pseudo-total content), acid (27.4 mg kg^{-1} or 5.2%), reducible (37.8 mg kg^{-1} or 7.1%), and oxidizing (41.6 mg kg^{-1} or 7.8%). In turn, the detection limits for Hg were: water (1.1 mg kg^{-1}), acid (2.4 mg kg^{-1}), reducing (3.1 mg kg^{-1}), and oxidizing (6.6 mg kg^{-1}).

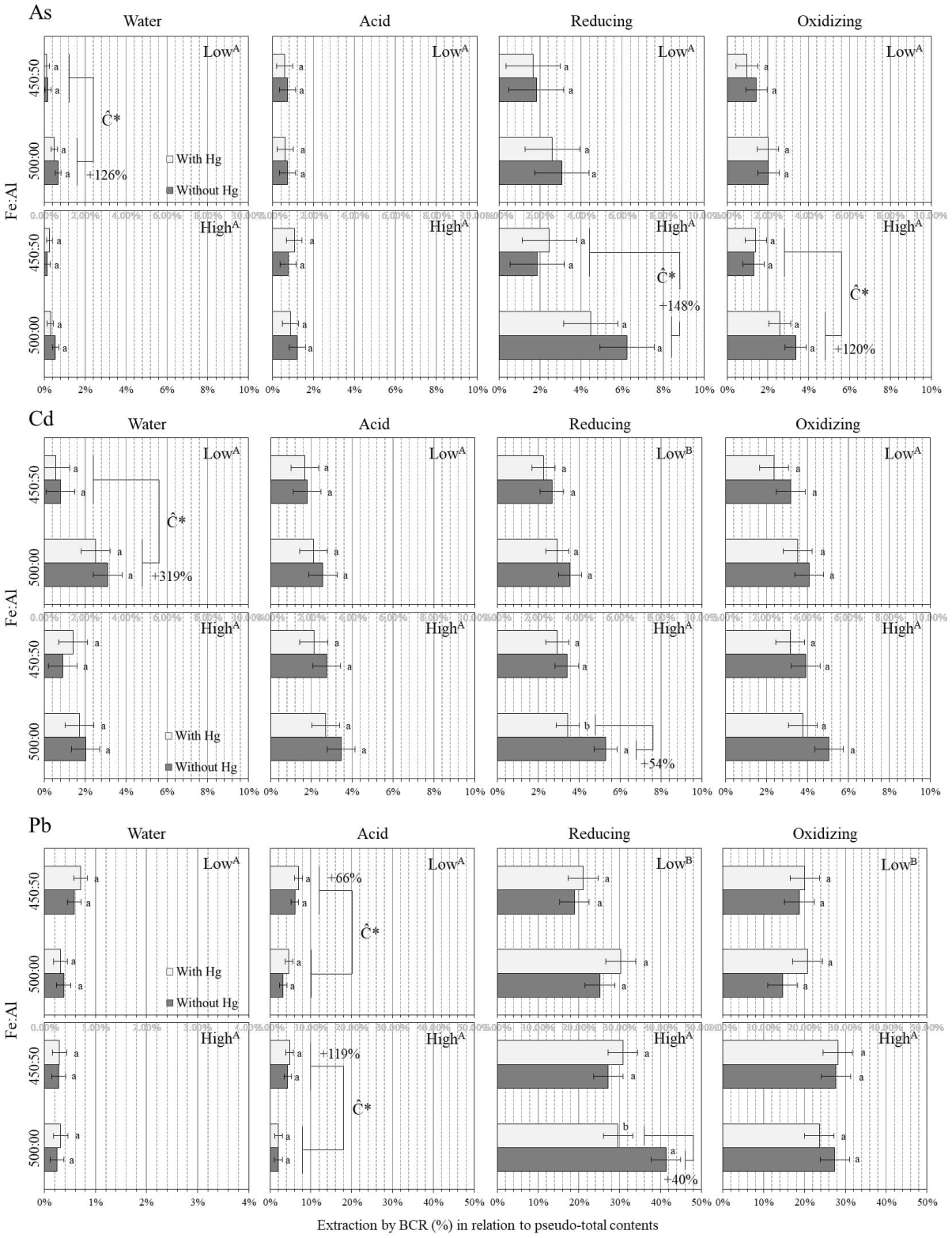

Figure 9 – Extraction (%) of arsenic (As), cadmium (Cd) and lead (Pb) by BCR discrete extractions (water, acid, reducing and oxidizing) in relation to pseudo-total contents (Method 3051A). Fe:Al molar ratio (500:0 or 450:50), trace elements concentrations (low or high) and mercury (without or with). Different lowercase letters (a, b), uppercase letters (A, B) and contrast effect (Ĉ*) indicate significant differences ($P \leq 0.05$) due to mercury, trace elements concentration and Fe:Al ratio, respectively. Thin lines correspond to experimental standard error.

Lanthanum was the most soluble element in water (average 18.3% of pseudo-total content or 46.6 mg kg^{-1}), acid (52.1% or 118.4 mg kg^{-1}), reducing (69.1% or 157.6 mg kg^{-1}), and oxidizing (81.2% or 185.2 mg kg^{-1}) BCR extractants (Figure 10). Ytterbium was more soluble from treatments 450:50 (from 62% to 110%) than from treatments 500:0 (Fe:Al molar ratio), as indicated by the significant contrast effects ($P < 0.05$). On the contrary, water-extraction released 198% more Yb from 500:0 than from 450:50 treatments, at low trace elements concentrations.

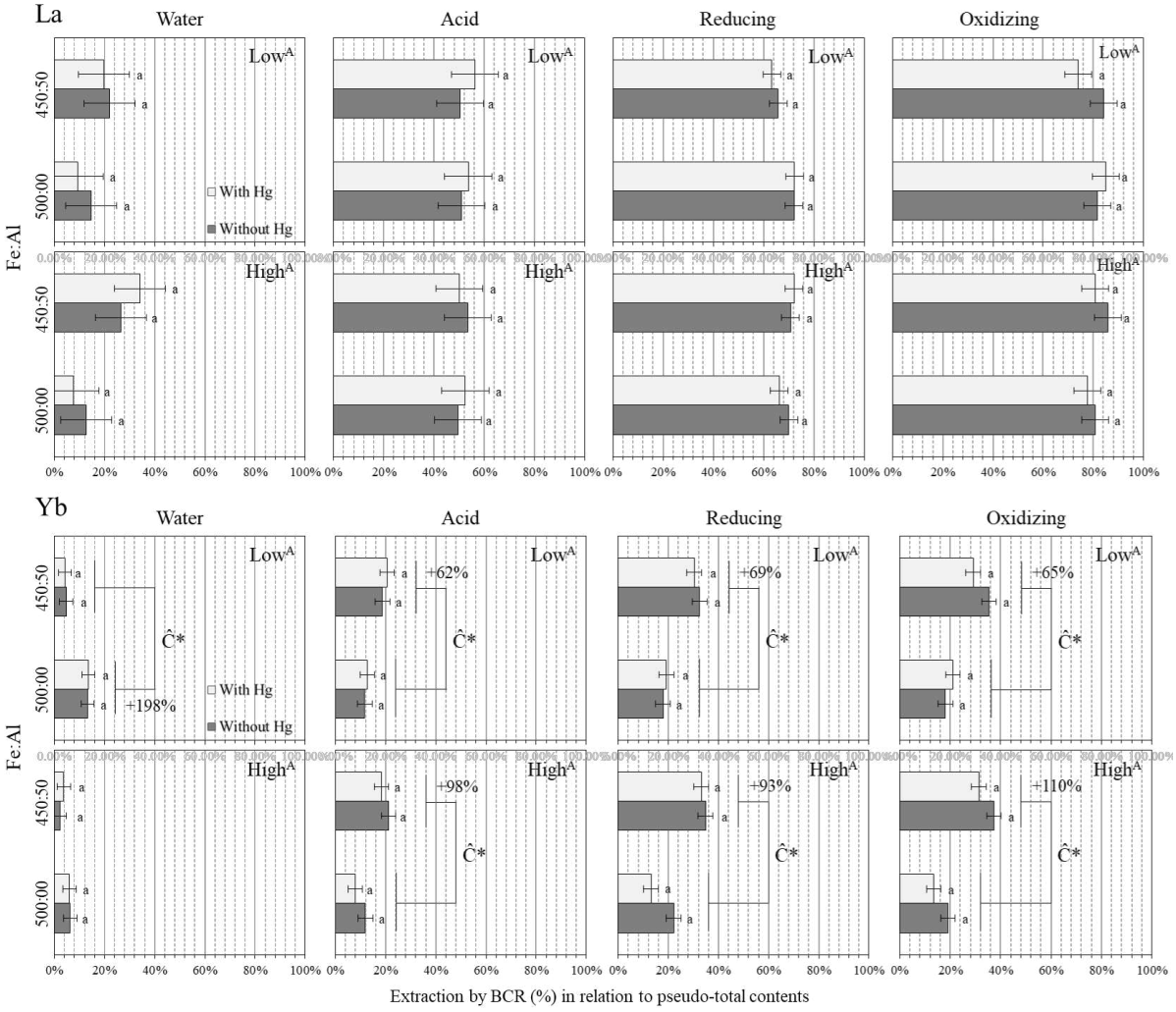

Figure 10 – Extraction (%) of lanthanum (La) and ytterbium (Yb) by BCR discrete extractions (water, acid, reducing and oxidizing) in relation to pseudo-total contents (Method 3051A). Fe:Al molar ratio (500:0 or 450:50), trace elements concentrations (low or high) and mercury (without or with). Different lowercase letters (a, b), uppercase letters (A, B) and contrast effect ($\hat{C}$*) indicate significant differences ($P \leq 0.05$) due to mercury, trace elements concentration and Fe:Al ratio, respectively. Thin lines correspond to experimental standard error.

3.3 Bioaccessibility and risk assessment

The bioaccessible iron, arsenic and cadmium were lower than 2%, 4%, and 6% of the pseudo-total contents, respectively. There were no significant differences ($P > 0.05$) in amounts of Fe, As or Cd extracted by the simplified bioaccessibility test (SBET), despite a trend towards higher extractions percentages from treatments without aluminum (500:0 Fe:Al molar ratio) (Figure 11).

Lead bioaccessibility varied from 12.2% to 34.1% of the pseudo-total content (35.5 to 195.5 mg kg^{-1}) (Figure 11). At low trace elements concentration, treatments with 500:0 Fe:Al molar ratio released 90% more Pb than 450:50 treatments. Conversely, at high concentration, treatments with 450:50 Fe:Al molar ratio released 38% more Pb than 500:0 treatments ($P < 0.05$). Moreover, there was 83% more bioaccessible Pb in treatments 500:0 due to the absence of Hg, at low trace elements concentration.

Lanthanum bioaccessibility was the highest among the elements under study: between 50.0% and 84.9% of the pseudo-total content, corresponding to 146.1 and 267.0 mg kg^{-1}, respectively. Lanthanum bioaccessibility was significantly higher in 450:50 Fe:Al molar ratio (73.3% or 253.9 mg kg^{-1}) than in 500:0 treatments (52.1% or 149.6 mg kg^{-1}) at high trace elements concentration ($P < 0.05$). In turn, ytterbium bioaccessibility was 147% higher in treatments with 450:50 than with 500:0 Fe:Al molar ratio, at high trace elements concentration ($P < 0.05$).

Similar to BCR extractions, bioaccessible antimony and mercury concentrations were below detection limit in all treatments. The detection limit for Sb was 173.0 mg kg^{-1} (32.5% of pseudo-total contents) and for Hg was 11.3 mg kg^{-1}.

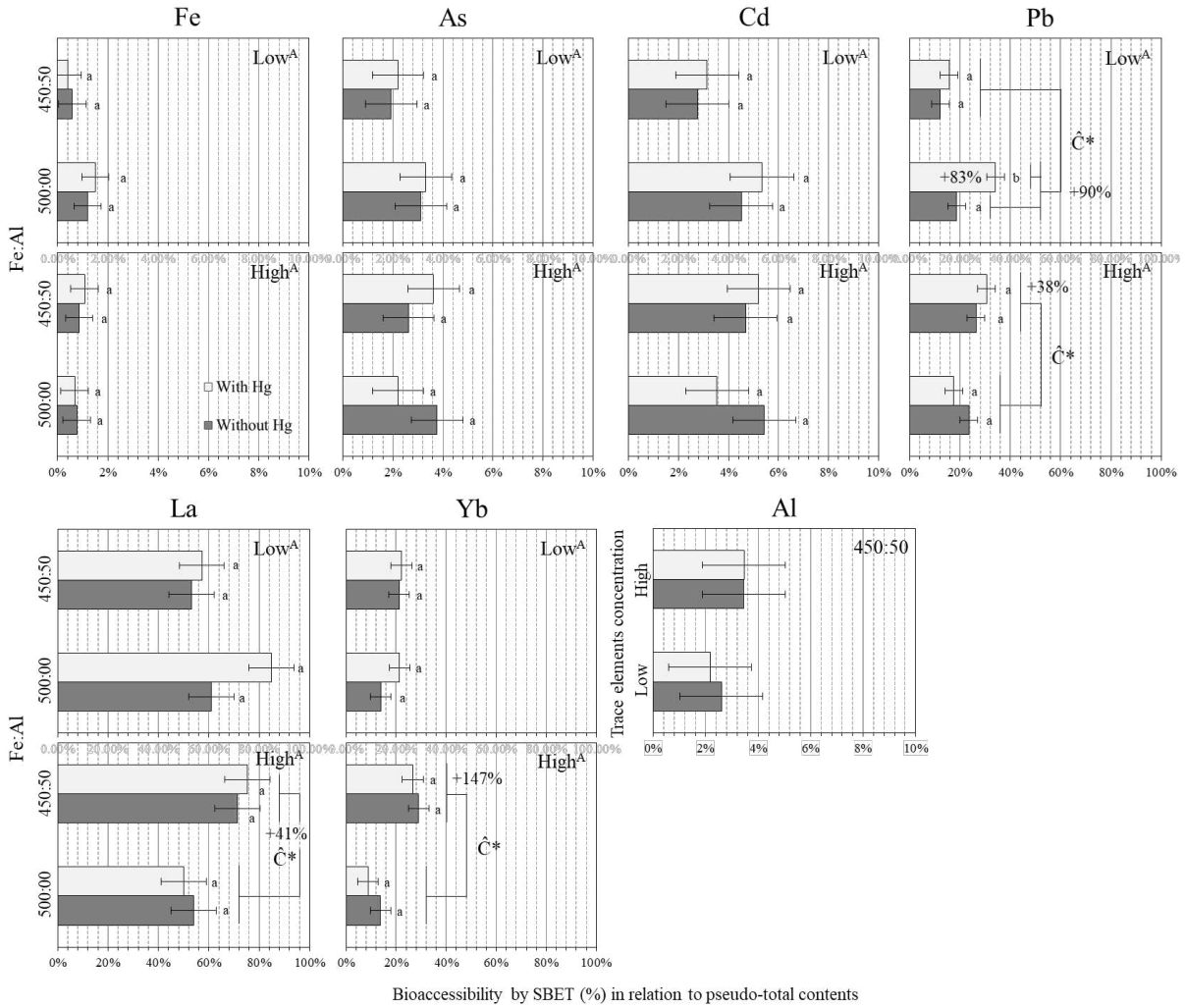

Figure 11 – Bioaccessible (%) iron (Fe), arsenic (As), cadmium (Cd), lead (Pb), lanthanum (La), ytterbium (Yb) and aluminum (Al) by simplified extraction test (SBET) in relation to pseudo-total contents (Method 3051A). Fe:Al molar ratio (500:0 or 450:50), trace elements concentration (low or high) and mercury (without or with). Different lowercase letters, uppercase letters and contrast effect ($\hat{C}$*) indicate significant differences ($P \leq 0.05$) due to mercury, trace elements concentration and Fe:Al ratio, respectively. Thin lines correspond to experimental standard error.

Human exposure by oral intake was assessed from the bioaccessible As, Cd, Pb, La and Yb contents, extracted by SBET method. The non-carcinogenic risk was evaluated through the Hazardous Quotient (*HQ*), i.e., the ratio of a substance exposure level to a reference dose over a specified time period (Eq. 4 and 5) (USEPA, 2007b).

The *HQ* results (Table 6) showed that the non-carcinogenic risks for adults are very low for Cd, La, and Yb (< 0.01) but higher for As (0.14 – 0.43) and Pb (0.03 – 0.09). Anyway, the precipitates can be considered safe material for adults. On the other hand, the *HQ*s are around ten times higher for children: As (1.26 – 4.06), Pb (0.19 – 0.82), La (0.02 – 0.06), and Cd (0.01 – 0.02), with the bioaccessible As representing risk (*HQ* > 1). At low trace elements concentrations, the *HQ* values were higher for treatments without Al (500:0 Fe:Al molar ratio).

Conversely, the highest *HQ* values were for treatments with Al (450:50 Fe:Al molar ratio) at high trace elements concentrations.

Table 6 – Bioaccesibility (mg kg^{-1}) and hazard quotient (*HQ*) for arsenic (As), cadmium (Cd), lead (Pb), lanthanum (La) and ytterbium (Yb) of Fe-oxides synthesized from different treatments.

Treatments[a]							
Fe:Al ratio[b]	Trace Elements Concentration[c]	As	Pb	Cd	La	Yb	∑ (*HQ*)[d]
		Extraction SBET (mg kg^{-1})					
500:00	Low	111.4	68.6	6.2	82.1	3.7	
450:50	Low	83.0	41.4	4.4	87.6	5.7	
500:00	High	255.2	115.2	13.2	149.6	5.3	
450:50	High	266.7	180.0	14.6	253.9	14.9	
		Hazard Quotient (adults)					
500:00	Low	0.18	0.03	< 0.01	< 0.01	< 0.01	0.22
450:50	Low	0.14	0.02	< 0.01	< 0.01	< 0.01	0.16
500:00	High	0.42	0.06	< 0.01	< 0.01	< 0.01	0.48
450:50	High	0.43	0.09	< 0.01	< 0.01	< 0.01	0.53
		Hazard Quotient (children)					
500:00	Low	1.69	0.31	0.01	0.02	< 0.01	2.04
450:50	Low	1.26	0.19	0.01	0.02	< 0.01	1.48
500:00	High	3.88	0.53	0.02	0.03	< 0.01	4.46
450:50	High	4.06	0.82	0.02	0.06	< 0.01	4.96

[a] Treatments for Fe-oxides coprecipitation with trace elements in laboratory. [b] Fe:Al molar ratio = 500:0 or 450:50 mmol L^{-1}. [c] Trace elements concentration in coprecipitation solution: ∑(As, Sb, Pb, Cd, La, Yb) = 5.2 or 10.5 mmol L^{-1} low or high, respectively. [d] ∑(*HQ*) = sum of all elements *HQ*s.

4. DISCUSSION

4.1 Iron oxides and trace elements stability

The results from BCR extractions (Figure 8Figure 9, Figure 10) suggest that the trace elements coprecipitated with Fe-oxides were sorbed through different mechanisms.

Iron extraction (Figure 8) was significantly higher in BCR reducing solution: up to 7.6% in treatments with lepidocrocite (Table 3). The Fe solubilized in reducing solution is attributed to Fe(III) in lepidocrocite, goethite, and poorly crystalized oxides not identified by XRD (e.g., ferrihydrite or green rusts). This result also corroborate that well crystalized Fe-oxides are not significantly solubilized by BCR reducing solution. Lower percentages of Fe extracted from oxidizing solution (< 1.0%) indicates low amounts of Fe(II) susceptible to oxidation in poorly crystallized oxides and magnetite.

Lower percentages of Fe were soluble in water and acid (average 0.3%). The water- and acid-soluble Fe is attributed to very poorly crystallized Fe-oxides and sulfate salts not identified by XRD. Sulfates could be precipitated over Fe-oxides, since sulfate salts were used in the experiment, mainly as sources of Fe and Al (Kroehling et al. in press). Indeed, only easily soluble salts are completely extracted in the first acid acetic 0.11 mol L^{-1} washing (Tong et al., 2020). Nevertheless, two consecutive water washings extracted slightly more Fe than one acid extraction (Figure 8).

Arsenic extraction was also higher in BCR reducing solution, although less than 7% of the pseudo-total contents (Figure 9). These results are in line with previous studies that reported low As extraction from coprecipitated Fe-oxides (Mello et al., 2018; Vasques et al., 2018a, 2018b). The low As extraction percentage is attributed to As incorporated to Fe-oxides structure through coprecipitation (Ciminelli et al., 2018; Freitas et al., 2015; Jeong et al., 2017).

Therefore, only a significant dissolution of the solid phase would be capable of extracting the incorporated As, which could not be recovered by water or acid BCR steps. Dissolution of Fe-oxides plays a major role in As release in the environment, especially in reducing conditions, although reduction of adsorbed As(V) to As(III) can happen without solubilizing the Fe(III)-oxide solid phase (Langner and Inskeep, 2000). Indeed, we suppose that a fraction of As, typically less than 0.5% of the pseudo-total content (Figure 9), was only adsorbed, not occluded in Fe-oxides and more easily extractable. This result suggests that there is a limit for As incorporation to Fe-oxides.

Similar to arsenic, cadmium extraction percentages were considered low (< 6.0% of the pseudo-total content). Although Cd presents lower affinity for Fe-oxides than As, Sb or Pb in pH ≤ 8, it can be also adsorbed via inner-sphere complexation over a wide range of pH and Cd concentrations (Randall et al., 1999; Schwertmann and Taylor, 1989; Sposito, 2008). Furthermore, the adsorbed Cd could migrate into Fe-oxides micropores and also isomorphically replace Fe in Fe-oxides structure during coprecipitation (Ainsworth et al., 1994; Bruemmer et al., 1988). Hence, similar to arsenic, Cd low extraction percentages might be associated to Cd trapped inside Fe-oxides structure. Therefore, these results suggest that most of the coprecipitated As and Cd (> 93%) were incorporated into the Fe-oxides structure.

Lead extraction was significantly higher than As and Cd extraction by the reducing and oxidizing BCR solutions (from 14.7% to 41.3% of Pb pseudo-total contents). Although Pb^{2+} has high affinity for Fe-oxide surface, it could completely desorb from the oxide surface and would have a lower capacity to incorporate into the Fe-oxide structure due to the larger ionic radius of Pb^{2+} (0.119 nm) (Ainsworth et al., 1994; Padmanabham, 1983). Therefore, most of the lead ions extracted were probably only adsorbed onto Fe-oxides surface. Notwithstanding, Pb ions can also be incorporated into Fe-oxides (Lu et al., 2011) and the higher recovery of Pb by the reducing BCR solution could also suggest its incorporation into poorly crystalized Fe-oxides structure.

Rare earth elements presented a lower capacity to be sorbed through coprecipitation with Fe-oxides. Lanthanum and ytterbium extraction percentages were the highest among the studied trace elements, with oxidizing extraction up to 85.8% and 37.3% of the pseudo-total contents for La and Yb, respectively (Figure 10). These results can be ascribed to the larger ionic radii of La^{2+} and Yb^{2+} (0.103 and 0.101 nm, respectively) in relation to Fe^{3+}, As^{3+} or Cd^{2+} (0.065, 0.058 and 0.095 nm), which could impair occlusion in Fe-oxides structure. Ytterbium extractions were lower compared to La, which is in line with the general idea that heavy rare earth elements show greater affinity for Fe-oxides than light rare earth elements (Liu et al., 2018). Pietralonga et al. (2017) also reported that La could be easily recovered from coprecipitated Fe-oxides by acetic acid 0.11 mol L^{-1} due to La segregation in discrete phases.

Antimony contents recovered from coprecipitates by BCR extractants were below the ICP-OES detection limit for all samples. Then, in the worst case, Sb extraction percentages would be less than 7.8% of the pseudo-total content, considering the detection limit for calculation. This is comparable to As and Cd extraction percentages, which is in agreement with previous studies that suggest strong inner-sphere surface complex of Sb^{3+} and Sb^{5+} (ionic

radii 0.090 and 0.074 nm) with Fe-oxides and incorporation into the Fe-oxide structure (Burton et al., 2020; Leuz et al., 2006; Shangguan et al., 2016). Therefore, similar to As and Cd, more than 90% of Sb ions could be trapped into the Fe-oxide lattice during coprecipitation.

Contents of mercury extracted from coprecipitates by BCR solutions, as well as their pseudo-total contents, were also below the detection limit (< 6.6 and < 2.5 mg kg^{-1}, respectively). Then it was not possible to make any assumption on Hg sorption by Fe-oxides. Notwithstanding, it is well known that Hg^{2+} (ionic radius of 0.102 nm) presents high affinity for Fe-oxides and can form inner-sphere surface complexes with surface hydroxyl groups (Bonnissel-Gissinger et al., 1999; Gil-Díaz et al., 2021; Gong et al., 2019; Richard et al., 2016).

In summary, reducing extraction released higher amounts of Fe, Al, and trace elements, followed by oxidizing, acid, and water extractions. Water and acid extractions could be attributed to very poorly crystallized Fe-oxides, sulfates salts, and weakly adsorbed ions. In turn, reducing and oxidizing extractions were capable of dissolving Fe(III) and Fe(II) from Fe-oxides and extract incorporated trace elements. Low extraction percentages of cadmium, arsenic, and antimony were assigned to incorporation of more than 90% of these ions into Fe-oxides structure. On the other hand, higher extraction percentages of lanthanum, ytterbium, and lead are assigned to adsorption of these elements on the surface of Fe-oxides, since they would not be incorporated into Fe-oxides structure to the same extent as As, Cd and Sb due to La, Yb and Pb larger ionic radii.

4.2 Mineral phases and aluminum isomorphic substitution

In general, precipitates from 450:50 (Fe:Al molar ratio) treatments presented lower Fe, As, and Cd recovery by BCR discrete extractions than precipitates from 500:0. This difference was significant ($P < 0.05$) for water-soluble Fe, As, and Cd, for acid-soluble for Fe, and also for oxidizing and reducing extractions of As (Figure 8 Figure 9). Therefore, Al isomorphic substitution reduces Fe-oxides solubility, and increases As and Cd sorption stabilities. Nevertheless, the presence of Al also contributed for a higher removal efficiency of As and Cd during coprecipitation with Fe-oxides, favoring Al-goethite formation over lepidocrocite (Kroehling et al. in press).

Previous studies also reported that Al isomorphic substitution increases goethite stability and plays a role in stabilizing As in Fe-oxides coprecipitated (Freitas et al., 2016; Silva et al., 2010; Vasques et al., 2018a, 2018b). It is well known that Al isomorphic substitution decreases Fe-oxides unit cell size, inducing structural defects that are compensated by an increase in

surface hydroxyl sites (Al- or Fe-OH) related to As sorption (Schulze, 1984; Schwertmann and Taylor, 1989; Souza et al., 2021). Furthermore, Al substitution in goethite decreases the interplanar distance d(110), what could be assigned to a higher Cd retention since the crystallographic surface (110) is the dominant for Cd adsorption on goethite (Randall et al., 1999).

In contrast with As and Cd, the presence of Al (treatments with 450:50 Fe:Al molar ratio) decreased Yb and La sorption stability. There were significant increases ($P < 0.05$) in Yb and La bioaccessibility (SBET extractions) due to the presence of Al in coprecipitates at high trace elements concentration (Figure 11). Ytterbium recovery from coprecipitates by acid, reducing, and oxidizing BCR extractants also increased (Figure 10). Notwithstanding, water-soluble Yb (BCR extraction) was the only exception, which is attributed to Yb precipitated with soluble sulfate salts. Treatments with 450:50 Fe:Al molar ratio were also less effective than treatments 500:0 to remove La and Yb from solution by coprecipitation with Fe-oxides (Kroehling et al. in press). Aluminum presence increases Fe-oxides isoelectric point (Souza et al., 2021), which could decrease rare earth elements sorption.

The effect of Al isomorphic substitution on stability of Pb coprecipitated with Fe-oxides was rather controverse. Significantly more Pb ($P < 0.05$) was recovered from Al substituted Fe-oxides (450:50 Fe:Al molar ratio) by BCR acid (Figure 9) and SBET (Figure 11) extractions, but only at high trace elements concentration for bioaccessible Pb (SBET). Conversely, more bioaccessible Pb was recovered from treatments without Al (500:0 Fe:Al molar ratio) by SBET extraction at low trace elements concentration (Figure 11). Therefore, further studies are required in order to elucidate Al effects on sorption stability of Pb coprecipitated with Fe-oxides.

The high trace elements concentration contributed to a significantly higher recovery of Cd and Pb from Fe-oxides by BCR reducing and oxidizing extractions (Figure 9). This higher recovery might be ascribed to lower crystallinity and higher solubility of Fe-oxides precipitated from solutions with high concentration of trace elements (Barcelos et al., 2018; Pietralonga et al., 2017; Vasques et al., 2018a). Furthermore, high concentration of trace elements in 500:0 Fe:Al treatments favored lepidocrocite precipitation (Table 3), which is less stable than goethite or magnetite (Lindsay, 1979; Schwertmann and Taylor, 1989). Nevertheless, there is probably a limit concentration for ion incorporation into Fe-oxides, such that the remaining ions not incorporated would be adsorbed on the surfaces and would be easily extractable as this threshold is overpassed due high concentrations in solution.

Although mercury was not detected in any sample, its presence significantly influenced some of the results related to the stability of the precipitates. Indeed, treatments with 500:0 Fe:Al molar ratio, at high concentration, presented higher BCR extractions in the absence of Hg than in its presence. There were significant differences ($P < 0.05$) for Cd and Pb recovered by BCR reducing extraction (Figure 9 Figure 10). However, these differences may not be due to Hg itself, as they were significant only for these treatments. Actually, these extraction differences could be related to differences in mineral compositions.

Lepidocrocite was the only Fe-oxide identified in treatment with 500:0 Fe:Al molar ratio at high trace elements concentration and without Hg, whereas goethite was also identified in this same treatment with Hg (Table 3). Lepidocrocite is more soluble than goethite (Lindsay, 1979; Schwertmann and Taylor, 1989), which could explain the higher extraction of trace elements from treatments with more lepidocrocite. Indeed, treatments with lepidocrocite (i.e., 500:0 Fe:Al ratio at high trace elements concentration) released more Fe, As, Cd, and Pb than any other treatment, especially in BCR reducing extraction. In contrast, the rare earth elements (i.e., La and Yb) coprecipitated with lepidocrocite were more stable than in treatments with Al-goethite.

In general, bioaccessible contents (SBET extraction) were higher in the presence of Hg for treatments with 500:0 Fe:Al molar ratio at low trace elements concentration, but this difference was significant ($P < 0.05$) for Pb only. As mentioned above, this difference might not be due to Hg itself, but to different mineral compositions. Magnetite was also identified in treatment with 500:0 Fe:Al ratio at low trace elements concentration without Hg. Hence, a lower recovery of the trace elements coprecipitated with Fe-oxides could be ascribed to a lower solubility of magnetite (Schwertmann and Taylor, 1989).

In summary, our results corroborate that the sorption stability depends on both the trace element sorbate and the solid phase sorbent. Arsenic and Cd coprecipitated with Al-goethite were more stable than with lepidocrocite or Al-free-goethite. Conversely, lanthanum and ytterbium sorbed onto Al-goethites were less stable than on Al-free-goethite or even lepidocrocite. In turn, high concentration of trace elements in precipitates decreased stability and increased solubility of Fe-oxides, and favored lepidocrocite precipitation. Finally, we assumed that there is a limit for trace elements incorporation into Fe-oxides and the ions not incorporated would be only adsorbed on the Fe-oxide surfaces.

4.3 Bioaccessibility and risk assessment

Extractions by SBET (Figure 11) were closely related to extractions by BCR method (Figure 8Figure 9Figure 10). Indeed, lanthanum, lead, and ytterbium presented the highest bioaccessibility in relation to pseudo-total contents (average 63.4%, 22.3% and 19.6% respectively). It was recently reported that these elements can be highly bioaccessible in different environments (Cánovas et al., 2023; Ferreira et al., 2022). The high bioaccessibility was associated to a weaker adsorption and lower incorporation of these ions into Fe-oxides structure (Ainsworth et al., 1994; Pietralonga et al., 2017).

On the other hand, arsenic and cadmium presented the lowest SBET extraction percentages (average 2.8% and 4.3%, respectively). Arsenic bioaccessibility assessed in this study is in line with previous reports (0.3% – 5.0%) using soil samples from Paracatu, Brazil (Antônio et al., 2021; Ciminelli et al., 2018). In turn, Cánovas et al. (2023) also found low Cd bioaccessibility (< 8.0%) from sulfide mine wastes and ascribed it to the Cd sorption by Fe-oxides. In this study, we suggest that most of As and Cd ions (> 90%) coprecipitated with Fe-oxides could be trapped inside the structure of these precipitates, which would be related to their lower bioaccessibility.

Although As bioaccessibility was lower than 4% of the pseudo-total content, there is an associated health risk for children due to the high pseudo-total content of As in the precipitates (Table 5 Table 6). The content of As and other trace elements coprecipitated with Fe-oxides is significantly higher than reference values for soils in Brazilian guidelines (CONAMA, 2011; COPAM, 2011) or previously reported contents in sediments and soils from Paracatu (Table 7) (Antônio et al., 2021; Ciminelli et al., 2018). It is worth to note that soils and sediments are natural multi-component materials, whilst only Fe-oxides and some trace elements were considered in this study. Therefore, the role of Fe-oxides was here isolated as the main sink of trace elements in soils and sediments.

The concentrations of iron and trace elements in this study were based on their average content at the Paracatu Formation (Mello et al. unpublished; Oliver et al., 2015). Iron and trace elements (except for Cd and La) are enriched in Paracatu stream sediments compared to the parent material due to their lower mobility in environmental conditions (Table 7). Indeed, Fe-oxides precipitation during weathering is one of the main processes for trace elements immobilization in natural systems (Antônio et al., 2021; Ciminelli et al., 2018; Freitas et al., 2016, 2015). Therefore, the higher concentrations of Fe and trace elements in this study are due

to our focus being on Fe-oxides for better understanding the correlation among the trace elements in experimental conditions.

The high pseudo-total concentrations of As led to bioaccessibility up to 266.7 mg kg^{-1} and hazard quotients that represent health risk for children (HQ > 1.0 for all treatments), although considered safe (HQ < 1.0) for adults (Table 6). Children are more susceptible to contamination due to lower corporal weight and higher soil ingestion rate compared to adults (USEPA, 2007b). Lead presented, after arsenic, the highest HQs due to its high total content in Fe-oxides and high bioaccessibility, but was still considered safe (up to 0.82 for children). Cadmium, lanthanum and ytterbium presented low HQs (< 0.06) due to higher reference doses and lower contents coprecipitated with Fe-oxides (Eq. 4 and 5).

In summary, the bioaccessibility (SBET extractions) of the elements coprecipitated with Fe-oxides proved to be solubility dependent, being closely related to the BCR extractions. For instance, La, Yb, and Pb presented higher bioaccessibility and also higher BCR extraction percentages than As and Cd. Aluminum in treatments 450:50 (Fe:Al molar ratio) increased La and Yb bioaccessibility, and reduced As and Cd bioaccessibility. Moreover, the high contents of As in Fe-oxides represent risk children health. These high contents are rarely found in natural samples, even in soils and sediments impacted by mining operations, but Fe-oxides are widely known as one of the main reservoirs for As, Pb, and other trace elements. However, it can be seen that the Fe:As ratio in Paracatu sediments match the Fe:As in treatments with low As content, justifying the associations made here.

Table 7 – Reference values in Brazilian guidelines, contents found in Paracatu (Minas Gerais, Brazil) and pseudo-total contents for the elements under study.

Metal(loid)	Quality Ref. Value[a]	Prevention Value[b]	Paracatu Formation[c]	Paracatu Sediments[c]	Pseudo-total contents[d]	
					Low	High
	mg kg^{-1}					
Fe	n.e.	n.e.	44,200	111,200	271,539	
As	8.0	15.0	871	1,413	3,741	8,363
Sb	0.5	2.0	1.1	3.9	372	1,057
Pb	19.5	72.0	24.8	55.5	286	607
Cd	< 0.4	1.3	0.5	0.3	138	293
La	66.1[e]	n.e.	19.0	11.0	137	319
Yb	0.8[e]	n.e.	0.3	0.4	24	52

[a] COPAM (2011). [b] CONAMA (2009). [c] Mello et al. (unpublished). [d] Microwave assisted acid digestion average results from the present study. [e] Ferreira et al. (2021). n.e. Not established.

4.4 Environmental applications

Iron oxides precipitation in the environment or in laboratory involves nucleation, crystal growth and transformation (Schwertmann and Cornell, 2000). Trace elements in solution interact with the first embryonic nuclei of Fe in solution, following Fe-oxides crystal growth and phases transformations. The adsorption of trace elements onto newly-formed Fe-oxides nanoparticles can be followed by particles aggregation, coalescence, and entrapment of trace elements inside larger Fe-oxides crystal structure (Freitas et al., 2015; Waychunas et al., 2005). Ions octahedrally coordinated (CN = 6) with ionic radius close to Fe^{3+} (0.065 nm) are more likely to be incorporated into Fe-oxides structure (Burton et al., 2020; Cooper et al., 2006).

Trace elements incorporated to Fe-oxides forming a solid solution would be released only with the solid phase dissolution, differently from adsorbed ions that can be extracted without solubilizing the Fe-oxide. In this study, extractions following BCR and SBET methods solubilized less than 10% of the pseudo-total content of Fe (Figure 8 Figure 11). Therefore, these extractions released preferably adsorbed ions, sulfate salts, and part of the poorly crystallized Fe-oxides, since more than 90% of the Fe remained stable in solid phase. Only a small fraction of incorporated ions rather located close to Fe-oxides particle surface could be extracted following the solid phase dissolution, especially under reducing conditions.

The extraction percentages of As, Cd, and Sb were low (< 10%) compared to La, Pb, and Yb extractions (up to 85.8%, 41.3% and 37.3%, respectively). The residual fraction of these elements would be entrapped in Fe-oxide particles forming a solid solution, unreachable for the extractors. Therefore, based on these indirect methods, we suggest that As, Sb, and Cd were less extracted because of a higher incorporation into Fe-oxides compared to Pb, Yb, and La. Further studies are recommended to confirm this incorporation preference.

5. CONCLUSIONS

Trace elements sorb on Fe-oxides through different mechanisms during coprecipitation, and the sorption stability depends on characteristics of both sorbate and sorbent. Smaller ions are more likely to incorporate into the Fe-oxides structure, resulting in a lower mobility, whilst larger ions are rather adsorbed on the particle surfaces. Aluminum isomorphic substitution in Fe-oxides can increase or reduce the trace element sorption stability, depending on which element is sorbed. The stability of Fe-oxide with high content of trace elements is reduced, and there might be a concentration limit for ions incorporation into Fe-oxide structure. Finally, the results discussed here are anticipated to enhance comprehension of trace elements sorption onto Fe-oxides, encompassing stability and bioavailability of contaminants in the environment.

6. REFERENCES

Ainsworth, C.C., Gassman, P.L., Pilon, J.L., Van Der Sluys, W.G., 1994. Cobalt, Cadmium, and Lead Sorption to Hydrous Iron Oxide: Residence Time Effect. Soil Science Society of America Journal 58, 1615. https://doi.org/10.2136/sssaj1994.03615995005800060005x

Antônio, D.C., Caldeira, C.L., Freitas, E.T.F., Delbem, I.D., Gasparon, M., Olusegun, S.J., Ciminelli, V.S.T., 2021. Effects of aluminum and soil mineralogy on arsenic bioaccessibility. Environmental Pollution 274. https://doi.org/10.1016/j.envpol.2021.116482

Baig, J.A., Kazi, T.G., Arain, M.B., Shah, A.Q., Sarfraz, R.A., Afridi, H.I., Kandhro, G.A., Jamali, M.K., Khan, S., 2009. Arsenic fractionation in sediments of different origins using BCR sequential and single extraction methods. J Hazard Mater 167, 745–751. https://doi.org/10.1016/j.jhazmat.2009.01.040

Barcelos, G.S., Veloso, R.W., de Mello, J.W.V., Gasparon, M., 2018. Immobilization of Eu and Ho from synthetic acid mine drainage by precipitation with Fe and Al (hydr)oxides. Environmental Science and Pollution Research 25, 18813–18822. https://doi.org/10.1007/s11356-018-2100-5

Bauer, A., Velde, B.D., 2014. Geochemistry at the Earth's Surface. Springer Berlin Heidelberg, Berlin, Heidelberg. https://doi.org/10.1007/978-3-642-31359-2

Bonnissel-Gissinger, P., Alnot, M., Lickes, J.-P., Ehrhardt, J.-J., Behra, P., 1999. Modeling the Adsorption of Mercury(II) on (Hydr)oxides II: α-FeOOH (Goethite) and Amorphous Silica. J Colloid Interface Sci 215, 313–322. https://doi.org/10.1006/jcis.1999.6263

Brazil, 2010. Guidelines for Evaluation of Risks to Human Health from Exposure to Chemical Contaminants (in Portuguese). Brasília.

Bruemmer, G.W., Gerth, J., Tiller, K.G., 1988. Reaction kinetics of the adsorption and desorption of nickel, zinc and cadmium by goethite. I. Adsorption and diffusion of metals. Journal of Soil Science 39, 37–52. https://doi.org/10.1111/j.1365-2389.1988.tb01192.x

Burton, E.D., Hockmann, K., Karimian, N., 2020. Antimony Sorption to Goethite: Effects of Fe(II)-Catalyzed Recrystallization. ACS Earth Space Chem 4, 476–487. https://doi.org/10.1021/acsearthspacechem.0c00013

Cánovas, C.R., Quispe, D., Macías, F., Callejón-Leblic, B., Arias-Borrego, A., García-Barrera, T., Nieto, J.M., 2023. Potential release and bioaccessibility of metal/loids from mine wastes deposited in historical abandoned sulfide mines. Environmental Pollution 316, 120629. https://doi.org/10.1016/j.envpol.2022.120629

Ciminelli, V.S.T., Antônio, D.C., Caldeira, C.L., Freitas, E.T.F., Delbem, I.D., Fernandes, M.M., Gasparon, M., Ng, J.C., 2018. Low arsenic bioaccessibility by fixation in nanostructured iron (Hydr)oxides: Quantitative identification of As-bearing phases. J Hazard Mater 353, 261–270. https://doi.org/10.1016/j.jhazmat.2018.03.037

CONAMA, 2011. Resolução 430/2011 (in Portuguese).

CONAMA, 2009. Resolução 420/2009 (in Portuguese).

Cooper, D.C., Picardal, F.F., Coby, A.J., 2006. Interactions between Microbial Iron Reduction and Metal Geochemistry: Effect of Redox Cycling on Transition Metal Speciation in Iron Bearing Sediments. Environ Sci Technol 40, 1884–1891. https://doi.org/10.1021/es051778t

COPAM, 2011. Deliberação Normativa 166/2011 (in Portuguese).

Cornell, R.M., Schwertmann, U., 2003. The Iron Oxides. Wiley. https://doi.org/10.1002/3527602097

Ferreira, M. da S., Fontes, M.P.F., Bellato, C.R., Marques Neto, J. de O., Lima, H.N., Fendorf, S., 2021. Geochemical signatures and natural background values of rare earth elements in soils of Brazilian Amazon. Environmental Pollution 277, 116743. https://doi.org/10.1016/j.envpol.2021.116743

Ferreira, M. da S., Fontes, M.P.F., Lima, M.T.W.D.C., Cordeiro, S.G., Wyatt, N.L.P., Lima, H.N., Fendorf, S., 2022. Human health risk assessment and geochemical mobility of rare earth elements in Amazon soils. Science of The Total Environment 806, 151191. https://doi.org/10.1016/j.scitotenv.2021.151191

Freitas, E.T.F., Montoro, L.A., Gasparon, M., Ciminelli, V.S.T., 2015. Natural attenuation of arsenic in the environment by immobilization in nanostructured hematite. Chemosphere 138, 340–347. https://doi.org/10.1016/j.chemosphere.2015.05.101

Freitas, E.T.F., Stroppa, D.G., Montoro, L.A., de Mello, J.W.V., Gasparon, M., Ciminelli, V.S.T., 2016. Arsenic entrapment by nanocrystals of Al-magnetite: The role of Al in crystal growth and As retention. Chemosphere 158, 91–99. https://doi.org/10.1016/j.chemosphere.2016.05.044

Gil-Díaz, M., Rodríguez-Alonso, J., Maffiotte, C.A., Baragaño, D., Millán, R., Lobo, M.C., 2021. Iron nanoparticles are efficient at removing mercury from polluted waters. J Clean Prod 315, 128272. https://doi.org/10.1016/j.jclepro.2021.128272

Gong, Y., Huang, Y., Wang, M., Liu, F., Zhang, T., 2019. Application of Iron-Based Materials for Remediation of Mercury in Water and Soil. Bull Environ Contam Toxicol 102, 721–729. https://doi.org/10.1007/s00128-019-02559-4

Jeong, S., Yang, K., Jho, E.H., Nam, K., 2017. Importance of chemical binding type between As and iron-oxide on bioaccessibility in soil: Test with synthesized two line ferrihydrite. J Hazard Mater 330, 157–164. https://doi.org/10.1016/j.jhazmat.2017.02.009

Kroehling, D.R.C., Veloso, R.W., Mello, J.W.V., Carvalho, A.M.X., Oliveira, M.F., Vasques, I.C.F., in press. Coprecipitation of Fe-Al-oxides and trace elements from an orogenic gold deposit environment.

Langner, H.W., Inskeep, W.P., 2000. Microbial Reduction of Arsenate in the Presence of Ferrihydrite. Environ Sci Technol 34, 3131–3136. https://doi.org/10.1021/es991414z

Leuz, A.-K., Mönch, H., Johnson, C.A., 2006. Sorption of Sb(III) and Sb(V) to Goethite: Influence on Sb(III) Oxidation and Mobilization. Environ Sci Technol 40, 7277–7282. https://doi.org/10.1021/es061284b

Lindsay, W.L., 1979. Chemical Equilibria in Soils. John Wiley & Sons.

Liu, H., Pourret, O., Guo, H., Martinez, R.E., Zouhri, L., 2018. Impact of Hydrous Manganese and Ferric Oxides on the Behavior of Aqueous Rare Earth Elements (REE): Evidence from a Modeling Approach and Implication for the Sink of REE. Int J Environ Res Public Health 15, 2837. https://doi.org/10.3390/ijerph15122837

Lu, P., Nuhfer, N.T., Kelly, S., Li, Q., Konishi, H., Elswick, E., Zhu, C., 2011. Lead coprecipitation with iron oxyhydroxide nano-particles. Geochim Cosmochim Acta 75, 4547–4561. https://doi.org/10.1016/j.gca.2011.05.035

Mello, J.W.V., Gasparon, M., Silva, J., 2018. Effectiveness of arsenic co-precipitation with Fe-Al hydroxides for treatment of contaminated water. Rev Bras Cienc Solo 42. https://doi.org/10.1590/18069657rbcs20170261

Mello, J.W. V., Nepomuceno, A.L., Matos, A.A.S., Guimarães, P.J., Mendonça, G. V., Silva, S.C., unpublished. Antimony, mercury and other elements as tracers for geogenic origin and impacts of artisanal mining on arsenic distribution in sediments from an orogenic gold mineralization area. Unsubmitted.

Melo, V.F., Batista, A.H., Gilkes, R.J., Rate, A.W., 2016. Relationship between heavy metals and minerals extracted from soil clay by standard and novel acid extraction procedures. Environ Monit Assess 188, 668. https://doi.org/10.1007/s10661-016-5690-8

Mo, X., Siebecker, M.G., Gou, W., Li, L., Li, W., 2021. A review of cadmium sorption mechanisms on soil mineral surfaces revealed from synchrotron-based X-ray absorption fine structure spectroscopy: Implications for soil remediation. Pedosphere 31, 11–27. https://doi.org/10.1016/S1002-0160(20)60017-0

Oliver, N.H.S., Thomson, B., Freitas-Silva, F.H., Holcombe, R.J., Rusk, B., Almeida, B.S., Faure, K., Davidson, G.R., Esper, E.L., Guimarães, P.J., Dardenne, M.A., 2015. Local and Regional Mass Transfer During Thrusting, Veining, and Boudinage in the Genesis of the Giant Shale-Hosted Paracatu Gold Deposit, Minas Gerais, Brazil. Economic Geology 110, 1803–1834. https://doi.org/10.2113/econgeo.110.7.1803

Padmanabham, M., 1983. Comparative study of the adsorption-desorption behaviour of copper(II), zinc(II), cobalt(II) and lead(II) at the goethite solution interface. Soil Research 21, 515. https://doi.org/10.1071/SR9830515

Pietralonga, A.G., de Mendonça, B.A.F., Barcelos, G.S., de Mello, J.W.V., Abrahão, W.A.P., 2017. Lanthanum immobilization by iron and aluminum colloids. Environ Earth Sci 76. https://doi.org/10.1007/s12665-017-6583-z

Randall, S.R., Sherman, D.M., Ragnarsdottir, K. V, Collins, C.R., 1999. The mechanism of cadmium surface complexation on iron oxyhydroxide minerals. Geochim Cosmochim Acta 63, 2971–2987. https://doi.org/10.1016/S0016-7037(99)00263-X

Rauret, G., López-Sánchez, J.F., Sahuquillo, A., Rubio, R., Davidson, C., Ure, A., Quevauviller, Ph., 1999. Improvement of the BCR three step sequential extraction procedure prior to the certification of new sediment and soil reference materials. Journal of Environmental Monitoring 1, 57–61. https://doi.org/10.1039/a807854h

Richard, J.-H., Bischoff, C., Ahrens, C.G.M., Biester, H., 2016. Mercury (II) reduction and co-precipitation of metallic mercury on hydrous ferric oxide in contaminated groundwater. Science of The Total Environment 539, 36–44. https://doi.org/10.1016/j.scitotenv.2015.08.116

Schulze, D.G., 1984. The Influence of Aluminum on Iron Oxides. VIII. Unit-Cell Dimensions of Al-Substituted Goethites and Estimation of Al From Them. Clays Clay Miner 32, 36–44. https://doi.org/10.1346/CCMN.1984.0320105

Schwertmann, U., Cornell, R.M., 2000. Iron Oxides in the Laboratary. Wiley-VCH Verlag GmbH. https://doi.org/10.1002/9783527613229

Schwertmann, U., Taylor, R.M., 1989. Iron Oxides. https://doi.org/10.2136/sssabookser1.2ed.c8

Shangguan, Y., Qin, X., Zhao, L., Wang, L., Hou, H., 2016. Effects of iron oxide on antimony(V) adsorption in natural soils: transmission electron microscopy and X-ray photoelectron spectroscopy measurements. J Soils Sediments 16, 509–517. https://doi.org/10.1007/s11368-015-1229-9

Silva, J., Mello, J.W.V., Gasparon, M., Abrahão, W.A.P., Ciminelli, V.S.T., Jong, T., 2010. The role of Al-Goethites on arsenate mobility. Water Res 44, 5684–5692. https://doi.org/10.1016/j.watres.2010.06.056

Souza, T.G.F., Freitas, E.T.F., Mohallem, N.D.S., Ciminelli, V.S.T., 2021. Defects induced by Al substitution enhance As(V) adsorption on ferrihydrites. J Hazard Mater 420, 126544. https://doi.org/10.1016/j.jhazmat.2021.126544

Sposito, G., 2008. The Chemistry of Soils, Second edition. ed. Oxford University Press, New York.

Sun, G., Li, Z., Liu, T., Chen, J., Wu, T., Feng, X., 2017. Rare earth elements in street dust and associated health risk in a municipal industrial base of central China. Environ Geochem Health 39, 1469–1486. https://doi.org/10.1007/s10653-017-9982-x

Tong, L., He, J., Wang, F., Wang, Y., Wang, L., Tsang, D.C.W., Hu, Q., Hu, B., Tang, Y., 2020. Evaluation of the BCR sequential extraction scheme for trace metal fractionation of alkaline municipal solid waste incineration fly ash. Chemosphere 249, 126115. https://doi.org/10.1016/j.chemosphere.2020.126115

Ure, A.M., 1991. Trace element speciation in soils, soil extracts and solutions. Microchimica Acta 104, 49–57. https://doi.org/10.1007/BF01245495

Ure, A.M., Quevauviller, Ph., Muntau, H., Griepink, B., 1993. Speciation of Heavy Metals in Soils and Sediments. An Account of the Improvement and Harmonization of Extraction Techniques Undertaken Under the Auspices of the BCR of the Commission of the European Communities. Int J Environ Anal Chem 51, 135–151. https://doi.org/10.1080/03067319308027619

USEPA, 2008. Standard Operating Procedure for an In Vitro Bioaccessibility Assay for Lead in Soil.

USEPA, 2007a. Method 3051A (SW-846): Microwave Assisted Acid Digestion of Sediments, Sludges, and Oils. Washington, DC.

USEPA, 2007b. Guidance for Evaluating the Oral Bioavailability of Metals in Soils for Use in Human Health Risk Assessment 1–18.

USEPA, 1991. IRIS Assessment on inorganic arsenic (CASRN 7440-38-2).

Vasques, Isabela C.F., de Mello, J.W.V., Veloso, R.W., Ferreira, V.P., Abrahão, W.A.P., 2018. Arsenite removal from contaminated water by precipitation of aluminum, ferrous and ferric (hydr)oxides. Environmental Science and Pollution Research 25, 12967–12980. https://doi.org/10.1007/s11356-018-1458-8

Vasques, Isabela C. F., de Mello, J.W. V., Veloso, R.W., Ferreira, V. de P., Abrahão, W.A.P., 2018. Effectiveness of Ferric, Ferrous, and Aluminum (Hydr)Oxide Coprecipitation to Treat Water Contaminated with Arsenate. J Environ Qual 47, 1339–1346. https://doi.org/10.2134/jeq2018.01.0014

Wang, C.-C., Zhang, Q.-C., Kang, S.-G., Li, M.-Y., Zhang, M.-Y., Xu, W.-M., Xiang, P., Ma, L.Q., 2023. Heavy metal(loid)s in agricultural soil from main grain production regions of China: Bioaccessibility and health risks to humans. Science of The Total Environment 858, 159819. https://doi.org/10.1016/j.scitotenv.2022.159819

Waychunas, G.A., Kim, C.S., Banfield, J.F., 2005. Nanoparticulate Iron Oxide Minerals in Soils and Sediments: Unique Properties and Contaminant Scavenging Mechanisms. Journal of Nanoparticle Research 7, 409–433. https://doi.org/10.1007/s11051-005-6931-x

Yang, M., Liang, X., Li, Y., He, H., Zhu, R., Arai, Y., 2021. Ferrihydrite Transformation Impacted by Adsorption and Structural Incorporation of Rare Earth Elements. ACS Earth Space Chem 5, 2768–2777. https://doi.org/10.1021/acsearthspacechem.1c00159

CONSIDERAÇÕES FINAIS

A coprecipitação de óxidos de Fe e elementos-traço se provou mais uma vez eficaz no tratamento de água contaminada. Entretanto, elementos-traço correlacionados nos depósitos orogênicos de ouro não apresentam a mesma correlação na coprecipitação em condições ambientais. Este trabalho mostrou que a imobilização de As, Pb, Sb e Yb é mais rápida que a de Cd e La durante a coprecipitação.

A substituição isomórfica do Al nos óxidos de Fe afeta a imobilização dos elementos-traço. A presença de Al aumentou a imobilização de La e Yb no curto-prazo, mas reduziu a imobilização desses elementos terras raras em longo-prazo. Por outro lado, o efeito do Al na precipitação de As e Cd foi o oposto: menor imobilização no curto-prazo, mas maior imobilização no longo-prazo. Os efeitos do Al durante a coprecipitação devem estar relacionados com a transformação de fases minerais durante o crescimento dos cristais de óxidos de Fe.

O Al estrutural também afeta a mineralogia e a estabilidade dos óxidos de Fe. Os tratamentos com Al formaram apenas goethita com substituição isomórfica (Al-goethita) devido à alta capacidade da goethita em incorporar Al. Além disso, menor quantidade de Fe foi extraída da Al-goethita do que da goethita ou lepidocrocita sem Al, indicando que o Al estrutural reduz a solubilidade da goethita. Não obstante, nossos resultados indicaram que As e Cd são mais estáveis coprecipitados com Al-goethita, enquanto La e Yb são mais estáveis com goethita e lepidocrocita sem Al.

Os elementos-traço coprecipitados apresentaram diferentes mecanismos de sorção nos óxidos de ferro. A menor extração de As, Sb e Cd (< 10%) pode estar relacionada com a maior incorporação desses na estrutura do óxido de Fe. Por outro lado, altas porcentagens de extração de La, Pb e Yb (até 86%, 41% e 37%, respectivamente) indicam que esses elementos não têm a mesma capacidade de incorporação. Íons menores e mais parecidos com Fe^{2+} ou Fe^{3+} devem ter uma maior capacidade de incorporação no óxido de Fe coprecipitado.

As razões molares entre Fe e elementos-traço neste trabalho (500:5 e 500:10) são altas quando comparadas com as razões encontradas em sistemas naturais, mesmo em áreas contaminadas. Isso fez com que os teores bioacessíveis de As nos precipitados (apesar de serem menores que 4% do conteúdo pseudo-total) representem risco para a saúde de crianças. Além disso, altas concentrações de elementos-traço favorecem a precipitação de lepidocrocita, mas apenas na ausência do Al.

O mercúrio não influenciou significativamente a remoção ou a estabilidade dos elementos-traço. A concentração de Hg no experimento pode não ter sido alta o suficiente para afetar a sorção dos outros elementos. Portanto, a hipótese de que Hg compete com os outros elementos por sítios de adsorção nos óxidos de ferro não foi confirmada.

Por fim, a discussão proposta neste trabalho tratou de aspectos relevantes sobre a dinâmica de elementos-traço em sistemas naturais, e avançou na compreensão dos mecanismos de sorção em óxidos de ferro. Espera-se que o trabalho contribua para um maior embasamento científico na remediação de áreas contaminadas, principalmente aquelas afetadas por drenagem ácida de mina.

SUPPLEMENTARY MATERIAL

Table S1 – Supernatant pH measured during coprecipitation period.

Treat*	0	1d	4d	7d	14d	21d	35d	68d	90d
a1b1c1	2.7	7.9	7.6	7.7	6.6	6.3	6.8	4.8	6.1
a1b1c1	2.3	7.5	6.7	7.0	6.4	6.8	6.2	3.8	5.8
a1b1c1	2.2	7.6	6.8	6.9	6.0	6.3	5.4	4.9	6.0
a1b1c2	2.3	7.3	6.8	6.7	6.1	6.5	6.8	5.6	5.9
a1b1c2	2.3	7.4	6.9	6.5	5.9	6.8	6.1	3.5	5.9
a1b1c2	2.2	7.3	7.0	6.4	6.1	6.2	5.7	5.2	6.2
a1b2c1	2.0	6.9	6.9	6.9	6.3	6.6	6.2	5.6	4.1
a1b2c1	2.0	7.2	6.8	6.3	6.1	6.2	6.4	5.8	5.7
a1b2c1	2.0	7.0	6.4	6.6	6.1	6.3	3.6	3.6	6.6
a1b2c2	2.1	7.1	6.7	6.9	6.1	6.8	6.3	5.3	4.5
a1b2c2	2.1	7.1	6.3	7.2	6.1	6.2	6.1	5.5	5.0
a1b2c2	2.1	5.7	6.0	6.9	6.0	6.7	6.1	3.2	3.5
a2b1c1	1.9	6.6	6.2	6.8	5.9	6.3	6.0	5.4	5.1
a2b1c1	1.8	6.6	6.3	6.0	6.0	6.2	5.4	4.1	6.8
a2b1c1	1.8	6.7	6.5	7.2	6.0	6.0	5.8	4.2	4.4
a2b1c2	1.8	7.2	6.4	6.5	6.1	6.6	6.2	4.6	4.7
a2b1c2	1.9	6.6	6.2	6.0	5.8	6.2	5.4	4.0	6.5
a2b1c2	1.9	6.4	6.3	6.3	5.9	6.0	6.1	5.3	4.6
a2b2c1	1.8	5.8	5.7	6.5	5.8	6.2	5.1	4.4	6.0
a2b2c1	1.8	6.9	5.9	6.0	5.9	6.1	4.5	5.6	5.2
a2b2c1	1.8	6.9	6.4	6.0	5.9	6.2	5.9	5.3	5.2
a2b2c2	1.8	6.4	6.3	6.3	5.9	6.2	5.8	5.3	4.6
a2b2c2	1.7	6.6	5.9	6.4	6.0	6.0	5.8	5.1	4.8
a2b2c2	1.8	6.4	6.3	6.0	6.0	6.2	5.5	4.7	5.0
e1	2.6	7.4	7.0	7.1	6.4	6.4	5.9	5.7	5.9
e1	2.5	7.4	7.0	7.2	6.6	6.5	6.6	4.9	5.9
e1	2.6	7.4	6.9	7.4	6.3	6.3	6.6	3.4	3.9
e2	2.0	6.6	6.5	6.6	5.8	6.5	6.2	5.9	4.9
e2	2.0	6.9	6.4	6.1	5.7	6.1	5.4	4.3	4.7
e2	2.0	7.2	6.8	6.2	5.8	6.3	5.9	4.5	4.8

* Treatments: a1) Fe:Al = 500:0, a2) 450:50, b1) Trace elements concentrations = Low, b2) High, c1) Without Hg, c2) With Hg, e1) Control 500:0, e2) Control 450:50.

Table S2 – Supernatant concentration (mg L^{-1}) by ICP-OES during coprecipitation period.

Treat*	Fe				Al				As			
	2h	1d	21d	90d	2h	1d	21d	90d	2h	1d	21d	90d
a1b1c1	4857	8912	1727	1430	5.52	6.05	5.57	5.34	2.05	111.55	0.49	0.00
a1b1c1	10458	10842	5577	2108	5.43	5.39	5.45	5.36	0.78	1.40	0.23	0.18
a1b1c1	7169	8573	3552	840	5.40	5.57	5.54	5.53	1.71	2.26	1.12	0.48
a1b1c2	8689	10775	3846	1029	5.95	5.39	5.49	5.45	1.72	1.07	1.02	0.16
a1b1c2	9452	11242	5327	1197	5.37	5.42	5.51	5.40	1.30	0.83	0.59	0.33
a1b1c2	8450	10675	4661	911	5.61	5.37	5.51	5.40	1.68	3.32	0.71	1.24
a1b2c1	10592	11458	4149	1735	5.75	5.33	5.55	5.42	2.91	1.08	1.23	10.65
a1b2c1	9922	10034	3518	1903	5.31	5.37	5.51	5.51	2.59	1.54	2.78	4.06
a1b2c1	10438	10100	6519	108	5.29	5.49	5.41	5.41	2.92	1.93	1.43	0.64
a1b2c2	10849	10909	3626	2099	5.30	5.40	5.52	5.61	2.37	1.33	1.55	4.07
a1b2c2	10186	9718	4654	1970	5.42	5.53	5.47	5.42	2.76	3.28	2.14	4.91
a1b2c2	10365	10287	5904	2371	5.26	5.56	5.51	5.54	13.95	1.83	0.83	2.11
a2b1c1	9248	9028	4515	588	5.50	6.41	5.60	8.61	4.66	3.76	0.61	0.54
a2b1c1	9136	9389	3133	61	5.51	6.26	5.75	5.48	8.84	3.75	0.45	0.25
a2b1c1	9094	9048	5377	1426	5.42	5.69	5.68	27.71	3.13	2.79	0.19	0.65
a2b1c2	8416	8557	2838	1239	5.42	5.60	5.65	15.72	2.40	2.59	0.30	0.61
a2b1c2	9944	9180	4207	108	5.31	5.84	5.66	5.47	4.50	3.68	0.24	0.31
a2b1c2	9751	8992	4864	610	5.38	6.33	5.62	11.68	12.33	4.27	0.21	0.33
a2b2c1	10941	10430	4724	0	5.21	6.02	5.61	5.53	97.87	15.11	0.28	0.23
a2b2c1	8634	9661	4291	0	5.43	5.74	5.62	5.66	4.05	4.32	0.63	0.37
a2b2c1	9907	9821	3831	831	5.31	5.74	5.59	6.46	19.99	5.03	0.42	0.85
a2b2c2	9150	9235	4024	514	5.39	5.86	5.60	12.08	13.68	6.94	1.13	0.81
a2b2c2	9102	10246	4741	985	5.42	5.58	5.61	8.56	24.83	6.53	0.25	1.11
a2b2c2	9378	9547	3358	0	5.35	5.56	5.65	6.32	23.33	6.59	0.50	0.35
e1	10371	10541	6980	1871	5.17	5.39	5.55	5.45	-6.36	-6.57	-1.12	-0.53
e1	10027	10483	5995	2197	5.24	5.32	5.63	5.41	-6.16	-6.27	-0.94	-0.60
e1	10384	11123	5114	2945	5.21	5.37	5.59	5.42	-6.33	-7.56	-0.87	-0.74
e2	9470	9425	4920	601	5.39	5.45	5.60	4.14	-5.61	-5.79	-0.87	-0.11
e2	9113	11063	5705	332	5.61	5.11	6.13	8.99	-5.14	-7.58	-0.74	-0.20
e2	8968	9249	6404	538	6.00	5.48	5.72	10.86	-5.15	-5.83	-0.71	0.14

* Treatments: a1) Fe:Al = 500:0, a2) 450:50, b1) Trace elements concentrations = Low, b2) High, c1) Without Hg, c2) With Hg, e1) Control 500:0, e2) Control 450:50.

Table S3 – Supernatant concentration (mg L^{-1}) by ICP-OES during coprecipitation period.

Treat*	Sb				Pb				Cd			
	2h	1d	21d	90d	2h	1d	21d	90d	2h	1d	21d	90d
a1b1c1	-0.18	-0.03	0.07	0.14	0.00	8.83	0.02	0.00	0.03	2.64	0.15	0.24
a1b1c1	-1.06	-1.05	0.01	0.13	0.54	0.60	0.06	-0.01	0.47	0.08	0.16	0.28
a1b1c1	-0.67	-0.81	0.07	0.11	0.00	0.03	0.01	0.00	-0.04	-0.03	0.19	0.19
a1b1c2	-0.39	-1.16	-0.10	0.10	0.07	0.54	0.04	0.03	0.24	0.10	0.11	0.21
a1b1c2	-0.64	-1.16	0.04	0.06	0.32	0.61	0.06	0.01	0.16	0.09	0.20	0.25
a1b1c2	-0.71	-0.83	-0.01	0.12	0.09	0.68	0.11	0.01	0.17	0.10	0.17	0.22
a1b2c1	-0.92	-1.17	-0.01	-0.05	0.66	1.09	0.13	0.10	0.74	0.58	0.16	1.48
a1b2c1	-0.94	-0.85	0.26	0.13	0.48	0.42	0.14	0.01	0.60	0.10	0.30	0.63
a1b2c1	-1.10	-0.88	0.19	0.09	0.63	0.46	0.04	-0.05	0.79	0.19	0.44	0.07
a1b2c2	-0.83	-1.30	0.03	0.11	0.71	0.78	0.02	-0.02	0.78	0.23	0.17	0.77
a1b2c2	-0.94	-0.80	0.24	0.05	0.51	0.42	0.06	0.00	0.72	0.13	0.26	0.90
a1b2c2	-0.58	-0.98	0.13	-0.04	0.87	0.39	0.12	-0.01	1.06	0.27	0.18	0.76
a2b1c1	-0.89	-0.45	-0.02	0.12	0.28	0.24	0.04	0.02	0.34	0.34	0.14	0.28
a2b1c1	-0.65	-0.83	-0.08	0.12	0.35	0.32	0.02	-0.03	0.58	0.36	0.24	0.06
a2b1c1	-0.88	-0.52	-0.08	0.08	0.34	0.16	0.00	0.04	0.29	0.31	0.16	0.51
a2b1c2	-0.42	-0.48	0.00	0.06	0.14	0.17	-0.01	0.10	0.18	0.13	0.10	0.36
a2b1c2	-0.89	-0.88	0.04	0.01	0.52	0.29	0.06	-0.01	0.39	0.22	0.25	0.06
a2b1c2	-0.72	-0.66	-0.06	0.15	0.49	0.34	0.06	0.06	0.61	0.27	0.21	0.30
a2b2c1	-0.97	-0.79	0.04	0.14	2.06	0.91	-0.02	-0.01	1.00	1.27	0.23	0.10
a2b2c1	-0.69	-0.63	0.08	0.07	0.13	0.29	0.06	0.03	0.38	0.54	0.53	0.34
a2b2c1	-0.73	-0.75	0.00	0.09	0.57	0.35	0.01	0.10	1.17	0.55	0.19	0.58
a2b2c2	-1.10	-0.61	0.16	-0.06	0.28	0.32	0.10	0.06	0.92	0.61	0.41	0.62
a2b2c2	-0.83	-0.72	-0.04	0.17	0.50	0.53	0.03	0.19	0.96	0.78	0.19	0.59
a2b2c2	-0.61	-0.81	0.14	0.14	0.59	0.41	0.01	0.04	1.35	0.61	0.38	0.28
e1	-1.10	-0.83	-0.14	0.08	0.58	0.64	0.16	0.07	0.00	-0.02	0.11	0.08
e1	-0.80	-0.98	0.13	0.24	0.47	0.59	0.05	0.07	-0.04	-0.02	0.09	0.08
e1	-0.98	-1.29	0.08	-0.07	0.58	0.93	0.08	0.11	-0.02	0.05	0.10	0.09
e2	-1.01	-0.59	0.15	Lost	0.30	0.27	0.04	Lost	-0.05	-0.04	0.08	Lost
e2	-0.94	-1.11	0.24	0.06	0.27	0.90	-0.01	0.04	-0.05	0.01	0.07	0.06
e2	-0.82	-0.79	0.09	0.21	0.22	0.28	0.05	0.11	-0.05	-0.09	0.08	0.50

* Treatments: a1) Fe:Al = 500:0, a2) 450:50, b1) Trace elements concentrations = Low, b2) High, c1) Without Hg, c2) With Hg, e1) Control 500:0, e2) Control 450:50.

Table S4 – Supernatant concentration (mg L^{-1}) by ICP-OES during coprecipitation period.

Treat*	La				Yb				Hg			
	2h	1d	21d	90d	2h	1d	21d	90d	2h	1d	21d	90d
a1b1c1	0.99	6.33	0.34	0.33	-0.10	0.59	0.18	-0.54	-0.80	-0.93	-0.97	-0.44
a1b1c1	14.80	9.56	0.34	0.32	0.05	0.04	0.19	-0.86	-1.59	-1.11	-1.09	-0.61
a1b1c1	8.04	6.91	0.35	0.34	-0.07	-0.04	0.19	-0.86	-0.85	-0.74	-1.02	-0.68
a1b1c2	12.03	8.60	0.37	0.33	0.00	0.03	0.20	-0.53	-1.23	-1.01	-0.74	-0.38
a1b1c2	11.47	9.57	0.37	0.33	0.02	0.04	0.22	-0.69	-1.19	-1.17	-1.00	-0.39
a1b1c2	11.21	10.18	0.36	0.34	-0.02	0.05	0.21	-0.77	-1.18	-1.14	-1.07	-0.55
a1b2c1	24.31	24.82	0.51	0.33	0.16	0.12	0.23	-0.91	-1.23	-1.49	-0.82	-0.43
a1b2c1	24.55	17.97	0.35	0.34	0.07	0.02	0.26	-1.05	-1.34	-1.00	-1.23	-0.94
a1b2c1	25.41	20.10	0.36	0.33	0.11	0.03	0.20	-1.18	-1.44	-1.08	-1.30	-0.79
a1b2c2	28.02	19.78	0.76	0.34	0.14	0.06	0.20	-1.06	-1.53	-1.20	-0.69	-0.11
a1b2c2	22.92	15.23	0.36	0.34	0.07	0.02	0.23	-0.98	-1.27	-0.85	-0.98	-0.63
a1b2c2	24.48	20.05	0.37	0.33	0.32	0.05	0.21	-0.72	-1.21	-1.21	-0.96	-0.93
a2b1c1	7.13	5.01	0.43	0.35	-0.01	-1.00	0.25	-0.32	-1.11	-0.82	-0.90	-0.53
a2b1c1	6.99	5.28	0.42	0.33	-0.01	-0.01	0.19	-0.54	-1.13	-0.96	-0.85	-0.25
a2b1c1	6.73	4.91	0.50	0.33	-0.01	-0.02	0.19	-0.60	-1.11	-0.95	-1.08	-0.04
a2b1c2	5.70	4.53	0.42	0.34	-0.03	-0.04	0.18	-0.47	-1.01	-0.84	-0.64	-0.45
a2b1c2	8.57	5.18	0.43	0.34	0.03	-0.02	0.19	-0.46	-1.35	-0.81	-0.98	-0.31
a2b1c2	8.19	4.73	0.58	0.34	0.02	-0.02	0.22	-0.39	-1.31	-0.83	-1.10	-0.07
a2b2c1	21.98	12.85	0.44	0.34	0.12	0.05	0.19	-0.49	-1.59	-1.09	-0.63	-0.23
a2b2c1	12.91	11.69	0.38	0.34	-0.02	0.00	0.19	-0.44	-0.98	-1.03	-1.05	-0.14
a2b2c1	18.80	11.94	0.39	0.34	0.05	0.01	0.20	-0.44	-1.43	-1.06	-0.73	-0.24
a2b2c2	15.04	10.37	0.42	0.33	0.01	0.00	0.34	-0.48	-1.09	-0.93	-1.05	-0.43
a2b2c2	14.42	14.12	0.38	0.34	0.01	0.04	0.20	-0.50	-1.08	-1.21	-1.04	-0.43
a2b2c2	16.76	11.64	0.35	0.37	0.03	0.01	0.18	-0.30	-1.17	-0.94	-0.72	-0.47
e1	-0.43	-0.43	0.31	0.32	0.04	0.03	0.20	-1.02	-1.25	-1.17	-1.42	-0.25
e1	-0.41	-0.42	0.32	0.32	0.01	0.03	0.19	-0.99	-1.12	-1.10	-1.12	-0.81
e1	-0.43	-0.45	0.31	0.32	0.04	0.08	0.20	-1.16	-1.34	-1.39	-1.27	-0.92
e2	-0.40	-0.40	0.32	0.33	-0.01	-0.02	0.19	-0.34	-1.13	-0.90	-0.95	Lost
e2	-0.39	-0.46	0.32	0.33	-0.02	0.07	0.19	-0.42	-0.98	-1.68	-0.84	0.01
e2	-0.37	-0.39	0.32	0.33	-0.02	-0.02	0.19	-0.44	-1.03	-0.92	-1.04	-0.34

* Treatments: a1) Fe:Al = 500:0, a2) 450:50, b1) Trace elements concentrations = Low, b2) High, c1) Without Hg, c2) With Hg, e1) Control 500:0, e2) Control 450:50.

Table S5 – Pseudo-total contents of precipitates (mg kg^{-1}) extracted by Method 3051A (USEPA, 2007a).

Treat*	Fe	Al	As	Pb	Cd	La	Yb	Sb	Hg
a1b1c1	224,683	- 10	2,931	393	108	99	17.7	328	0.1
a1b1c1	238,647	- 10	3,169	220	116	103	19.6	383	- 5.4
a1b1c1	297,172	- 5	4,711	327	174	156	28.5	330	- 2.8
a1b1c2	250,306	- 30	3,464	245	127	116	21.4	297	- 4.8
a1b1c2	230,600	- 37	3,046	209	112	102	18.7	402	- 4.6
a1b1c2	254,211	- 38	3,544	243	131	112	22.5	286	0.1
a1b2c1	320,111	- 32	9,782	657	332	330	56.2	1,236	- 1.0
a1b2c1	304,512	- 34	8,773	595	302	311	52.7	1,143	- 0.9
a1b2c1	248,278	- 30	6,384	449	243	213	37.7	881	-12.3
a1b2c2	318,224	- 36	9,870	662	337	332	56.7	1,352	- 0.7
a1b2c2	302,596	- 34	8,838	584	305	296	52.1	1,224	- 0.2
a1b2c2	271,719	- 37	7,392	540	257	264	41.0	967	- 9.7
a2b1c1	265,486	21,579	4,117	309	151	164	27.9	504	- 8.5
a2b1c1	257,132	19,906	3,735	287	140	149	27.0	441	- 8.9
a2b1c1	255,788	20,103	3,885	280	141	155	21.6	344	- 6.1
a2b1c2	274,975	21,428	4,205	320	152	172	25.9	441	- 4.5
a2b1c2	264,835	20,124	4,019	286	149	155	27.0	308	-12.2
a2b1c2	270,501	21,441	4,062	308	149	164	26.6	396	- 6.7
a2b2c1	272,295	21,015	7,763	618	278	330	53.7	948	-10.7
a2b2c1	270,573	20,557	7,565	631	267	350	52.8	915	- 6.9
a2b2c1	275,939	21,725	8,176	627	286	333	51.9	924	- 7.0
a2b2c2	280,569	21,704	8,488	627	297	360	53.4	902	- 2.4
a2b2c2	294,697	23,402	9,398	648	328	346	56.2	1,185	0.2
a2b2c2	273,084	21,095	7,922	644	279	359	53.7	1,005	- 7.3

* Treatments: a1) Fe:Al = 500:0, a2) 450:50, b1) Trace elements concentrations = Low, b2) High, c1) Without Hg, c2) With Hg, e1) Control 500:0, e2) Control 450:50.

Table S6 – Water extraction (mg kg^{-1}) by two consecutives washing.

Treat*	Fe	Al	As	Pb	Cd	La	Yb	Sb	Hg
a1b1c1	2,294	2.8	18.8	1.7	4.0	10.7	2.5	9.3	- 2.9
a1b1c1	3,980	3.6	21.7	0.8	3.5	9.7	2.6	13.9	- 6.0
a1b1c1	1,398	2.0	33.8	1.1	4.4	37.6	3.6	10.2	- 2.3
a1b1c2	2,853	2.4	20.3	0.5	2.9	11.4	2.8	- 12.4	- 2.8
a1b1c2	1,902	1.6	15.4	0.5	3.0	11.7	3.0	14.4	- 5.2
a1b1c2	1,424	2.9	13.4	1.2	3.3	7.2	2.6	6.0	- 2.8
a1b2c1	759	1.0	70.9	1.6	8.4	103.4	4.7	4.6	- 3.5
a1b2c1	752	0.8	75.2	1.6	10.6	20.2	5.6	8.8	- 3.0
a1b2c1	6	0.1	4.5	1.0	0.0	0.1	0.0	- 3.1	1.0
a1b2c2	465	1.4	39.6	1.5	4.8	42.1	3.2	- 1.2	- 2.9
a1b2c2	828	0.9	31.2	1.6	6.1	13.6	3.0	7.7	- 4.5
a1b2c2	968	0.8	11.5	2.4	4.4	13.7	2.7	- 1.6	- 3.2
a2b1c1	678	53.3	12.9	1.9	2.1	44.0	1.2	7.6	- 0.5
a2b1c1	4	0.5	1.3	0.9	- 0.1	0.1	0.0	10.4	0.3
a2b1c1	32	151.6	7.6	2.2	1.4	60.3	2.1	- 11.6	- 0.6
a2b1c2	192	184.2	7.5	3.7	1.4	61.7	2.4	15.4	- 1.0
a2b1c2	8	1.2	0.6	1.5	- 0.0	1.4	0.0	0.9	0.9
a2b1c2	55	32.2	5.4	1.4	1.1	37.2	1.0	- 0.5	0.5
a2b2c1	1	0.4	3.6	1.0	0.5	38.5	0.0	5.8	- 0.6
a2b2c1	0	3.5	8.5	2.0	2.2	128.1	1.0	- 0.2	- 0.8
a2b2c1	977	52.5	23.9	2.2	4.8	104.1	2.4	1.7	- 0.6
a2b2c2	16	34.3	10.7	2.1	2.2	99.8	1.8	- 0.7	- 1.2
a2b2c2	1,851	53.5	51.3	1.8	9.4	165.3	3.2	- 4.0	- 3.2
a2b2c2	11	8.2	8.5	1.8	1.7	95.9	1.2	- 0.5	- 1.7

* Treatments: a1) Fe:Al = 500:0, a2) 450:50, b1) Trace elements concentrations = Low, b2) High, c1) Without Hg, c2) With Hg, e1) Control 500:0, e2) Control 450:50.

Table S7 – Acid extraction (mg kg^{-1}) by method BCR (Rauret et al., 1999).

Treat*	Fe	Al	As	Pb	Cd	La	Yb	Sb	Hg
a1b1c1	2,055	12.4	32.3	16.5	4.0	58.4	2.5	30.7	2.6
a1b1c1	1,552	5.3	17.0	7.1	2.2	40.6	1.6	17.7	1.5
a1b1c1	1,274	3.7	25.3	7.2	3.6	85.0	3.5	- 1.1	1.2
a1b1c2	1,635	3.2	23.9	13.0	2.9	76.3	3.0	- 6.6	0.3
a1b1c2	905	2.2	14.1	6.7	1.9	38.8	2.0	- 4.9	0.0
a1b1c2	1,496	2.8	23.1	13.3	3.1	64.2	2.9	- 0.1	1.3
a1b2c1	819	2.7	133.1	16.5	8.4	223.2	4.3	10.3	- 2.2
a1b2c1	33	1.2	65.3	8.3	8.4	82.2	4.9	1.4	- 2.3
a1b2c1	39	3.3	95.2	10.2	12.2	115.6	7.1	- 10.3	- 7.0
a1b2c2	1,008	2.5	114.3	17.6	8.8	188.1	5.2	- 21.3	- 6.2
a1b2c2	1,363	1.8	101.8	12.5	11.4	172.7	4.9	0.5	- 8.7
a1b2c2	780	2.0	19.6	8.2	4.4	111.5	2.1	- 8.6	- 3.1
a2b1c1	1,041	986.5	55.3	21.2	3.8	96.2	6.1	2.4	0.1
a2b1c1	23	143.7	15.4	14.2	2.1	65.1	5.0	- 4.9	- 3.2
a2b1c1	257	523.6	16.4	17.9	1.9	75.4	3.4	5.0	- 0.4
a2b1c2	577	800.7	24.3	28.1	2.2	107.4	5.3	18.9	- 1.4
a2b1c2	46	207.7	21.3	12.4	2.8	76.7	5.2	7.8	- 3.2
a2b1c2	408	597.5	24.5	24.0	2.5	93.6	5.9	3.3	- 1.5
a2b2c1	174	377.2	62.2	26.9	8.6	217.7	14.3	- 7.5	- 3.7
a2b2c1	124	206.9	25.4	22.4	4.7	153.1	8.9	1.1	- 2.6
a2b2c1	955	942.4	89.6	31.9	9.5	168.0	10.3	27.8	- 2.3
a2b2c2	164	359.4	35.5	26.8	4.0	147.4	7.6	- 13.6	- 1.3
a2b2c2	2,085	1,152.0	212.2	40.7	10.8	214.5	12.6	- 22.6	0.4
a2b2c2	211	268.4	37.3	24.6	4.8	170.7	9.8	- 9.8	- 2.6

* Treatments: a1) Fe:Al = 500:0, a2) 450:50, b1) Trace elements concentrations = Low, b2) High, c1) Without Hg, c2) With Hg, e1) Control 500:0, e2) Control 450:50.

Table S8 – Reducing extraction (mg kg^{-1}) by method BCR (Rauret et al., 1999).

Treat*	Fe	Al	As	Pb	Cd	La	Yb	Sb	Hg
a1b1c1	13,530	12.7	127.9	129.9	5.2	79.0	3.7	11.5	2.1
a1b1c1	3,159	7.8	60.0	47.0	3.7	75.1	3.0	10.3	- 3.8
a1b1c1	8,437	4.7	138.6	68.8	4.7	99.5	4.9	- 5.1	0.5
a1b1c2	2,597	3.5	64.6	69.9	3.2	79.7	3.4	28.4	- 0.7
a1b1c2	2,420	1.7	59.2	64.3	3.5	77.0	4.1	4.9	- 2.5
a1b1c2	19,381	17.1	141.5	76.3	4.2	81.6	4.4	1.9	2.0
a1b2c1	20,826	2.4	689.6	224.3	16.7	225.1	10.3	19.0	- 7.4
a1b2c1	20,456	2.1	702.0	227.5	16.6	220.9	10.1	15.3	- 4.9
a1b2c1	23,620	3.2	235.1	231.7	13.1	150.9	10.9	7.9	-12.8
a1b2c2	21,160	2.9	636.5	210.7	11.6	214.5	8.7	28.5	- 1.3
a1b2c2	17,919	3.0	516.2	179.4	13.3	181.8	7.0	- 7.0	- 5.2
a1b2c2	2,211	1.5	84.0	141.5	6.6	191.9	4.2	5.1	- 5.1
a2b1c1	12,084	2,436.5	129.2	56.4	4.8	107.8	9.3	4.9	- 1.7
a2b1c1	2,625	623.4	33.9	57.2	4.3	101.9	10.2	- 9.1	- 5.2
a2b1c1	4,828	1,539.0	54.7	51.7	2.5	98.0	5.7	8.7	- 1.6
a2b1c2	6,914	1,953.0	79.1	88.2	2.9	115.3	7.3	- 6.6	- 1.5
a2b1c2	3,063	748.8	56.6	46.6	4.1	92.4	8.1	14.9	- 4.1
a2b1c2	5,332	1,597.2	68.1	59.4	3.2	104.2	8.7	31.0	- 2.2
a2b2c1	4,722	1,051.7	105.9	163.2	9.4	221.2	18.3	23.9	- 3.8
a2b2c1	4,584	858.2	73.3	178.8	8.0	250.6	17.8	2.7	- 3.7
a2b2c1	16,261	2,808.1	267.0	168.1	11.1	245.5	19.1	16.7	- 2.7
a2b2c2	3,950	1,328.7	124.6	188.1	7.2	257.4	16.9	- 6.0	- 2.4
a2b2c2	28,046	3,522.0	449.2	200.3	13.7	267.1	21.4	- 7.1	1.8
a2b2c2	3,436	732.9	88.8	201.6	6.2	243.4	16.0	5.1	- 3.4

* Treatments: a1) Fe:Al = 500:0, a2) 450:50, b1) Trace elements concentrations = Low, b2) High, c1) Without Hg, c2) With Hg, e1) Control 500:0, e2) Control 450:50.

Table S9 – Oxidizing extraction (mg kg^{-1}) by method BCR (Rauret et al., 1999).

Treat*	Fe	Al	As	Pb	Cd	La	Yb	Sb	Hg
a1b1c1	2,601	2.7	51.0	90.5	5.8	95.8	3.9	- 25.6	- 0.4
a1b1c1	2,365	5.4	74.3	21.8	4.4	81.4	3.3	- 22.9	- 9.5
a1b1c1	2,015	0.8	94.0	35.9	5.3	107.2	4.4	- 21.2	- 4.0
a1b1c2	1,515	9.3	73.9	47.5	4.2	94.3	3.9	0.6	- 3.2
a1b1c2	1,342	5.4	72.3	49.0	4.1	89.8	4.6	- 24.5	- 7.9
a1b1c2	2,293	0.6	53.8	47.2	4.7	96.1	4.5	- 23.2	- 5.6
a1b2c1	1,017	1.9	340.5	125.6	12.1	285.0	7.2	31.6	- 5.2
a1b2c1	1,269	2.8	325.6	172.7	18.4	265.6	10.4	15.1	- 6.2
a1b2c1	170	0.8	184.3	153.4	13.3	151.3	9.4	- 38.4	-11.8
a1b2c2	1,122	7.6	310.7	175.8	11.7	247.4	8.6	- 17.1	-10.8
a1b2c2	1,279	11.9	292.8	147.0	14.8	224.8	7.3	19.4	-12.9
a1b2c2	958	8.3	95.3	104.2	7.6	218.0	4.6	- 3.8	- 7.8
a2b1c1	5,019	1,887.8	95.4	56.5	6.4	139.2	9.9	11.7	- 6.2
a2b1c1	302	442.7	29.0	50.7	4.0	124.6	10.8	- 9.7	- 5.7
a2b1c1	1,413	1,264.7	46.6	56.9	3.5	130.8	6.6	4.1	- 7.0
a2b1c2	1,799	1,413.9	44.7	87.1	3.2	137.4	6.9	32.0	- 2.5
a2b1c2	372	470.2	37.9	43.0	4.1	105.3	8.0	11.3	- 6.7
a2b1c2	1,131	1,075.1	36.7	55.5	3.4	122.2	8.2	- 14.4	- 3.2
a2b2c1	827	698.5	77.2	163.4	10.1	264.4	18.8	- 30.1	- 5.8
a2b2c1	952	617.7	56.8	183.1	9.1	300.7	19.0	17.8	- 6.2
a2b2c1	5,538	2,032.1	178.2	174.1	13.5	304.0	21.2	14.8	- 2.1
a2b2c2	789	983.6	93.2	183.2	7.8	300.9	16.6	- 5.9	- 8.1
a2b2c2	7,513	1,994.2	223.0	173.5	14.4	285.5	19.2	- 54.6	- 6.7
a2b2c2	522	492.8	57.4	183.8	6.9	273.2	15.4	21.6	- 0.7

* Treatments: a1) Fe:Al = 500:0, a2) 450:50, b1) Trace elements concentrations = Low, b2) High, c1) Without Hg, c2) With Hg, e1) Control 500:0, e2) Control 450:50.

Table S10 – Bioaccessibility (mg kg^{-1}) by SBET procedure (USEPA, 2008).

Treat*	Fe	Al	As	Pb	Cd	La	Yb	Sb	Hg
a1b1c1	4,020	12.7	96.8	80.5	5.5	55.6	2.4	- 27.4	9.9
a1b1c1	2,961	12.2	105.9	48.7	6.1	81.7	3.2	- 52.7	7.7
a1b1c1	1,678	4.9	127.6	43.7	5.6	74.5	3.4	- 81.5	4.8
a1b1c2	2,285	6.6	97.6	78.9	6.1	97.4	4.1	-190.1	3.3
a1b1c2	1,951	6.1	72.6	65.1	5.1	83.1	4.5	-315.4	- 5.4
a1b1c2	7,037	16.9	167.7	94.9	8.7	100.6	4.7	-117.5	1.1
a1b2c1	2,547	4.1	363.6	102.0	15.0	178.8	4.7	- 50.8	- 5.5
a1b2c1	2,863	3.5	324.3	129.1	17.4	157.7	6.3	-127.1	- 2.2
a1b2c1	1,403	5.4	248.6	149.9	14.6	122.7	7.9	-222.2	- 7.0
a1b2c2	2,175	3.1	229.2	90.7	10.4	122.5	4.4	- 86.1	- 2.9
a1b2c2	2,749	7.7	301.2	122.8	15.5	157.0	5.3	-128.6	- 3.4
a1b2c2	1,215	3.1	64.6	96.6	6.3	159.0	3.5	-204.6	- 4.1
a2b1c1	2,717	778.0	106.2	29.7	5.2	72.2	4.6	191.7	- 1.1
a2b1c1	591	218.8	61.0	40.6	3.9	94.3	7.7	65.5	1.5
a2b1c1	1,299	620.5	61.1	36.2	3.0	80.9	4.0	24.4	- 9.9
a2b1c2	1,298	564.1	72.0	49.3	3.4	76.7	3.9	- 1.6	0.5
a2b1c2	1,015	368.2	122.3	56.2	7.1	126.3	9.3	-118.4	- 2.1
a2b1c2	959	435.7	75.4	36.3	3.7	75.2	4.5	-188.1	- 2.3
a2b2c1	1,096	413.4	156.0	154.5	11.2	217.1	15.3	18.4	- 6.8
a2b2c1	1,132	367.4	99.6	156.2	8.1	234.6	13.7	- 6.3	- 7.6
a2b2c1	4,867	1,434.7	371.8	182.7	20.1	270.6	16.8	-275.5	3.5
a2b2c2	901	527.3	185.7	174.3	10.0	257.0	13.1	128.6	- 0.5
a2b2c2	7,322	1,482.8	629.4	206.4	28.7	286.3	16.6	-170.9	- 0.3
a2b2c2	1,140	343.1	157.4	205.8	9.8	257.7	13.9	-269.5	- 0.1

* Treatments: a1) Fe:Al = 500:0, a2) 450:50, b1) Trace elements concentrations = Low, b2) High, c1) Without Hg, c2) With Hg, e1) Control 500:0, e2) Control 450:50.